

PACIFIC EARTHQUAKE ENGINEERING RESEARCH CENTER

Concrete Column Blind Prediction Contest 2010: Outcomes and Observations

Vesna Terzic

Matthew J. Schoettler

Department of Civil and Environmental Engineering
University of California, Berkeley

José I. Restrepo

Department of Structural Engineering
University of California, San Diego

Stephen A. Mahin

Department of Civil and Environmental Engineering
University of California, Berkeley

PEER Report No. 2015/01

Pacific Earthquake Engineering Research Center
Headquarters at the University of California, Berkeley

March 2015

Disclaimer

The opinions, findings, and conclusions or recommendations expressed in this publication are those of the author(s) and do not necessarily reflect the views of the study sponsor(s) or the Pacific Earthquake Engineering Research Center.

Concrete Column Blind Prediction Contest 2010: Outcomes and Observations

Vesna Terzic

Matthew J. Schoettler

Department of Civil and Environmental Engineering
University of California, Berkeley

José I. Restrepo

Department of Structural Engineering
University of California, San Diego

Stephen A. Mahin

Department of Civil and Environmental Engineering
University of California, Berkeley

PEER Report No. 2015/01
Pacific Earthquake Engineering Research Center
Headquarters at University of California, Berkeley

March 2015

ABSTRACT

Performance-based earthquake engineering (PBEE) is based on the premise that the performance of engineered facilities can be predicted and evaluated with sufficient degree of confidence. However, prediction of system response greatly depends on the analyst's experience and modeling skills. Therefore, the uncertainty with which the engineering community can predict response of a system or one of its components should be realistically quantified in PBEE. A blind prediction contest of a full-scale reinforced-concrete bridge column exposed to six consecutive unidirectional ground motions of different intensity was conducted to identify the uncertainty of the predictions of important response quantities. Predictions submitted by forty-one teams were statistically analyzed, which showed great scatter in predictions of basic engineering response parameters. For instance, the average coefficients of variation in predicting maximum displacement and acceleration over six ground motions were 39% and 48%, respectively. Biases in median predicted responses were also significant, varying from 5% to 35% for displacement and from 25% to 118% for acceleration. Although the results of this blind prediction contest provide data regarding the modeling uncertainty of modern bridge columns, more than anything these results stress the need for a comprehensive analytical study that establishes guidelines on bridge column modeling, with the goal of reducing the uncertainties.

ACKNOWLEDGMENTS

This project was sponsored by the Pacific Earthquake Engineering Research Center (PEER) Program “Applied Earthquake Engineering Research of Lifelines Systems,” supported by the California Energy Commission, the California Department of Transportation, and the Pacific Gas and Electric Company. Additional support was provided from the Federal Highway Administration (FHA) Contract DTFH61-07-C-00031.

This work made use of the Earthquake Engineering Research Centers Shared Facilities supported by the National Science Foundation (NSF), under Award Number EEC-9701568 through PEER.

The authors are greatly appreciated of all of the experts that participated in the contest, especially of those who shared the requested information regarding their models. Any opinions, findings, and conclusions or recommendations expressed in this material are those of the authors, and do not necessarily reflect those of NSF or the FHA.

CONTENTS

ABSTRACT	iii
ACKNOWLEDGMENTS	v
TABLE OF CONTENTS	vii
LIST OF TABLES	ix
LIST OF FIGURES	xi
1 INTRODUCTION	1
1.1 Motivation for the Blind Prediction Contest	1
1.2 A Full-Scale Test of a Bridge Column	2
1.3 Organization of the Report	2
2 DESCRIPTION OF THE EXPERIMENTAL PROGRAM	5
2.1 Test Set-Up	5
2.1.1 Column.....	6
2.1.2 Footing.....	8
2.1.3 Superstructure Mass.....	8
2.2 Material Properties	8
2.3 Loading Protocol	11
3 TEST RESULTS	15
3.1 Digital Data Processing Procedures	15
3.2 Test EQ1	16
3.3 Test EQ2	17
3.4 Test EQ3	18
3.5 Test EQ4	19
3.6 Test EQ5	19
3.7 Test EQ6	19
3.8 Summary	20
4 BLIND PREDICTION CONTEST	23
4.1 Contest Description	23
4.2 Rules of the Contest	23
4.3 Rules for Scoring Contestants	27

4.4	Winners of Contest	27
4.5	Prediction of Failure Mode	36
4.6	Alternative Methods for Scoring Predictions.....	36
4.7	Winners based on Alternative Scoring Methods.....	37
5	STATISTICAL ANALYSIS OF DATA	45
5.1	Mean and Median Bias and Coefficient of Variations for Considered Response Quantities.....	45
5.1.1	Relative Lateral Displacement at the Top of the Column.....	46
5.1.2	Absolute Acceleration at the Top of the Column	46
5.1.3	Bending Moment at the Base of the Column.....	47
5.1.4	Base Shear.....	47
5.1.5	Compressive Axial Force.....	48
5.1.6	Maximum Average Curvature between 51 and 254 mm from the Bottom of the Column	48
5.1.7	Maximum Average Axial Strain 51 and 254 mm from the Bottom of the Column	48
5.1.8	Residual Displacement at the Top of the Column	49
5.2	Distributions of Average Error in Prediction of Contest-Specified Response Quantities.....	64
5.3	Error as a Function of Damage State of Column after an Earthquake.....	69
6	COMPARISON OF NUMERICAL MODELS OF BRIDGE COLUMN	75
7	SUMMARY AND CONCLUSIONS	83
	REFERENCES.....	85
	APPENDIX A: QUESTIONNAIRES	87

LIST OF TABLES

Table 2.1	Column concrete strength.	9
Table 2.2	Ground motion selection.....	12
Table 2.3	Ground motion scale factors and peak ground parameters.....	12
Table 3.1	Peak response quantities.	22
Table 4.1	Award of Excellence winners.	28
Table 4.2	Winners based on different scoring methods.....	38
Table 5.1	Average coefficient of variation (COV) for different response quantities.	46
Table 5.2	Median and dispersion (β) of the average error for different response quantities.....	65

LIST OF FIGURES

Figure 2.1	Test set-up.....	5
Figure 2.2	Column reinforcing details.	7
Figure 2.3	Column concrete stress-strain relationship at 42 days.....	9
Figure 2.4	Typical column longitudinal reinforcement tensile stress-strain relationship.....	10
Figure 2.5	Column transverse hoop reinforcement tensile stress-strain relationship.....	10
Figure 2.6	(a) Peak ground acceleration and (b) peak ground velocity replicated by the shake table.....	13
Figure 3.1	East face of the column base after (a) EQ1, (b) EQ2, (c) EQ3, (d) EQ4, (e) EQ5, and (f) EQ6.	17
Figure 3.2	Normalized base moment-curvature response for (a) EQ1, (b) EQ2, (c) EQ3, (d) EQ4, (e) EQ5, and (f) EQ6.	18
Figure 3.3	Normalized base shear-drift response for (a) EQ1, (b) EQ2, (c) EQ3, (d) EQ4, (e) EQ5, and (f) EQ6.	18
Figure 3.4	Input acceleration time histories.	20
Figure 3.5	Acceleration time histories of the column top.	20
Figure 3.6	Drift ratio time histories.....	21
Figure 3.7	Peak drift ratios achieved.....	21
Figure 4.1	Contest submittal spreadsheet.....	26
Figure 4.2	Analysis software used for analytical predictions.	29
Figure 4.3	Analysis software used by winning contestants and Award of Excellence recipients.	29
Figure 4.4	Predictions of “Max” displacement at the top of the column versus measured response.	30
Figure 4.5	Predictions of “Min” displacement at the top of the column versus measured response.	30
Figure 4.6	Predictions of “Max” acceleration at the top of the column versus measured response.	31

Figure 4.7	Predictions of “Min” acceleration at the top of the column versus measured response.	31
Figure 4.8	Predictions of “Max” bending moment at the base of the column versus measured response.	32
Figure 4.9	Predictions of “Min” bending moment at the base of the column versus measured response.	32
Figure 4.10	Predictions of “Max” shear force at the base of the column versus measured response.	33
Figure 4.11	Predictions of “Min” shear force at the base of the column versus measured response.	33
Figure 4.12	Predictions of maximum compressive axial force versus measured response.....	34
Figure 4.13	Predictions of “Max” average curvature between 51 and 254 mm from the bottom of the column versus measured response.	34
Figure 4.14	Predictions of “Max” average axial strain between 51 and 254 mm from the bottom of the column versus measured response.....	35
Figure 4.15	Predictions of residual displacement at the top of the column versus measured response.	35
Figure 4.16	Number of predictions for each of the six suggested failure modes.	36
Figure 4.17	Predictions of “Max” displacement at the top of the column versus measured response.	38
Figure 4.18	Predictions of “Min” displacement at the top of the column versus measured response.	39
Figure 4.19	Predictions of “Max” horizontal acceleration at the top of the column versus measured response.	39
Figure 4.20	Predictions of “Min” horizontal acceleration at the top of the column versus measured response.	40
Figure 4.21	Predictions of “Max” bending moment at the base of the column versus measured response.	40
Figure 4.22	Predictions of “Min” bending moment at the base of the column versus measured response.	41
Figure 4.23	Predictions of “Max” shear force at the base of the column versus measured response.	41
Figure 4.24	Predictions of “Min” shear force at the base of the column versus measured response.	42
Figure 4.25	Predictions of maximum compressive axial force versus measured response.....	42

Figure 4.26	Predictions of “Max” average curvature between 51 and 457 mm from the bottom of the column versus measured response.	43
Figure 4.27	Predictions of “Max” average axial strain between 51 and 457 mm from the bottom of the column versus measured response.....	43
Figure 4.28	Predictions of residual displacement at the top of the column versus measured response.	44
Figure 5.1	Statistical analysis of predictions of “Max” displacements at the top of the column: (a) analytical predictions with measured response, mean, and median marked on the graph; (b) mean and median bias; and (c) coefficient of variation.	50
Figure 5.2	Statistical analysis of predictions of “Min” displacements at the top of the column: (a) analytical predictions with measured response, mean, and median marked on the graph; (b) mean and median bias; and (c) coefficient of variation.	51
Figure 5.3	Statistical analysis of predictions of “Max” accelerations at the top of the column: (a) analytical predictions with measured response, mean, and median marked on the graph; (b) mean and median bias; and (c) coefficient of variation.	52
Figure 5.4	Statistical analysis of predictions of “Min” accelerations at the top of the column: (a) analytical predictions with measured response, mean, and median marked on the graph; (b) mean and median bias; and (c) coefficient of variation.	53
Figure 5.5	Statistical analysis of predictions of “Max” bending moment at the base of the column: (a) analytical predictions with measured response, mean, and median marked on the graph; (b) mean and median bias; and (c) coefficient of variation.	54
Figure 5.6	Statistical analysis of predictions of “Min” bending moments at the base of the column: (a) analytical predictions with measured response, mean, and median marked on the graph; (b) mean and median bias; and (c) coefficient of variation.	55
Figure 5.7	Statistical analysis of predictions of “Max” shear at the base of the column: (a) analytical predictions with measured response, mean, and median marked on the graph; (b) mean and median bias; and (c) coefficient of variation.	56
Figure 5.8	Statistical analysis of predictions of “Min” shear at the base of the column: (a) analytical predictions with measured response, with mean and median marked on the graph; (b) mean and median bias; and (c) coefficient of variation.	57

Figure 5.9	Statistical analysis of predictions of maximum compressive axial force: (a) analytical predictions with measured response, with mean and median marked on the graph; (b) mean and median bias; and (c) coefficient of variation.	58
Figure 5.10	Statistical analysis of predictions of “Max” average curvature (between 51 and 254 mm from the bottom of the column): (a) analytical predictions and measured response; (b) mean and median bias; and (c) coefficient of variation.	59
Figure 5.11	Statistical analysis of predictions of “Max” average curvature (between 51 and 457 mm from the bottom of the column): (a) analytical predictions and measured response; (b) mean and median bias; and (c) coefficient of variation.	60
Figure 5.12	Statistical analysis of predictions of “Max” average axial strain (between 51 and 254 mm from the bottom of the column): (a) analytical predictions and measured response; (b) mean and median bias; and (c) coefficient of variation.	61
Figure 5.13	Statistical analysis of predictions of “Max” average axial strain (between 51 and 457 mm from the bottom of the column): (a) analytical predictions and measured response; (b) mean and median bias; and (c) coefficient of variation.	62
Figure 5.14	Statistical analysis of predictions of residual displacements at the top of the column: (a) analytical predictions with measured response, with mean and median marked on the graph; (b) mean and median bias; and (c) coefficient of variation.	63
Figure 5.15	Lognormal distribution of average error in predicting absolute maximum horizontal displacement at the top of the column.	65
Figure 5.16	Lognormal distribution of average error in predicting absolute maximum horizontal acceleration at the top of the column.	66
Figure 5.17	Lognormal distribution of average error in predicting absolute maximum bending moment at the base of the column.	66
Figure 5.18	Lognormal distribution of average error in predicting maximum shear at the base of the column.	67
Figure 5.19	Lognormal distribution of average error in predicting maximum compressive axial force.	67
Figure 5.20	Lognormal distribution of average error in predicting maximum average curvature between 51 and 457 mm from the bottom of the column.	68
Figure 5.21	Lognormal distribution of average error in predicting maximum average axial strain between 51 and 457 mm from the bottom of the column.	68

Figure 5.22	Lognormal distribution of average error in predicting residual displacement at the top of the column.	69
Figure 5.23	Cumulative error over six earthquakes in predicting maximum horizontal displacement at the top of the column.	71
Figure 5.24	Average error in predicting maximum horizontal displacement at the top of the column considering different numbers of earthquakes (“n” represents number of considered earthquakes).	71
Figure 5.25	Cumulative error over six earthquakes in predicting maximum horizontal acceleration at the top of the column: (a) all contestants, and (b) the best 14 contestants.	72
Figure 5.26	Average error in predicting maximum horizontal acceleration at the top of the column considering different numbers of earthquakes (“n” represents number of considered earthquakes).	73
Figure 6.1	Average error over 6 earthquakes in predicting maximum horizontal displacement at the top of the column using four different element types: force based element (FB), displacement based element (DB), beam with distributed plastic hinges (DPH), and beam with concentrated plastic hinges (CPH).	77
Figure 6.2	Average error over six earthquakes in predicting minimum horizontal displacement at the top of the column using four different element types: force based element (FB), displacement based element (DB), beam with distributed plastic hinges (DPH), and beam with concentrated plastic hinges (CPH).	77
Figure 6.3	Average error over six earthquakes in predicting maximum horizontal acceleration at the top of the column using four different element types: force based element (FB), displacement based element (DB), beam with distributed plastic hinges (DPH), and beam with concentrated plastic hinges (CPH).	78
Figure 6.4	Average error over six earthquakes in predicting minimum horizontal acceleration at the top of the column using four different element types: force based element (FB), displacement based element (DB), beam with distributed plastic hinges (DPH), and beam with concentrated plastic hinges (CPH).	78
Figure 6.5	Average error over six earthquakes in predicting maximum bending moment at the base of the column using four different element types: force based element (FB), displacement based element (DB), beam with distributed plastic hinges (DPH), and beam with concentrated plastic hinges (CPH).	79

Figure 6.6	Average error over six earthquakes in predicting minimum bending moment at the base of the column using four different element types: force based element (FB), displacement based element (DB), beam with distributed plastic hinges (DPH), and beam with concentrated plastic hinges (CPH).....	79
Figure 6.7	Average error over six earthquakes in predicting maximum shear at the base of the column using four different element types: force based element (FB), displacement based element (DB), beam with distributed plastic hinges (DPH), and beam with concentrated plastic hinges (CPH).	80
Figure 6.8	Average error over six earthquakes in predicting minimum shear at the base of the column using four different element types: force based element (FB), displacement based element (DB), beam with distributed plastic hinges (DPH), and beam with concentrated plastic hinges (CPH).	80
Figure 6.9	Average error over six earthquakes in predicting maximum compressive axial force using four different element types: force based element (FB), displacement based element (DB), beam with distributed plastic hinges (DPH), and beam with concentrated plastic hinges (CPH).....	81
Figure 6.10	Average error over six earthquakes in predicting maximum average curvature between 51 and 457 mm from the bottom of the column using four different element types: force based element (FB), displacement based element (DB), beam with distributed plastic hinges (DPH), and beam with concentrated plastic hinges (CPH).....	81
Figure 6.11	Average error over six earthquakes in predicting maximum average axial strain between 51 and 457 mm from the bottom of the column using four different element types: force based element (FB), displacement based element (DB), beam with distributed plastic hinges (DPH), and beam with concentrated plastic hinges (CPH).....	82
Figure 6.12	Average error over six earthquakes in predicting residual displacement at the top of the column using four different element types: force based element (FB), displacement based element (DB), beam with distributed plastic hinges (DPH), and beam with concentrated plastic hinges (CPH).....	82

1 Introduction

1.1 MOTIVATION FOR THE BLIND PREDICTION CONTEST

Performance-based earthquake engineering (PBEE) implies design, evaluation, and construction of engineered facilities whose performance under common and extreme loads responds to the diverse needs of owners-users and society [Krawinkler 1999]. In the U.S., several conceptual PBEE frameworks for engineered facilities have been developed: some for design [SEAOC 1995; FEMA 1997; FEMA 2000b] and some for evaluation [ATC 1996; FEMA 2000a; Cornell and Krawinkler 2000]. Although some of these frameworks can account for effects of modeling uncertainty, PBEE evaluation is most commonly based on premise that the performance of engineered facilities can be predicted and evaluated with a high degree of confidence. However, prediction of system response greatly depends on the analyst's experience and modeling skills. Therefore, the uncertainty with which the engineering community can predict performance of a system or one of its components should be realistically quantified and considered in PBEE.

The *Concrete Column Blind Prediction Contest* of a full-scale reinforced-concrete (RC) bridge column subjected to six consecutive unidirectional ground motions was organized by the Pacific Earthquake Engineering Research Center (PEER) to identify the uncertainty of the predictions of important response quantities. Each contestant/team had to predict maximum global (displacement, acceleration, and residual displacement), intermediate (bending moment, shear, and axial force), and local (axial strain and curvature) response quantities of a structure subjected to six earthquakes. The contestants were supplied with the ground motions and structural details, including the results from shake table tests, the complete dimension of the test specimen, and mechanical one-dimensional (1D) properties of the steel and concrete. Predictions were submitted by forty-one teams from fourteen different countries: Australia, Canada, China, Colombia, Ecuador, Italy, Japan, New Zealand, Switzerland, Peru, Portugal, Puerto Rico, Taiwan, and the U.S. The contestants held either M.S. or PhD degrees, or were either researchers or engineering practitioners. The submitted predictions were statistically analyzed with the purpose of quantifying modeling uncertainty. Predictions were also used to explore different ways of scoring the predictions so that the best model could be objectively recognized.

The blind prediction contests also highlighted areas where current numerical models might be improved and thus enhance understanding of different modeling parameters on the accuracy of predictions. A questionnaire that contained questions related to model description (e.g., type of element, number of elements, etc.), mass and damping formulation, integration scheme, and output acceleration data signal processing was developed and sent to all

participants. Twenty-five participants responded to the questionnaires (see Appendix A), and their responses were analyzed to identify the effect of different modeling parameters on accuracy.

1.2 A FULL-SCALE TEST OF A BRIDGE COLUMN

The full-scale shake table test of a bridge column was performed to investigate the seismic performance of bridge columns built to current U.S. standards [Schoettler et al. 2014]. The column was detailed according to Caltrans' *Seismic Design Criteria* [2006] and *Bridge Design Specifications* [2004]. The 1.22-m- (4-ft-) diameter cantilever column spanned 7.31 m (24 ft) above the footing. With a height-to-diameter aspect ratio of six, the test specimen was intended to respond in the nonlinear range with predominantly flexural behavior. To mobilize its capacity during shake table tests, a large concrete block weighing 2.32 MN (521.9 kip) was cast on the top of the column. A total of ten earthquake simulations were conducted; however, only the first six were relevant to the blind prediction contest. The column was not straightened or repaired between tests.

The test specimen was densely instrumented to obtain high-quality response measurements under various ground motions. Testing was conducted over a span of two days on the NEES-UCSD shake table at the University of California, San Diego's Englekirk Structural Engineering Center on September 20th and 21st, 2010.

1.3 ORGANIZATION OF THE REPORT

The report contains seven chapters and one appendix. Chapter 2 describes the experimental program of a full-scale bridge column, and includes the test set-up along with the description of the column, footing and superstructure, properties of reinforcing steel and plain concrete, and loading protocol.

Chapter 3 describes instrumentation used to measure the response of the column to imposed ground motions. It then explains how the experimental measurements were utilized to generate the important response quantities (e.g., displacements, accelerations, bending moments, curvature, etc.). Performance of the column for each earthquake is described next, including moment-curvature and base shear-drift responses, as well as the time histories of displacements and accelerations at the top of the column.

Chapter 4 describes the organization of the contest, provides the rules of the contest along with the predicted response quantities and the criteria used to score the predictions, and based on these predictions and scoring criteria, how the winner was selected. In addition, it presents three alternative ways of scoring the predictions to determine the optimum scoring method that is most objective in evaluating submissions.

Chapter 5 presents the results of statistical analysis including: mean and median bias, coefficient of variation, lognormal distribution of average error over the six ground motions for

all predicted quantities, and histograms that show the error of a predicted displacement and acceleration quantities for subsequent earthquakes.

Chapter 6 includes basic model and analysis descriptions provided by contestants. For the purpose of showing the accuracy of different models as a function of the element type used for modeling the bridge column, the models were divided into four groups labeled by the names of element types: force-based beam-column element, displacement-based beam-column element, beam-column element with distributed plastic hinges, and beam-column element with concentrated plastic hinges. The average errors over all considered earthquakes with the contestants/teams predicted response quantities are presented for different types of elements.

Chapter 7 presents a summary of the main findings and conclusions.

Appendix A includes questionnaires received from 25 participants.

2 Description of the Experimental Program

2.1 TEST SET-UP

The experimental program is detailed by Schoettler et al [2014]. The test specimen consisted of a RC column cantilevered above its footing and supported a superstructure mass; see Figure 2.1. The footing was secured to the shake table with post-tensioning to prevent sliding or uplift. The large superstructure mass provided the axial load and the mass necessary to generate nonlinear response. To align its center of mass with the top of the column, a breakout in the superstructure mass enabled the column to extend halfway through, where a full moment-resisting connection anchored the superstructure mass to the column.

To protect site personnel and equipment, safety restraints were secured to the shake table and surrounded the test specimen. These safety restraints were located at the corners of the shake table and were fitted with horizontal guides to preclude out of plane motion. A clear 6.4-mm (0.25-in.) gap between the guide and superstructure block was greased to reduce friction should contact initiate during testing.



Figure 2.1 Test set-up.

Column displacement was limited to a 10% drift ratio. This restriction was imposed by inclined safety columns placed on either side of the column in the direction of shaking. These also provided gravity load restraint in the event of imminent collapse.

2.1.1 Column

The column was detailed according to Caltrans' *Seismic Design Criteria* [2006] and *Bridge Design Specifications* [2004]. Although detailed to these guidelines, it was not modeled after an existing prototype bridge column. The 1.22-m- (4-ft-) diameter cantilever column spanned 7.31 m (24 ft) above the footing. With a height-to-diameter aspect ratio of six, the test specimen was intended to respond in the nonlinear range with a predominant flexural behavior. The column was not straightened or repaired between tests.

Longitudinal reinforcement consisted of eighteen 35.8-mm-diameter (#11) bars in a single concentric layer. Butt-welded, double 15.9-mm-diameter (#5) hoops, spaced at 152 mm (6 in.) on-center, were used as transverse reinforcement. The term "double" refers to two hoops bundled together at each 152 mm spacing. The clear cover to the hoops was 51 mm (2 in.). Column reinforcement layout and the test specimen's geometry are provided in Figure 2.2, as is customary practice in bridge construction in California; all steel reinforcement was ASTM-A706, Grade 60.

The column's longitudinal reinforcement ratio ($\rho_l = 1.55\%$) is typical in current practice. The transverse reinforcement provided a volumetric confining ratio ($\rho_s = 0.95\%$). Reinforcement complied with Caltrans' minimum and maximum requirements [2004; 2006].

The as-built estimated axial load at the column base was 2.53 MN (570 kip). Accounting for the measured concrete strength at day one of testing, this axial load produced an axial load ratio of $N/A_g f'_c = 5.3\%$.

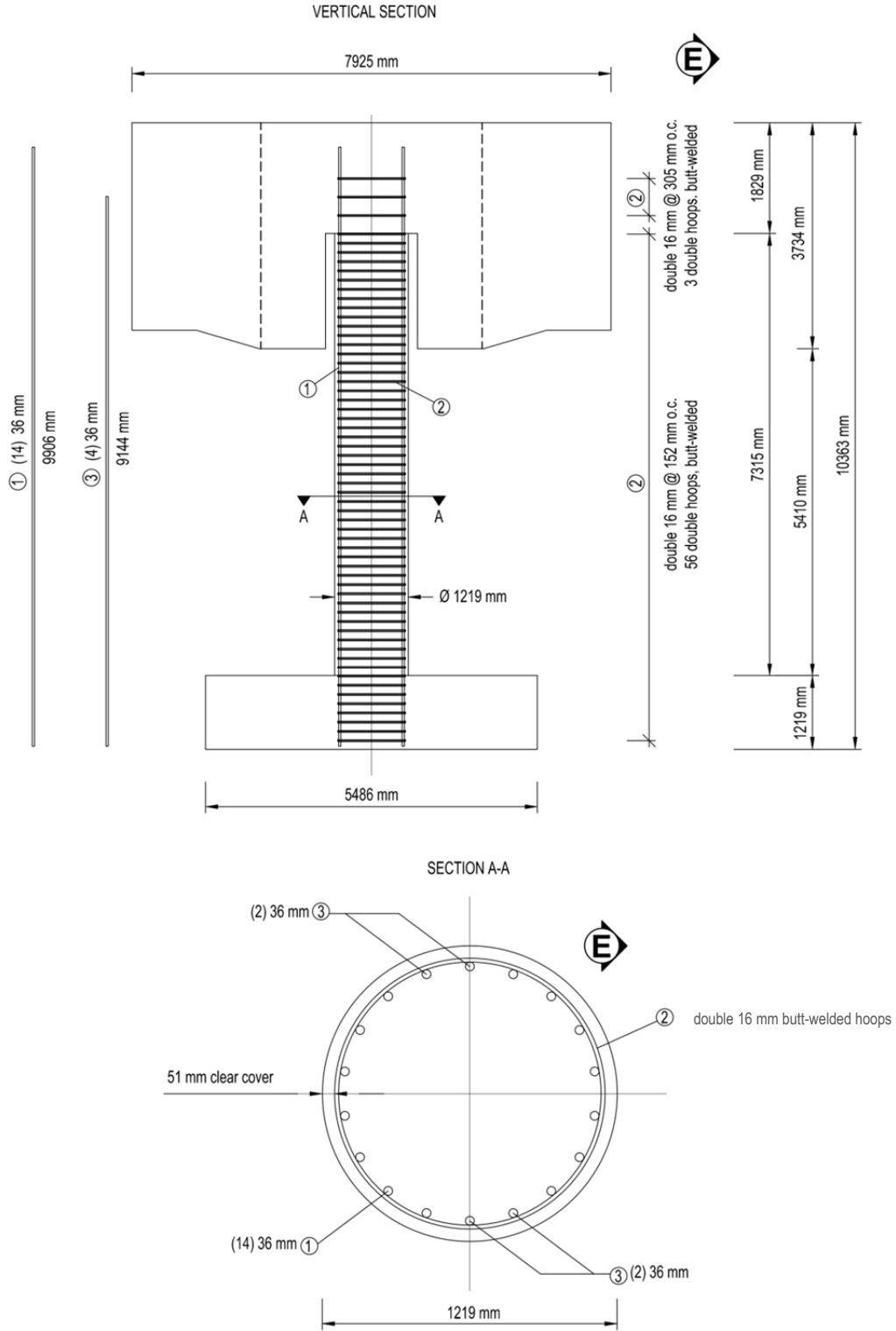


Figure 2.2 Column reinforcing details.

2.1.2 Footing

The footing—designed according to Caltrans’ *Seismic Design Criteria* [2006] and *Bridge Design Specifications* [2004] guidelines—consisted of a 5.49-m- (18-ft-) long, 1.83-m- (6-ft-) wide, 1.22-m- (4-ft-) deep RC block. The moment resisting connection between the footing and column was designed similar to a superstructure “T” joint [Caltrans 2006]. The footing was post-tensioned to the shake table to prevent decompression under maximum expected overturning moment and prevent sliding at maximum shear transfer to the shake table.

2.1.3 Superstructure Mass

The superstructure consisted of five cast-in-place concrete blocks. These blocks were arranged in a cruciform to accommodate placement of the safety restraints. The blocks were post-tensioned together and had a combined estimated weight of 2.32 MN (522 kip). This weight utilized the measured concrete unit weight with the specified geometry and accounted for the block reinforcement through holes for post-tensioning and post-tensioning bars. The combined block geometry was designed so its center-of-mass coincided with the top of the column. To ensure an unencumbered column height of 7.32 m (24 ft), a 152-mm (6-in.) gap was provided between the column and the central block for the bottom 1.91 m (6.25 ft) of the block.

2.2 MATERIAL PROPERTIES

The specified concrete strength of the column was 27.6 MPa (4.0 ksi). Maximum aggregate size was 25.4 mm (1.0 in.). At the time of casting, 152-mm- (6-in.-) diameter by 305-mm- (12-in.-) high concrete test cylinders were generated, for an average concrete unit weight of 23.6 kN/m³ (150 pcf). These cylinders were tested under monotonic compression in sets of three samples at 29, 42, and 43 days. Commencement of shake table testing corresponded to an age of forty-two days in the column concrete. The 43-day age corresponded to the second day of shake table testing. Of the three samples in a set, two samples were taken from the first batch of concrete delivered to the site, and one sample was from the second batch of concrete. This gave emphasis to the concrete strength in the plastic hinge region. Table 2.1 summarizes the results of these compression tests. A complete stress-strain relationship to peak load was obtained for one sample of each set of cylinders; see Figure 2.3. Strain was obtained as the average measurement from three concrete strain gages oriented in the longitudinal direction. These samples were taken from the first batch of concrete delivered to the site.

Column longitudinal and transverse reinforcement was specified as Grade 60 (414 MPa) steel conforming to ASTM A706. The #11 (35.8-mm-diameter) longitudinal reinforcement had a yield strength of 519 MPa (75.2 ksi) and an ultimate strength of 707 MPa (102.4 ksi). These strengths were obtained from monotonic tension tests. A complete stress-strain curve for this reinforcement is provided in Figure 2.4.

Table 2.1 Column concrete strength.

Age (days)	f'_c (MPa) [ksi]
29	40.3 [5.8] *
42	40.9 [5.9] +
43	42.0 [6.1] ‡

* Average of three samples.

+ Average of five samples.

‡ Average of six samples.

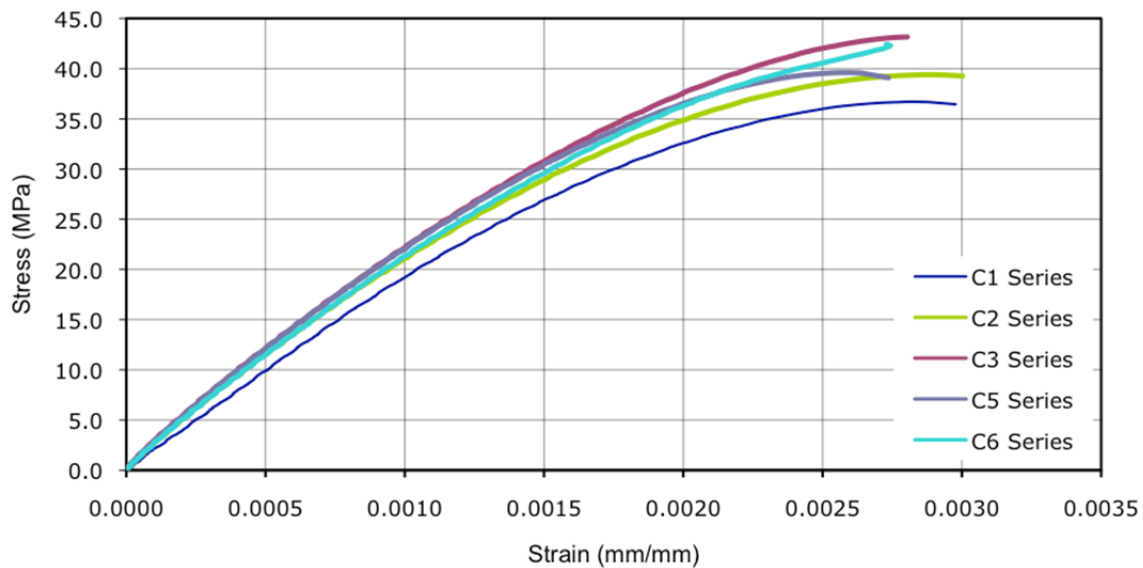


Figure 2.3 Column concrete stress-strain relationship at 42 days.

Samples taken from the #5 (15.9-mm-diameter) transverse hoops tested under monotonic tension did not exhibit a yield plateau. The peak stress was 592 MPa (85.9 ksi). A full stress-strain relationship of two samples is provided in Figure 2.5. These samples were cut from three bent hoops outside of the weld-affected region. The butt welds of the three sample hoops were also tested, and all failed outside of the weld. Yield strength based on the mill certification of the straight #5 bars was expected to be 454 MPa (65.8 ksi), and the ultimate tensile strength was expected to be 600 MPa (87.0 ksi).

Normal-weight concrete was utilized in both of these components. Samples from each of these components provided an average concrete unit weight of 23.5 kN/m³ (150 pcf) and 23.7 kN/m³ (151 pcf) for the footing and superstructure, respectively. The concrete in the footing had a specified strength of 27.6 MPa (4.0 ksi), and the mix design was the same as that used for the column. To accommodate the project schedule, however, the superstructure mass included high

early-strength concrete. The specified strength of this mix design was 35 MPa (5.1 ksi), with an expected strength of 31.3 MPa (4.7 ksi) at seven days.

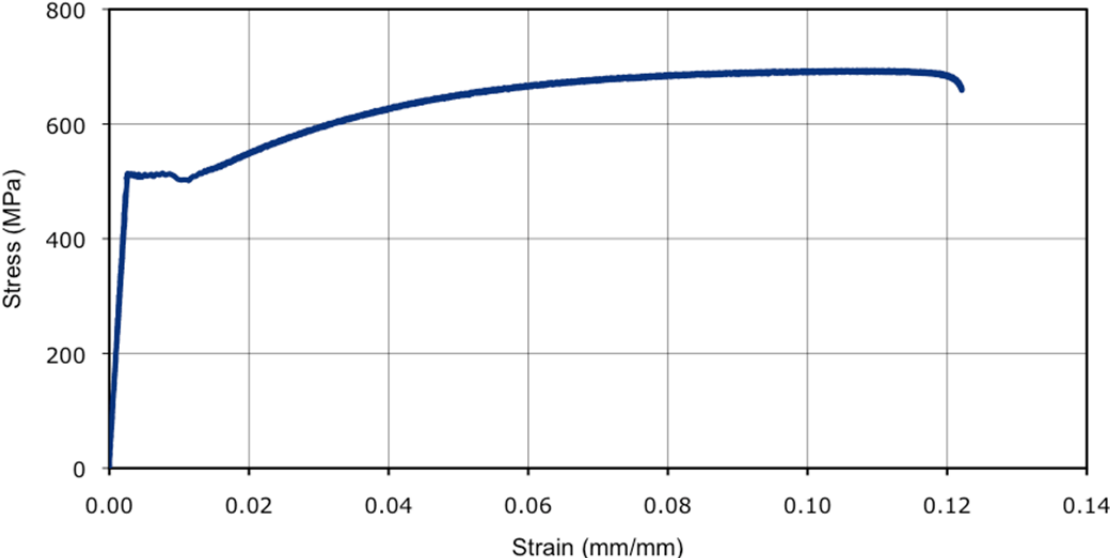


Figure 2.4 Typical column longitudinal reinforcement tensile stress-strain relationship.

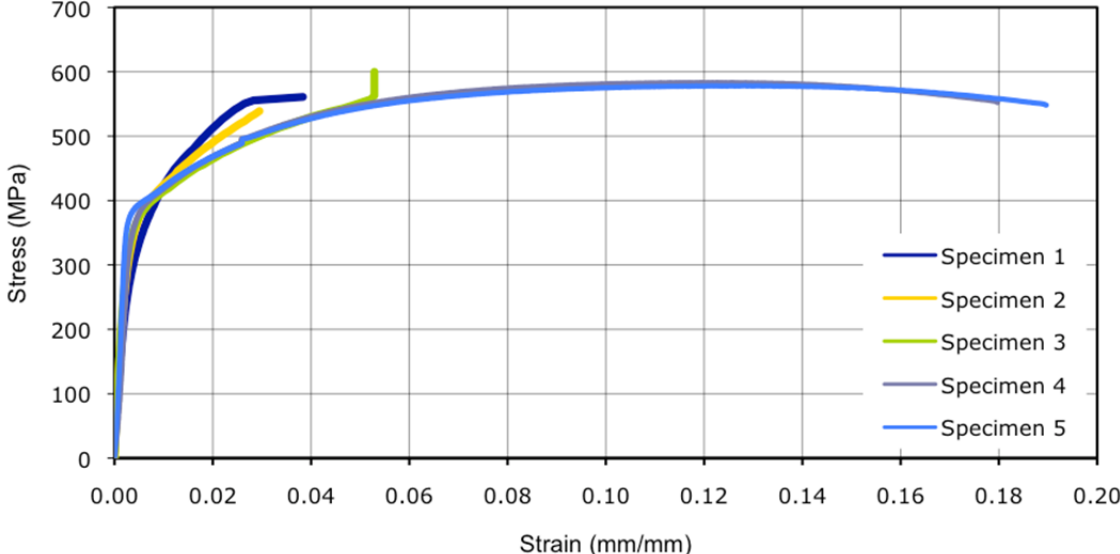


Figure 2.5 Column transverse hoop reinforcement tensile stress-strain relationship.

2.3 LOADING PROTOCOL

Input excitation consisted of a single horizontal component produced by the 7.6-m- (25-ft-) wide and 12.2-m- (40-ft-) long uni-axial shake table. The table has a velocity capacity of ± 1.8 m/sec (± 71 in/sec), a bare table peak acceleration of 4.2g, and a bare table overturning moment capacity of 35 MN-m (25,800 kip-ft) [NEES 2010].

The test protocol called for six earthquake simulation tests at targeted displacement ductilities of 1, 2, 4, 2, 8, and 4. An idealized yield displacement was computed analytically as 87 mm (3.41 in.), which corresponds to a drift ratio of 1.2%. Four historical earthquake recordings were selected as shake table input motions corresponding to the displacement ductility of 1, 2, 4, and 8. For the seismic hazard, a hypothetical site of San Francisco, California, was selected. For this site, earthquake recordings from a strike-slip fault mechanism were given preference. Three input motions were selected from the 1989 Loma Prieta earthquake. The fourth record selected was the Takatori station from the 1995 Kobe earthquake. These records are identified in Table 2.2.

Each of the recordings was obtained from PEER's strong-motion database [PEER 2007]. The targeted displacement ductility, station, scale factor, and recorded peak ground acceleration (PGA) obtained the table feedback are identified with the test names in Table 2.3. Before the first earthquake simulation, two, 5-minute-long, white noise table motions were conducted. These white noise table motions had 0.03g root mean square amplitude; the first was conducted as a quality control check on the instrumentation. The same input motion was repeated before earthquake testing commenced and repeated between subsequent earthquake simulations; this protocol was implemented to observe the period shift caused by damage accumulation.

With structural integrity intact after the planned loading protocol, the test sequence was expanded and an additional four tests were conducted. These tests used the Takatori ground motion from the Kobe earthquake. Results from the extended testing are not presented as the scope of the blind prediction competition was limited to the first six tests.

Table 2.2 Ground motion selection.

Test	Earthquake	Date	Moment magnitude	Station	Component
EQ1	Loma Prieta	10/18/1989	6.9	Agnew State Hospital	090
EQ2	Loma Prieta	10/18/1989	6.9	Corralitos	090
EQ3	Loma Prieta	10/18/1989	6.9	LGPC	000
EQ4	Loma Prieta	10/18/1989	6.9	Corralitos	090
EQ5	Kobe	01/16/1995	6.9	Takatori	000
EQ6	Loma Prieta	10/18/1989	6.9	LGPC	000

Table 2.3 Ground motion scale factors and peak ground parameters.

Test	Target displacement ductility	Earthquake	Station	Scale factor	Shaking table PGA (g)	Shaking table PGV (m/sec)
EQ1	1.0	Loma Prieta	Agnew State Hospital	1.0	-0.196	0.16
EQ2	2.0	Loma Prieta	Corralitos	1.0	0.411	0.37
EQ3	4.0	Loma Prieta	LGPC	1.0	0.515	0.89
EQ4	2.0	Loma Prieta	Corralitos	1.0	0.445	0.39
EQ5	8.0	Kobe	Takatori	-0.8	-0.540	0.95
EQ6	4.0	Loma Prieta	LGPC	1.0	-0.496	0.87

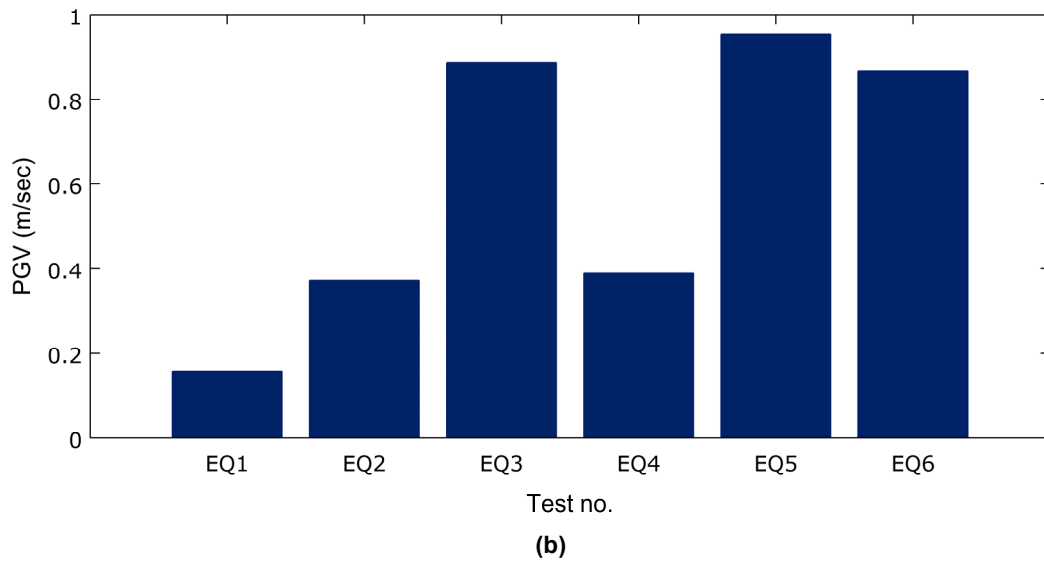
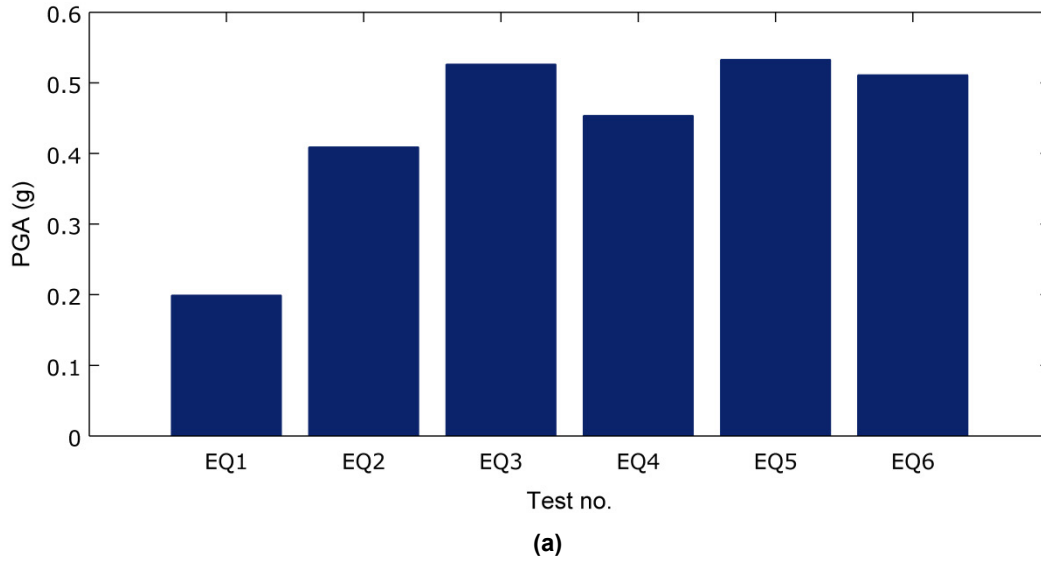


Figure 2.6 (a) Peak ground acceleration and (b) peak ground velocity replicated by the shake table.

3 Test Results

3.1 DIGITAL DATA PROCESSING PROCEDURES

Experimental results can be found in a companion report by Schoettler et al. [2015]; results relevant to the blind prediction competition are discussed below. Experimental measurements were filtered to present data within the range of frequencies capable of being produced by the shake table. Spurious recordings outside the useable frequency range of the shake table were filtered out. Acceleration data was band-pass filtered using an order 5000 FIR filter. The cut-off frequencies were 0.25 and 25 Hz. To retain the residual measurements from linear voltage displacement transducers and string potentiometers, the data from these instruments were low-pass filtered, with a cut-off frequency of 25 Hz and an order 5000 FIR filter.

Column top displacement was measured with string potentiometers mounted horizontally between the superstructure mass and the arched safety restraint towers. String potentiometers were located at an elevation consistent with the top of the column and not at the top of the superstructure mass. The horizontal displacement was computed as the average of measurements from string potentiometers on the north and south sides of the column, which was the relative displacement between the top of the column and the shake table. It does not include the dynamic response of the towers, which were assumed to be rigid. No corrections were made in this horizontal displacement to account for the towers' responses. A positive column displacement was considered to the east.

Mems accelerometers were installed in pairs on opposite sides of the test specimen for redundancy. The average recording of this pair was utilized as the acceleration at the accelerometers' elevation. Horizontal accelerations for the top of the column relied on accelerometers located at the appropriate elevation on the north and south faces of the superstructure block because it restricted access to the column's top.

Column shear forces were obtained from the inertial forces computed from measured accelerations and the tributary mass associated with the accelerometer pair. The tributary mass for the superstructure block included its estimated mass and one-half of the column's mass that was recessed in the superstructure block. Tributary mass for column accelerometers accounted for the one half of the column length between adjacent accelerometer pairs and the estimated column mass per unit length. The selected sign convention generated a positive shear force consistent with a column displacement to the east.

The bending moment anywhere along the column height was computed as the contribution of three components: (1) inertia forces generated in the superstructure mass and

column; (2) mass moment of inertia of the superstructure mass; and (3) P- Δ moment generated by the superstructure mass and laterally displaced column. The selected sign convention generated positive moments when the column was displaced to the east, which was considered a positive displacement. The moment generated by inertial forces relied on the inertial force and the average measured elevation of the accelerometer pair above the top of the footing. The mass moment of inertia was computed with the specified block geometry, accounting for blockouts and the estimated weight and the block's rotational acceleration. The rotational acceleration was obtained by calculating the average of three accelerometer pairs mounted either vertically or horizontally on the superstructure block, and the distance between the accelerometer pair. The P- Δ moment was computed with the estimated self-weight of the superstructure block and the column and horizontal displacements recorded by string potentiometers. This did not include variations in axial load due to changes in vertical inertial force.

Average column section curvature was calculated near the column base. The curvature was smeared over a 406 mm (16 in.) (1/3 column diameter) gage length from 51 mm (2 in.) to 457 mm (18 in.) above the footing. Measurements from linear voltage displacement transducers (LVDTs) located at the four corners of the column were normalized by the initial gage length to obtain average strain within this gage length. The horizontal distance between the vertical LVDTs on North side of the column was used to calculate curvature from the strain measurements. The same calculation was performed for the south side of the column, using the horizontal distance between these LVDTs; the mean value of these two was retained.

Average axial strain was smeared over the same one-third column diameter gage length used to compute the curvature. This quantity was computed as the mean axial strain computed from LVDTs on the north and south faces of the column. It was computed as the axial strain at the centroid of the column, and accounted for the location of the vertical LVDTs, which were used to find the strain at the centroid.

The column axial force was calculated from contributions of the superstructure mass and column. Vertical accelerometers were mounted on the east and west faces of the column, and on the top of the superstructure mass coinciding with the column centroid. Vertical accelerations, including gravitational acceleration, were multiplied by a tributary weight. Column vertical accelerations accounted for the pair of vertical accelerometers, while the single accelerometer on the superstructure mass was used with its entire weight.

3.2 TEST EQ1

The peak drift ratio measured in the column during test EQ1 was 0.85%; the residual drift ratio was 0.01%. There was no observable damage in the column post-test. Hairline cracks, defined here as less than 0.1 mm (0.004-in.), were found at the column-to-footing interface. No other cracks were observed post-test in the test specimen. Figure 3.1(a) shows a post-test view of the east face of the column base.

The peak column base moment was 3930 kN-m (2900 kip-ft). The moment-curvature response is shown in Figure 3.2(a). The peak shear force was 500 kN (112 kip). The lateral shear force and displacement response is shown in Figure 3.3(a).

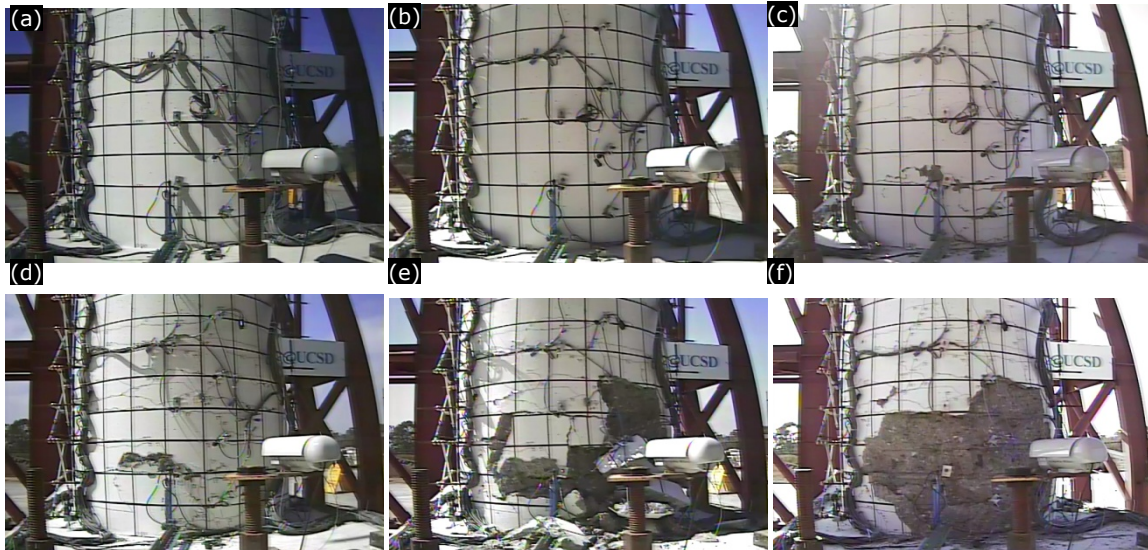


Figure 3.1 East face of the column base after (a) EQ1, (b) EQ2, (c) EQ3, (d) EQ4, (e) EQ5, and (f) EQ6.

3.3 TEST EQ2

This earthquake simulation produced a peak drift ratio of 1.82% at the top of the column; the residual drift ratio was 0.05%. A post-test view of the east face of the column base is shown in Figure 3.1(b). Because the video snapshot was taken before the cracks were marked, cracks are not visible in this figure.

Although this test initiated a nonlinear response of the column, plastic deformations were small; see the moment-curvature relationship shown in Figure 3.2(b). The peak column base moment was 5865 kN-m (4325 kip-ft), and peak shear force was 698 kN (157 kip). The lateral shear force and displacement response is shown in Figure 3.3(b); note the influence of the second mode of vibration due to the superstructure's rotational mass moment of inertia.

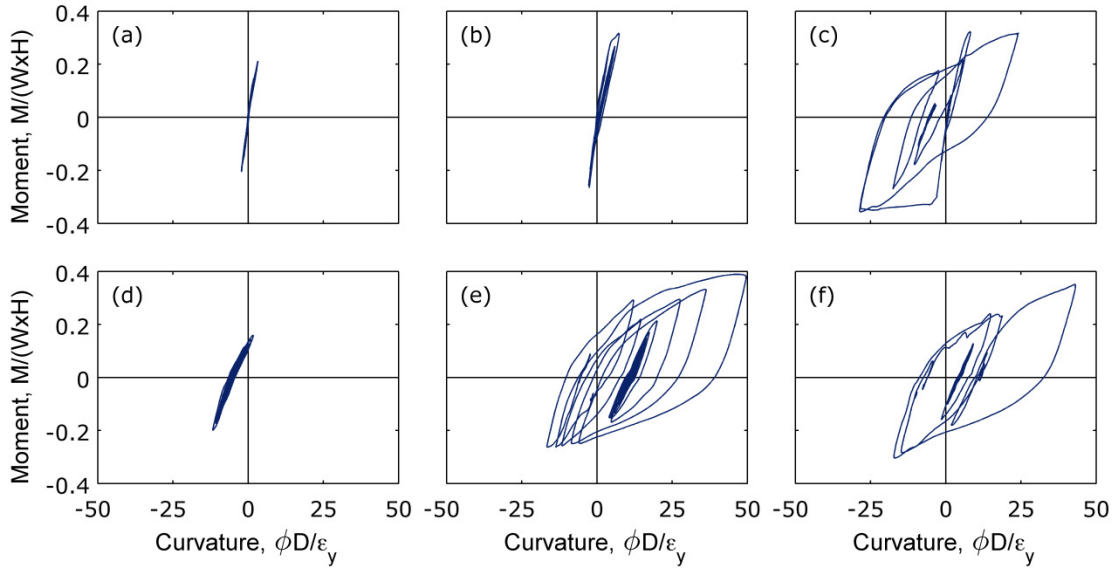


Figure 3.2 Normalized base moment-curvature response for (a) EQ1, (b) EQ2, (c) EQ3, (d) EQ4, (e) EQ5, and (f) EQ6.

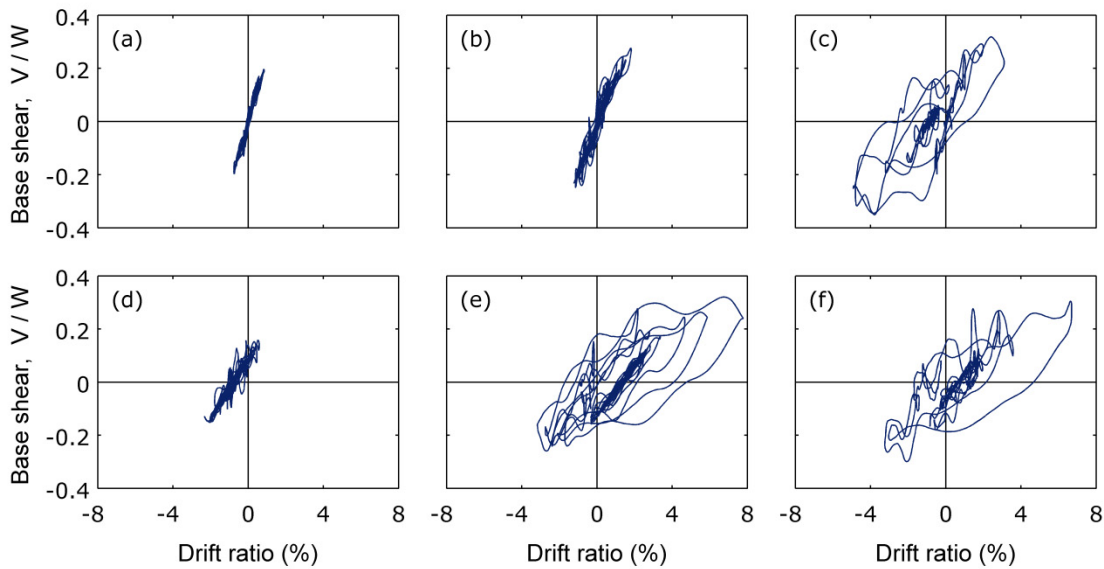


Figure 3.3 Normalized base shear-drift response for (a) EQ1, (b) EQ2, (c) EQ3, (d) EQ4, (e) EQ5, and (f) EQ6.

3.4 TEST EQ3

The peak drift ratio measured in the column after Test EQ3 was 4.93%, with a residual drift ratio of -0.87%, signaling nonlinear response. Spalling of the concrete cover was initiated at this level of testing and significant cracking developed; see Figure 3.1(c). Although this photograph was taken before cracks had been marked, the crack pattern and concrete flaking are visible.

As shown in Figure 3.2(c), significant nonlinearity occurred, which is reflected in the moment-curvature response. The peak column base moment was 6600 kN-m (4870 kip-ft). The peak shear force was 877 kN (200 kip). This was the largest shear force obtained in any of the tests. The lateral shear force and displacement response is shown in Figure 3.3(c), which shows clearly the contribution of the second mode.

3.5 TEST EQ4

Test EQ4 simulated an aftershock from EQ3, and the column achieved a peak drift ratio of 2.33%. A residual drift of -0.81% remained post-test. Regions that experienced spalling caused by Test EQ3 enlarged, but damage was less significant than that induced by EQ3. Figure 3.1(d) shows a post-test view of the east face of the column base.

As shown in Figure 3.2(d), a nearly linear response was obtained in terms of moment curvature. The peak column base moment was 3700 kN-m (2730 kip-ft). The peak shear force was 400 kN (90 kip). The lateral shear force and displacement response is shown in Figure 3.3(d), which shows clearly the contribution of the second mode of vibration.

3.6 TEST EQ5

When subjected to Test EQ5, the column achieved a peak drift ratio of 7.78%. This was the largest displacement measured in the loading protocol. The residual drift ratio was 1.43%. Continued concrete spalling occurred and extended to 1.07 m (3.5 ft) above the column base. Figure 3.1(e) shows a post-test view of the east face of the column base where concrete spalling is evident to a height of 0.76 m (2.5 ft).

The peak column base moment was 7220 kN-m (5320 kip-ft); see Figure 3.2(e) for the moment-curvature response. This was the largest moment demand obtained in the loading protocol. The peak shear force was 813 kN (183 kip). The lateral shear force and displacement response is shown in Figure 3.3(e), where undulations in the shear force from the second mode of vibration were generated by the superstructure mass's rotational mass moment of inertia.

3.7 TEST EQ6

A repeat of Test EQ3 resulted in the column exhibiting a peak drift ratio of 6.69%. A residual drift ratio of 0.68% remained post-test. Figure 3.1(f) shows a post-test view of the east face of the column base. Although concrete spalling is visible, it did not extend beyond the damage caused by Test EQ5.

The peak column base moment was 6510 kN-m (4800 kip-ft). Stable hysteretic loops are present in the moment-curvature response of Figure 3.2(f). The peak shear force was 766 kN (172 kip). The lateral shear force and displacement response is shown in Figure 3.3(f), where undulations in the shear force from the second mode of vibration were generated by the superstructure mass's rotational mass moment of inertia.

3.8 SUMMARY

Acceleration time histories for Tests EQ1 through EQ6 are shown in Figure 3.4. These accelerations represent the mean value recorded by four horizontal accelerometers located on the corners of the shake table. To facilitate comparison, the time histories have been trimmed to be 65 sec in duration. Accelerations recorded on the superstructure at its center-of-mass, coinciding with the top of the column, are shown in Figure 3.5. A comparison of these two figures demonstrates that the magnitude of peak acceleration in Test EQ1 is similar, while the ground acceleration is larger than that recorded at the top of the column in subsequent tests. This is consistent with nonlinear response. Period elongation is evident in Figure 3.5 during successive tests.

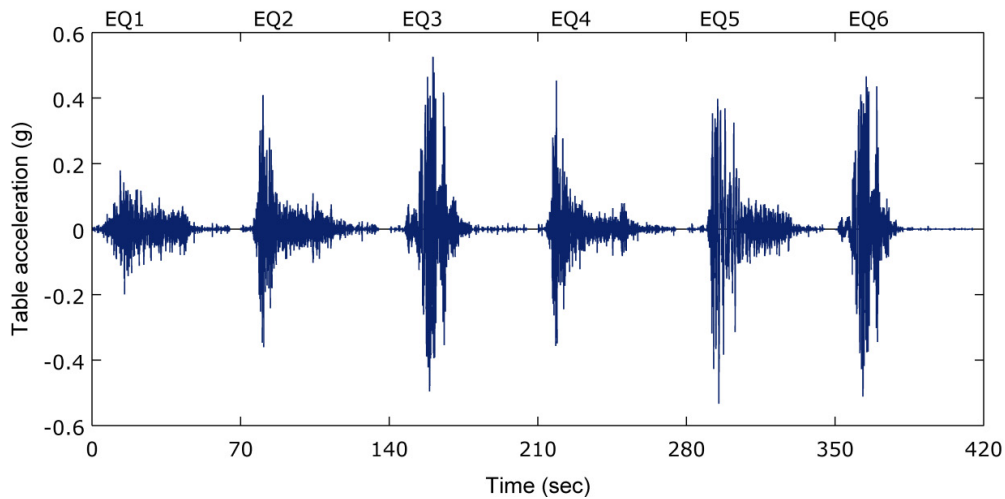


Figure 3.4 Input acceleration time histories.

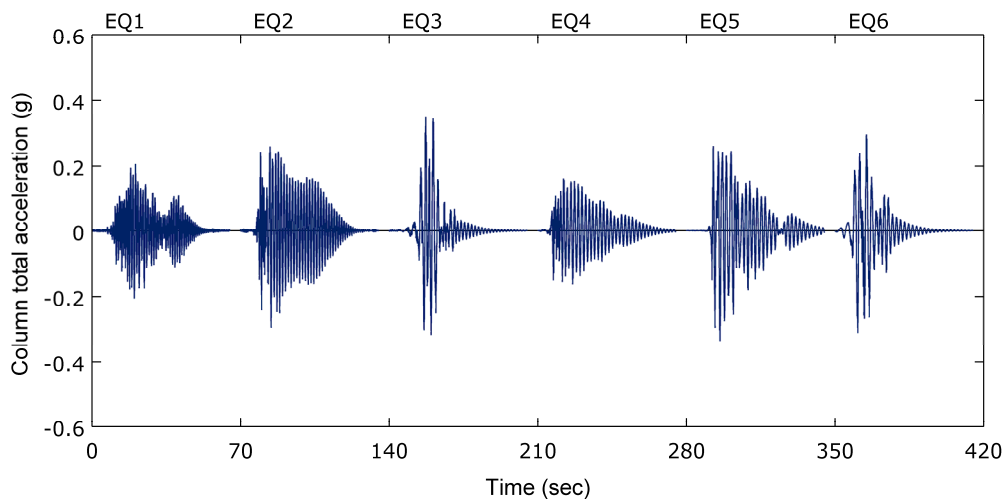


Figure 3.5 Acceleration time histories of the column top.

The drift time history of Figure 3.6 illustrates the initial displacement conditions of the tests. Residual displacement from a prior test was not corrected, and the column was tested without repair. The strategic decision to invert the polarity of the scaled Takatori ground motion in Test EQ5 prevented ratcheting of the column to one side. Peak drift ratios obtained in each test are summarized in Figure 3.7. A summary of the peak response quantities is provided in Table 3.1. These quantities were required in the blind prediction competition.

Test EQ6 concluded the loading protocol. At this stage of testing, damage was limited to concrete spalling within the plastic hinge. This provided the opportunity to extend the scope of testing, but results are not presented here.

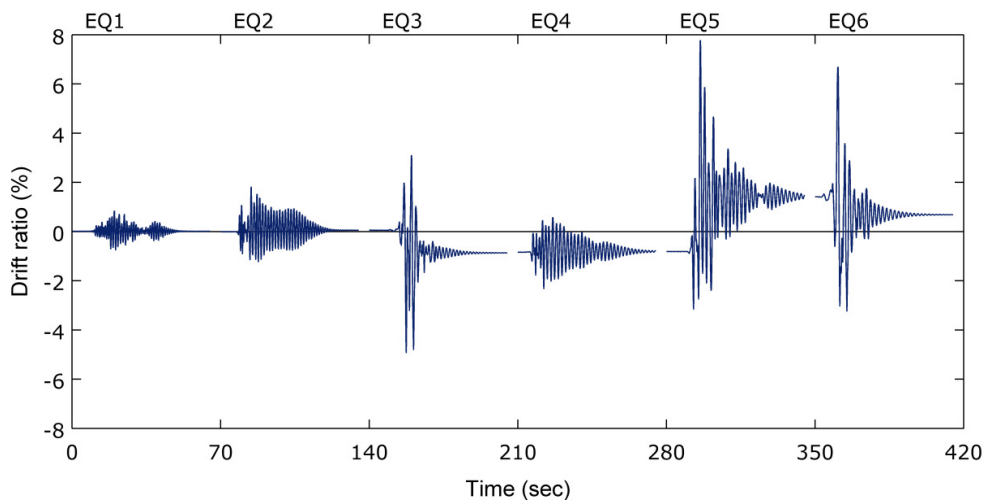


Figure 3.6 Drift ratio time histories.

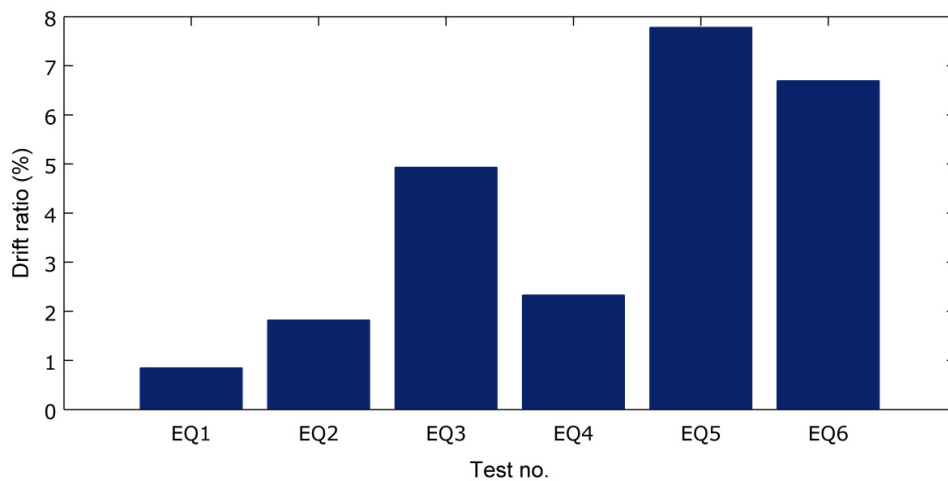


Figure 3.7 Peak drift ratios achieved.

Table 3.1 Peak response quantities.

Test	EQ1	EQ2	EQ3	EQ4	EQ5	EQ6
Horizontal displacement (mm)	62	133	361	170	569	490
Total acceleration (g)	0.207	0.295	0.348	0.163	0.335	0.310
Bending moment (kN-m)	3934	5866	6598	3698	7215	6506
Shear force (kN)	500	68	887	399	813	766
Average curvature (rad/km)	0.526	0.453	17	7.5	58	55
Average axial strain ($\times 10^6$)	543	906	2513	1712	17,817	16
Residual displacement (mm)	0.9	4.0	63	59	104	50
Compressive axial force (kN)	2605	2770	2816	2743	2779	2786

4 Blind Prediction Contest

4.1 CONTEST DESCRIPTION

The Concrete Column Blind Prediction Contest was conducted to identify the uncertainty in predicting important response quantities of a full-scale RC bridge column subjected to six consecutive unidirectional ground motions. Each contestant/team had to predict the maximum response for global, intermediate, and local response quantities for six earthquakes. The contest was advertised nationally and internationally among professional engineers and researchers. Predictions were submitted by forty-one teams from fourteen different countries: Australia, Canada, China, Colombia, Ecuador, Italy, Japan, New Zealand, Switzerland, Peru, Portugal, Puerto Rico, Taiwan, and the U.S. Although the contestants held either M.S. or PhD degrees, it was not a prerequisite. Two entry categories were formed based on the affiliation of the contestant/team. The contestants/teams that belonged to academic or research groups were designated as “Researchers,” and contestants/teams that belonged to structural engineering group were designated as “Professional Engineers.” A winner was chosen from each group.

4.2 RULES OF THE CONTEST

The rules of the contest were adopted from a Seven-Story Building-Slice Earthquake Blind Prediction Contest (2006) and were as follows:

1. A contest submittal can be from an individual or a team.
2. An individual can only be on one team.
3. If an individual is part of a team, the individual cannot submit separately as an individual.
4. The individual or team must use the contest Submittal Spreadsheet and input values as follows:
 - a. Relative horizontal displacements are to be provided with respect to the base of the footing ($y = 0.0$ mm) and are to be provided in millimeter units to one (1) place beyond the decimal point.
 - b. Accelerations will be obtained experimentally from accelerometers deployed at different locations in the test specimen. Accelerations are to be provided in units of g to three (3) places beyond the decimal point.

- c. Bending moments are to be provided in units of kN-m to one (1) place beyond the decimal point.
 - d. Shear forces are to be provided in units of kN to one (1) place beyond the decimal point.
 - e. Curvatures are to be provided in units of rad/km ($\text{rad/mm} \times 10^6$) to three (3) places beyond the decimal point.
 - f. Axial strains are to be provided in units of micro-strain as an integer.
 - g. Axial forces are to be provided in units of kN to one (1) place beyond the decimal point.
 - h. All values shall be input on the spreadsheet as positive values. The word “Maximum” written with the upper case letter “M” shall mean the largest of the absolute values of the maximum positive or maximum negative value under consideration. The word “maximum” written with the lowercase letter “m” shall mean the smallest of the absolute values of the maximum positive or maximum negative value under consideration.
 - i. Values shall be input for the six intensities of ground motion (EQ1, EQ2, EQ3, EQ4, EQ5, and EQ6).
5. The individual or team must declare one of the two categories on the Submittal Spreadsheet:
 - a. Researchers (including post docs and students)
 - b. Engineering Professional
 6. Structural drawings will be provided in U.S. customary units. However, data is requested in S.I. units. A translation from U.S. customary to S.I. units and vice versa can easily be done in the google.com prompt. For example, type in the google.com prompt:
 - a. 430000 pounds feet in kN m
 - b. 4 ft 3 inches in mm
 - c. 3500 psi in MPa
 7. The recorded data will be processed by band-pass filtering with a high-order (5000) FIR digital filter with a 0.25–25 Hz bandwidth. Forces will be determined from recorded accelerations and using an acceleration of gravity equal to 9.807 m/sec^2 , and the unit weight of the material. The unit weight for steel will be assumed equal to 77 kN/m^3 . The unit weight of concrete will be determined from tests and reported on September 1.
 8. The contest has two parts: pre-test and post-test. For the two parts of the contest the Submittal Spread Sheet (Figure 4.1) has to be filled in the following way:

- a. Pre-test phase of the contest requires filling general information (4 cyan fields) and response to question 9 (mode of failure).
 - b. Post-test phase of the contest requires filling general information (4 cyan fields) and response to first 8 questions (69 answers are expected).
9. The post-test analysis shall be performed using measured excitations, measured concrete strength on the day of the test, and measured steel strength. All necessary measurements will be provided no later than September 22.
10. Due dates for submitting results of pre-test and post-test analysis are September 7 and September 28, respectively. Winners in each category will be notified on September 30.
11. The following system will be used to judge the category winners. Error is defined as the absolute value of the measured parameter minus the value predicted by the contestant.
 - a. The team with minimum error in a question will receive 8 points
 - b. The second team will receive 5 points
 - c. The third team will receive 3 points
 - d. The fourth team will receive 1 point
 - e. All contestants that correctly predict failure mode (question 9) will get 8 points. All points will be added up and the team with the greatest total will be declared winner of its category. There will be one winner for each of the two categories. Winners will be awarded at the Quake Summit 2010.
12. A representative of the category winners will be invited to the Quake Summit 2010 that will be held in San Francisco, October 8-9. The representative will be asked to make a presentation on the techniques used (model and analysis) in making their winning predictions.
13. Except for category winners, all submittals will be kept anonymous.
14. Questions about the blind prediction contest or details of the structure or ground can be submitted to the Contest Organizing Committee. Questions and answers will be posted on the site's FAQ page.
15. Teams from UCSD are not allowed to participate.

Name of the firm representative:
Entry Category (Researcher or Practicing Engineer):
Computer platform used:
Type of element used to model the column:

NOTE: Values should be reported in absolute terms
NOTE: y=0.0 is at the platen surface

	Predicted Quantity					
	EQ1	EQ2	EQ3	EQ4	EQ5	EQ6
1 Relative horizontal displacement (mm) at level 6: y=8.534-m: Maximum maximum						
2 Total horizontal acceleration (g) at level 6: y=8.534-m: Maximum maximum						
3 Bending moment (kN-m) at level 0: y=1.219-m: Maximum maximum						
4 Shear force (kN) at level 0: y=1.219-m: Maximum maximum						
5 Average curvature (rad/km) between y = 1.270 and 1.473 m Maximum						
6 Average axial strain ($\times 10^5$) between y = 1.270 and 1.473 m Maximum						
7 Relative residual displacement (mm) at level 6: y=8.534-m:						
8 Largest column compressive axial force (kN) at level 0: y=1.219-m:						
9 Mode of failure (type corresponding number): Specify if "Other":						

- 1: None
- 2: Column shear failure
- 3: Column longitudinal bar anchorage failure
- 4: Column hoop fracture
- 5: Column longitudinal bar fracture
- 6: Other

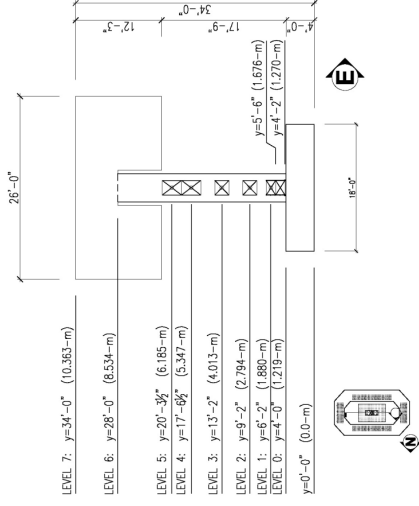


Figure 4.1 Contest submittal spreadsheet.

4.3 RULES FOR SCORING CONTESTANTS

The absolute error (AbsE) method was used for scoring the contestants. The absolute error of predicted to measured quantity was calculated for all 69 entries. For each predicted quantity, the four best predictions were awarded with 8, 5, 3, and 1 points (8 being for the best prediction). The prediction with the smallest absolute error from the measured response was considered the best prediction. The same weight was given to each response quantity. All contestants who correctly predicted the failure mode were awarded 8 additional points. These points were assumed to represent 5% of the winner's total points. All points were then totaled, and the team with the greatest total was declared winner of its category.

4.4 WINNERS OF CONTEST

A total of forty-one teams participated in PEER's Concrete Column Blind Prediction Contest 2010. Based on the contest rules, participants were classified into two categories: Professional Engineer and Researcher. A total of 17 teams were registered as "Professional Engineer" and 24 teams were registered as "Researcher." Based on a comparison of the submitted response predictions and measured response quantities, overall winners were identified in the two categories.

For the Professional Engineer category, Bill Tremayne and Lawrence Burkett tied for first place.

- Lawrence Burkett, of Rutherford Chekene, San Francisco, California, U.S., used the program SeismoStruct in conjunction with force-based fiber elements for his winning entry.
- Bill Tremayne, of Holmes Culley Structural Engineers, San Francisco, California, U.S., used the program ANSR-II for his predictions. The column was modeled using 3D beam-column elements with distributed plastic hinges that exhibit degrading strength and stiffness.

For the Research category, the entry from Dr. Zhe Qu was identified as the first-place winner.

- Dr. Zhe Qu, of the Tokyo Institute of Technology, Yokohama, Japan, used the program ABAQUS with two-node linear beam elements having end fiber sections employing special user-defined steel and concrete material property models.

In recognition of the many excellent submissions, the judges identified six other entries that were recognized for their excellence in being able to predict the broad array of response parameters required of the contestants. These Award of Excellence winners are listed alphabetically in Table 4.1. Each predicted some parameters better than others, but all achieved a superior level of fidelity.

A total of 12 different analysis software programs were used to numerically model and analyze the bridge column (see Figure 4.2). The largest number of contestants 15 (36%) used

OpenSees. SeismoStruct and SAP2000 were each used by five contestants (12%), ANSR-II and CANNY were each used by three contestants (7%), ABAQUS and PERFORM 3D were each used by two contestants (5%), and ANSYS, PISA 3D, MSC. MARK, Engineering Studio and NARCF were each used by one contestant (2.5%). Among the overall winners and the Award of Excellence recipients, three used SeismoStruct, two used OpenSees, two used ANSR-II, one used SAP2000, and one used ABAQUS (Figure 4.3).

Table 4.1 Award of Excellence winners.

Name	Category	Organization	Software	Element type
Eric Kelley and team	Engineering Professional	Parsons Brinckerhoff, Inc, Seattle, WA, United States	SAP2000	Displacement-based beam-column element with fiber sections
Otton Lara and team	Researcher	Escuela Superior Politécnica del Litoral, Guayaquil, Ecuador	OpenSees	Force-based beam-column element with fiber sections
Bruce Maison	Engineering Professional	Consulting Engineer, El Cerrito, CA, United States	ANSR-II	Beam with concentrated fiber-based hinges
Rui Pinho and team	Researcher	EUCENTRE, Pavia, Italy	SeismoStruct	Displacement-based beam-column element with fiber sections
Nelson Vila-Pouca and team	Researcher	Faculty of Engineering of University of Porto, Portugal	SeismoStruct	Force-based beam-column element with fiber sections
Andreas Schellenberg	Engineering Professional	Rutherford & Chekene, San Francisco, CA, United States	OpenSees	Force-based beam-column element with fiber sections

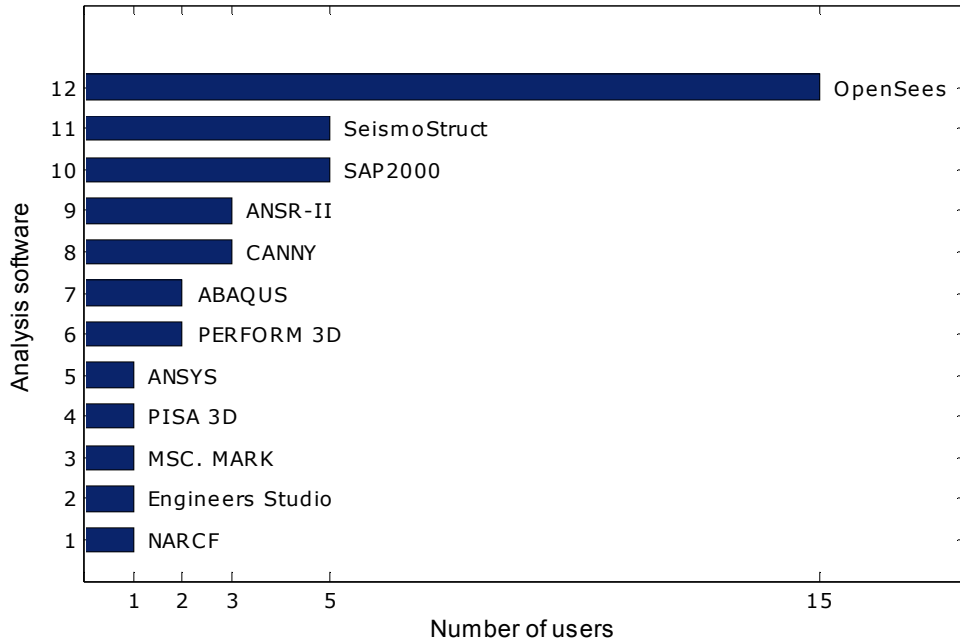


Figure 4.2 Analysis software used for analytical predictions.

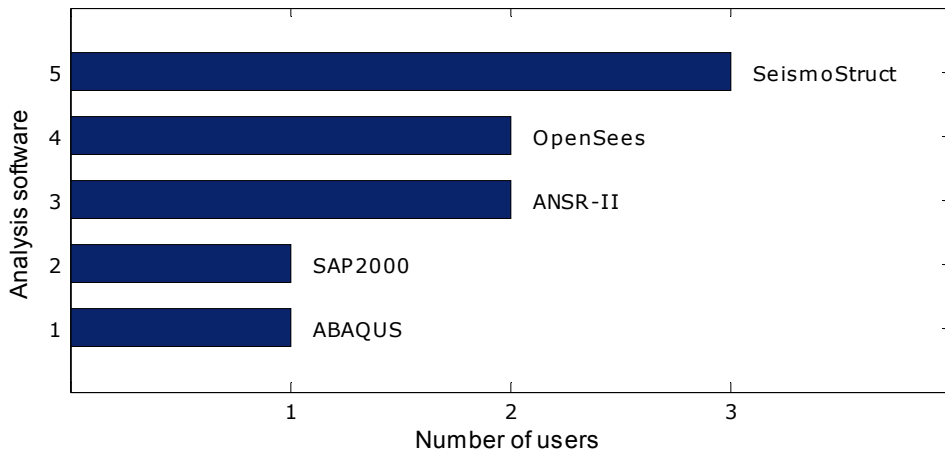


Figure 4.3 Analysis software used by winning contestants and Award of Excellence recipients.

Response predictions and measured (experimental) response quantities are shown in Figure 4.4 to Figure 4.15 for all predicted response quantities. The winners from the both categories are marked on plots. The winner from the Research category was designated as “Winner-R,” and the two winners from the Professional Engineer category were marked as “Winner-EP1” and “Winner-EP2”. Designation “Max” in the figures refers to the absolute maximum of the considered response. Designation “Min” refers to the peak in the other direction.

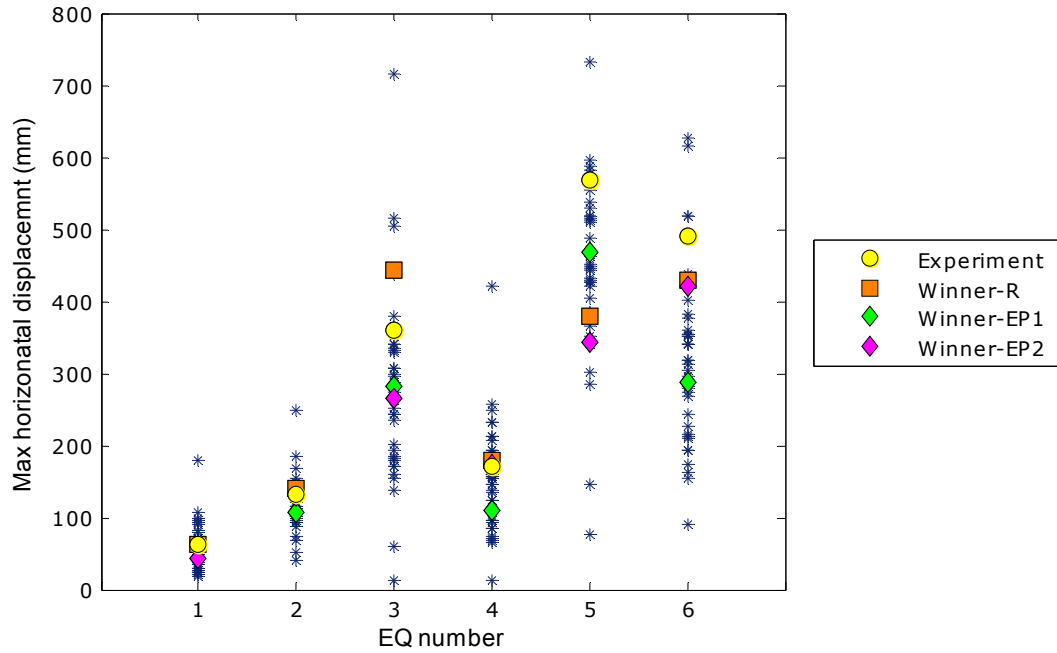


Figure 4.4 Predictions of “Max” displacement at the top of the column versus measured response.

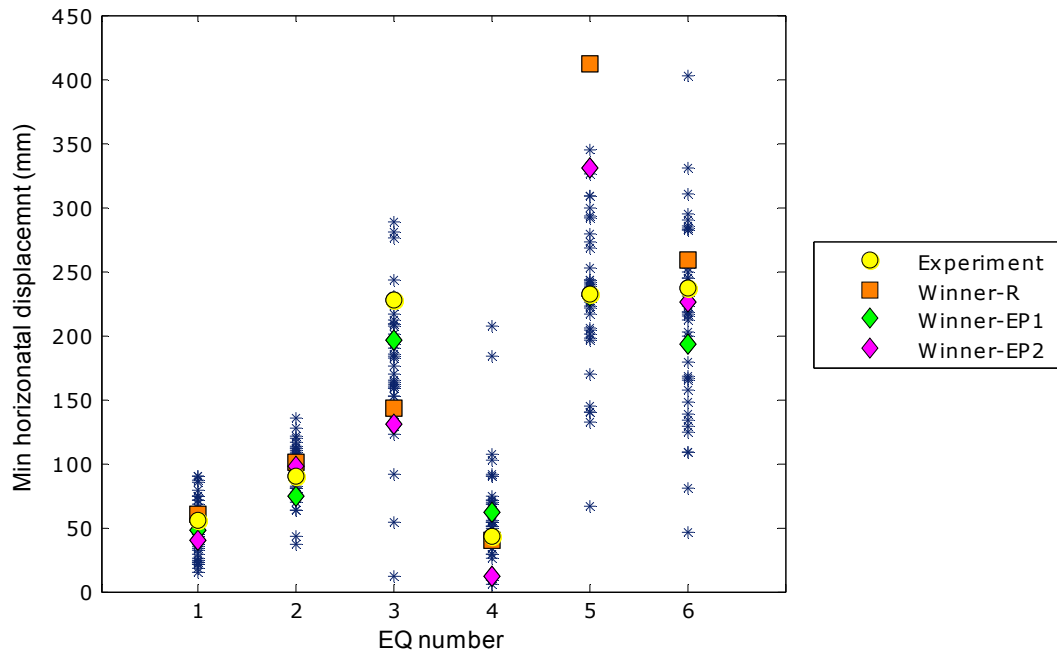


Figure 4.5 Predictions of “Min” displacement at the top of the column versus measured response.

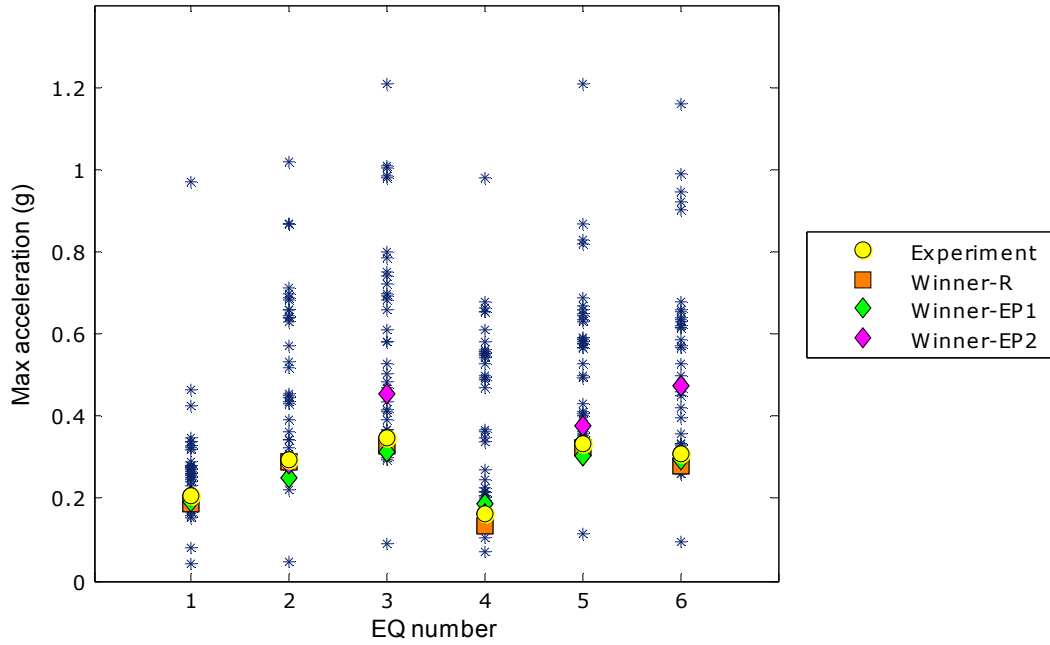


Figure 4.6 Predictions of “Max” acceleration at the top of the column versus measured response.

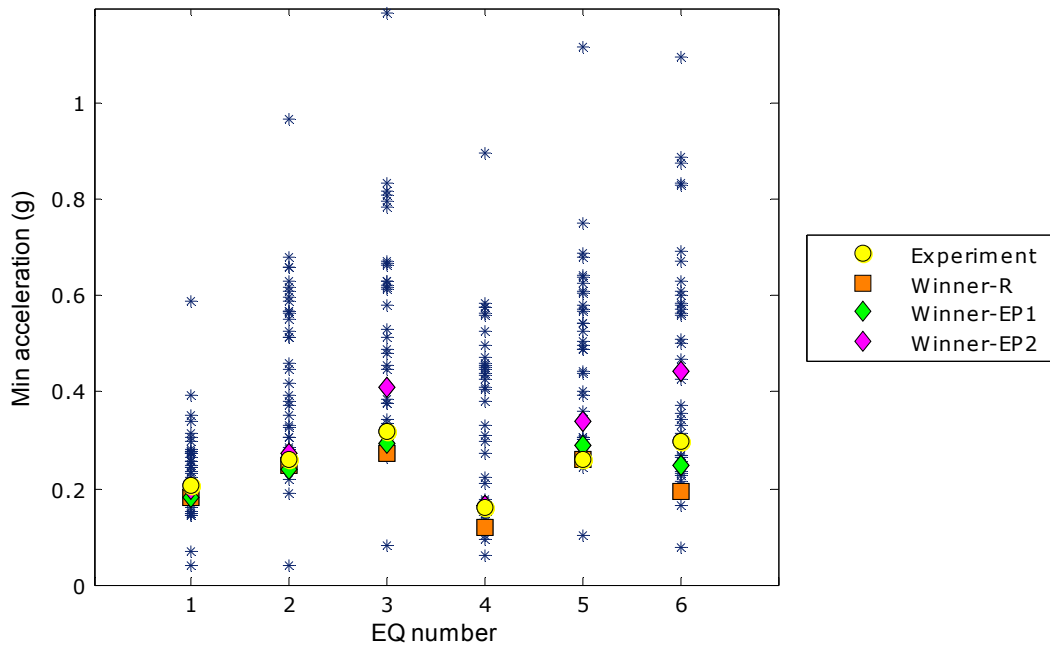


Figure 4.7 Predictions of “Min” acceleration at the top of the column versus measured response.

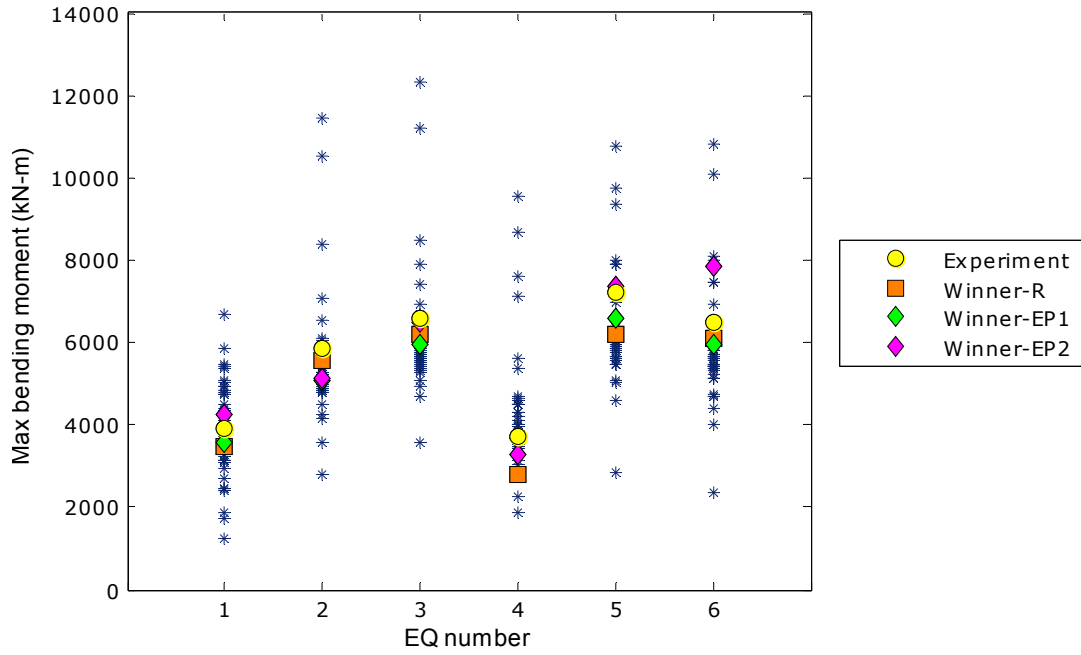


Figure 4.8 Predictions of “Max” bending moment at the base of the column versus measured response.

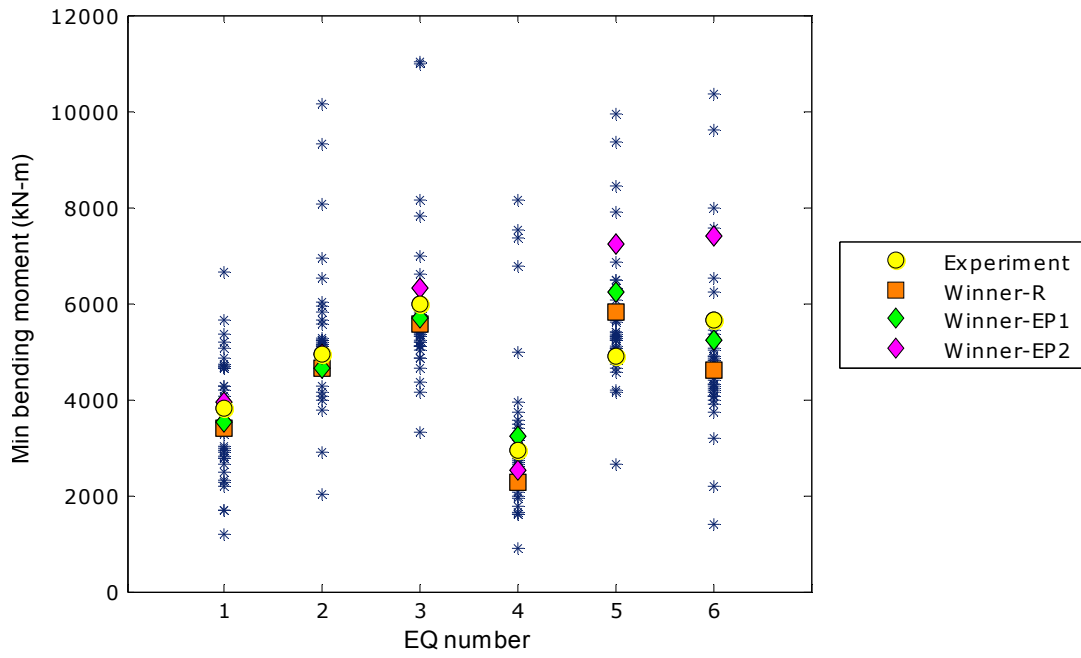


Figure 4.9 Predictions of “Min” bending moment at the base of the column versus measured response.

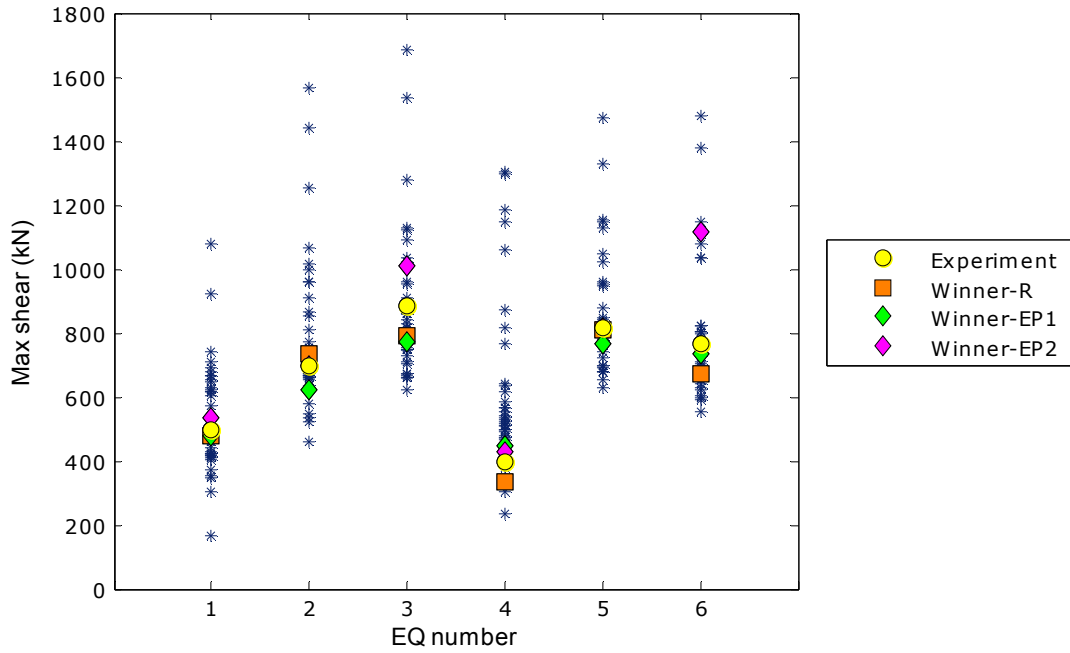


Figure 4.10 Predictions of “Max” shear force at the base of the column versus measured response.

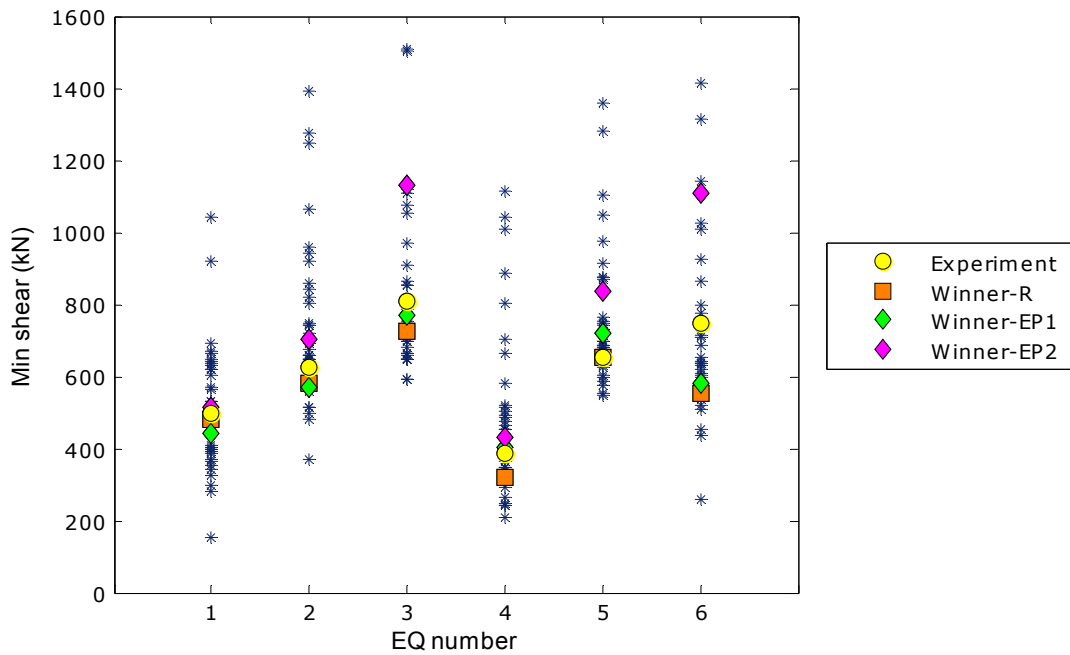


Figure 4.11 Predictions of “Min” shear force at the base of the column versus measured response.

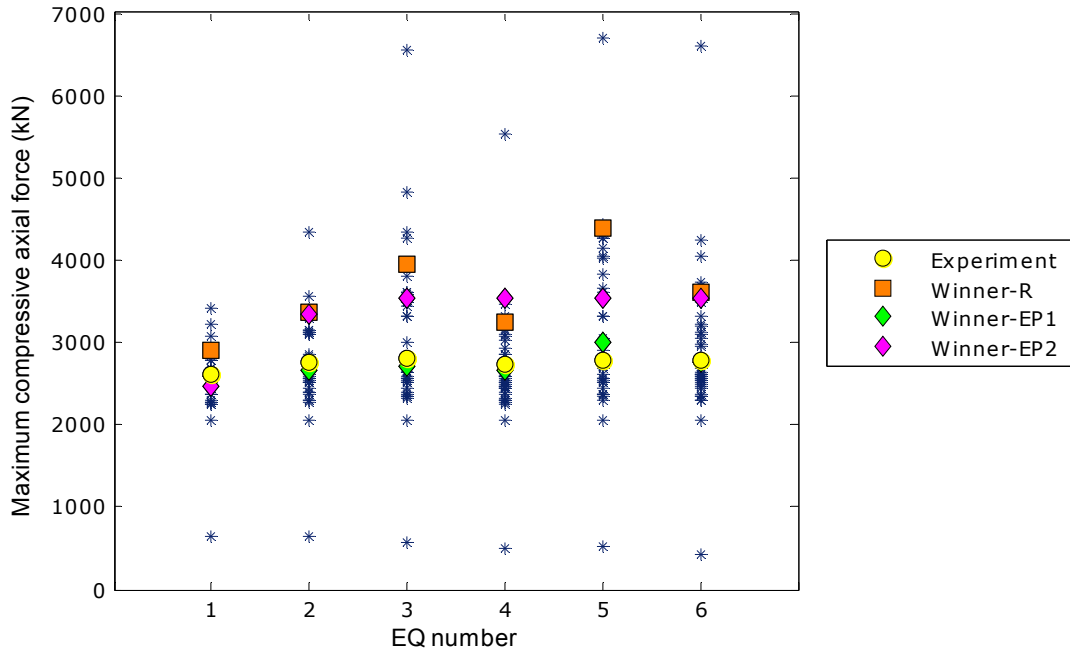


Figure 4.12 Predictions of maximum compressive axial force versus measured response.

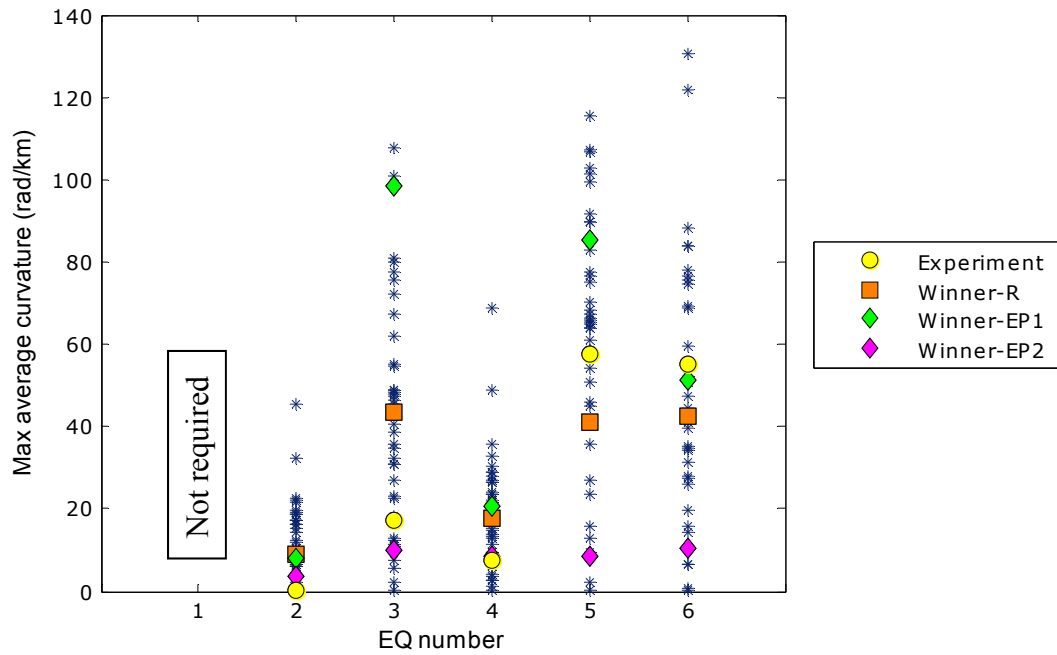


Figure 4.13 Predictions of “Max” average curvature between 51 and 254 mm from the bottom of the column versus measured response.

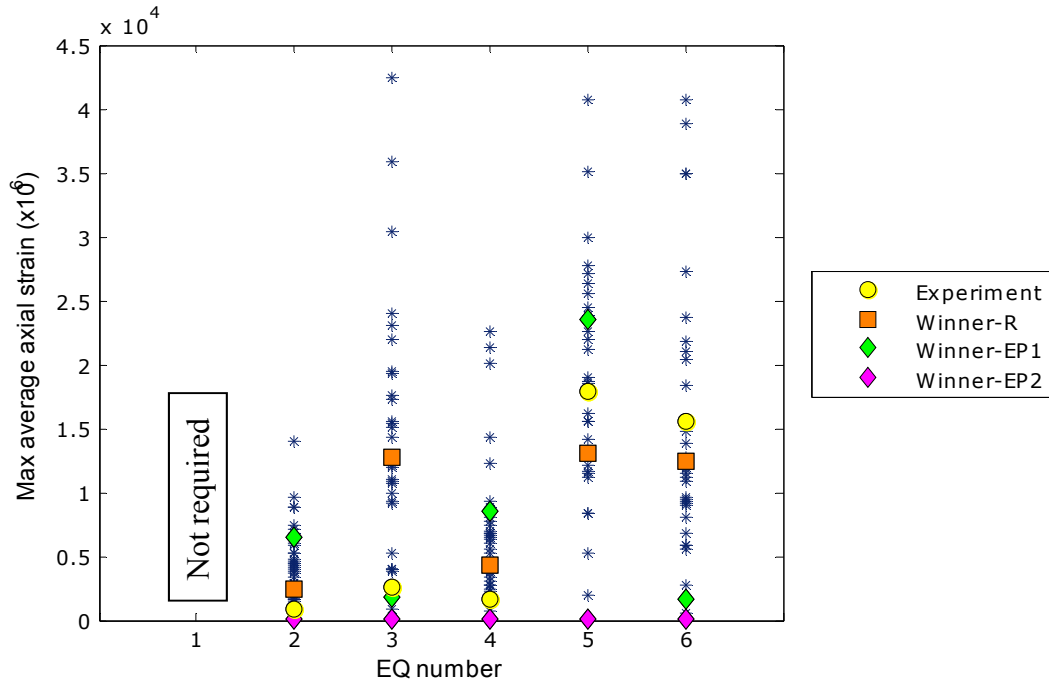


Figure 4.14 Predictions of “Max” average axial strain between 51 and 254 mm from the bottom of the column versus measured response.

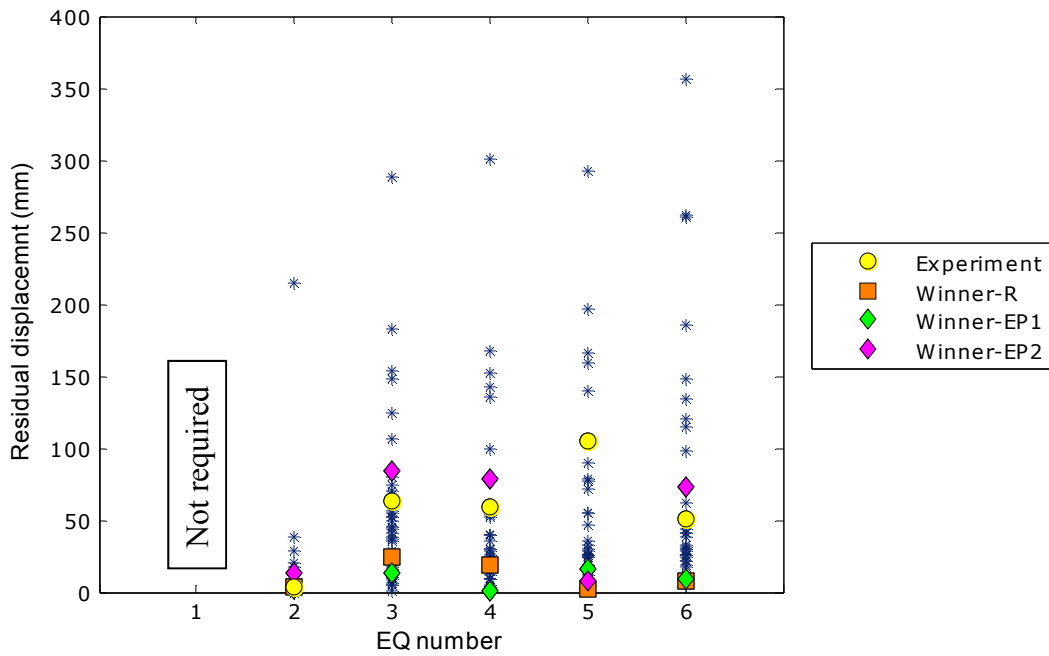


Figure 4.15 Predictions of residual displacement at the top of the column versus measured response.

4.5 PREDICTION OF FAILURE MODE

After being subjected to ground motion representing the six consecutive earthquakes, the column did not appear to fail. Out of forty-one contestants of the Concrete Column Blind Prediction Contest 2010, 14 contestants (33%) predicted that the column would not fail. Figure 4.16 shows number of predictions for each of the suggested failure modes. While the observed mode of failure had the highest frequency compared to the other modes of failure, the majority of contestants (67%) expected otherwise.

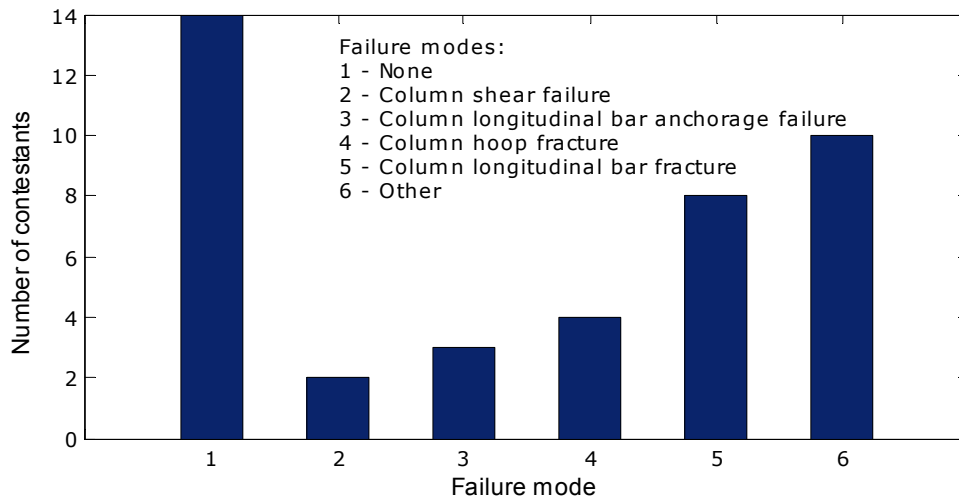


Figure 4.16 Number of predictions for each of the six suggested failure modes.

4.6 ALTERNATIVE METHODS FOR SCORING PREDICTIONS

Although the announced winners predicted with a good degree of accuracy most of the column responses, some predictions were greatly inaccurate. Therefore, three additional scoring methods were considered with the purpose of identifying a scoring scheme that recognized the best prediction. These are cumulative error (CE) method, average error (AvgE) method, and root-mean-square error (RMSE) method. To be consistent with the absolute error method, all three methods were assigned the same weight to all response quantities.

The cumulative error method is based on summation of errors in predicting each response quantity. The cumulative error for each contestant/team was calculated based on Equation (4.1),

$$CumErr = \sum_{i=1}^n abs \left[\frac{(R_a - R_{exp})}{R_{exp}} \right] \quad (4.1)$$

where n is the number of response quantities to be predicted, R_a is analytically predicted response, and R_{exp} is a measured response. The contestant/team with the smallest cumulative error was the winner. This method is not point-based but percentage-based, and thus did not

account for the correct prediction of a failure mode. However, this method identifies the analytical model that predicted all requested response quantities with greatest accuracy.

The average error method is based on calculating the average error of the predicted response quantity over a set of earthquakes and assigning 8, 5, 3, and 1 points to the four best predictions. The average error of a response quantity was calculated as follows:

$$AvgErr = \frac{1}{j} \sum_{i=1}^j abs \left[\left(R_a - R_{exp} \right) / R_{exp} \right] \quad (4.2)$$

where j is the number of earthquakes for one predicted response quantity. All contestants/teams that predicted the failure mode correctly were awarded 2 additional points. These points were assumed to represent 5% of the winner's total points. All points were then totaled, and the contestant/team with the greatest total was declared the winner.

The RMSE method is based on calculating the square-root of the sum of squares of a response quantity error over a set of earthquake, and assigning 8, 5, 3, and 1 points to the four best predictions. The RMS error of a response quantity was calculated as follows:

$$RMSErr = \sqrt{\sum_{i=1}^j \left(R_a - R_{exp} \right)^2} \quad (4.3)$$

where j is the number of earthquakes for predicted one response quantity. All contestants/teams that predicted the failure mode correctly were awarded additional 2 points. These points were assumed to represent 5% of the winner's total points. All points were then totaled, and the contestant/team with the greatest total was declared the winner.

4.7 WINNERS BASED ON ALTERNATIVE SCORING METHODS

The winners were judged based on absolute error (AbsE) method and the three alternative methods: cumulative error (CE), average error (AvgE), and root-mean-square error (RMSE), and are presented and compared in this section. For the purpose of this study, the maximum average curvature and the maximum average axial strain of the column were measured over a range extending from 51 mm (2 in.) to 457 mm (18 in.) from the bottom of the column. This distance corresponded to one-third the column diameter. The reasons for this choice of measuring length are described in Section 5.1.6.

The four different scoring methods identified two different winners of each category. The winners of the Research category are marked as R_1 and R_2 , and the winners of the Engineering Professional category are marked as EP_1 and EP_2 (Table 4.2). The AbsE method and CE method, which are based on scoring each prediction, identified the same winners for both categories (marked as R_1 and EP_1). The AvgE method and RMSE method, which are based on scoring a predicted response quantity over a set of earthquakes, identified the same winner for the Engineering Professional category (EP_2), but different winners for the Research category (R_1 and

R₂). The announced winners of the contest (Section 4.4) that are based on AbsE method and average curvature and axial strains of the column over a range of 203 mm (8 in.) are different from the winners presented in this section, except for winner EP1 (marked in Figures 4.4 to 4.15), which is the same as EP₂.

Figure 4.17 to Figure 4.28 show the response predictions and measured (experimental) response quantities for all response quantities. Based on the four scoring methods, the winners are marked on the plots. The predictions of winners based on the AbsE, CE, and AvgE methods (R₁, EP₁, and EP₂) were close (with few exceptions) to the measured response for all response quantities. Using the RMSE method, winner R₂'s predictions in some categories were very accurate; however, in other categories these predictions contained large errors, especially in regards to accelerations, curvature, and axial strain (see Figure 4.19, Figure 4.20, Figure 4.26, and Figure 4.27). This is the disadvantage of using this scoring method; the preferred winner should have consistent and small bias in all response quantities. Based on the analysis of different scoring schemes, it is recommended using the CE method as a basic scoring method and possibly in conjunction with AbsE or AvgE method. This recommendation is relevant to the sequential nature of this test.

Table 4.2 Winners based on different scoring methods

	AbsE	CE	AvgE	RMSE
Researcher	R ₁	R ₁	R ₁	R ₂
Engineering Professional	EP ₁	EP ₁	EP ₂	EP ₂

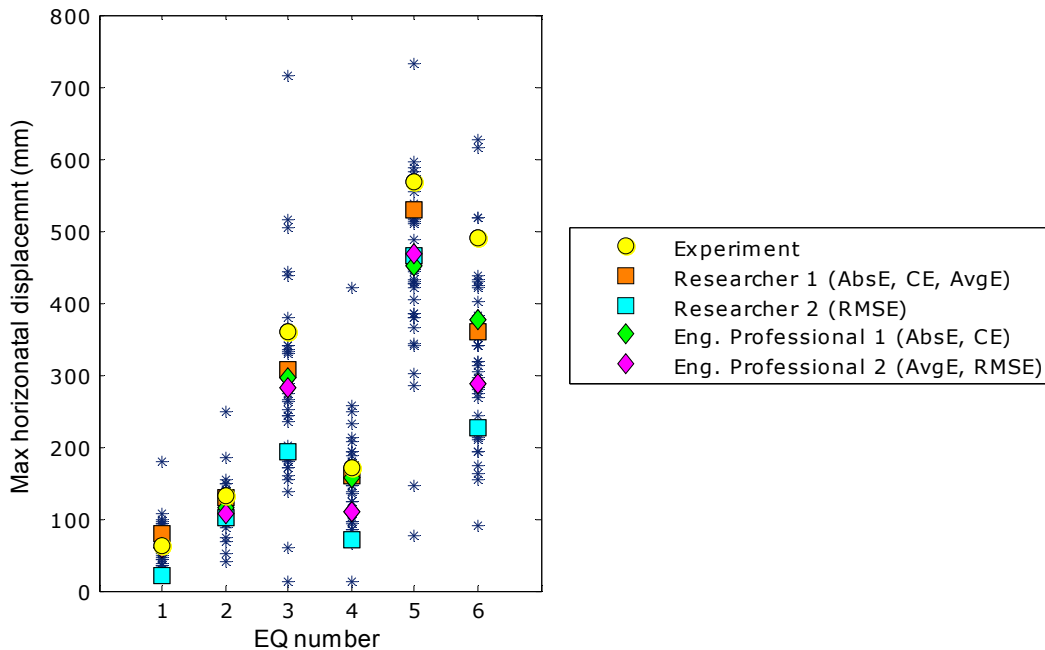


Figure 4.17 Predictions of “Max” displacement at the top of the column versus measured response.

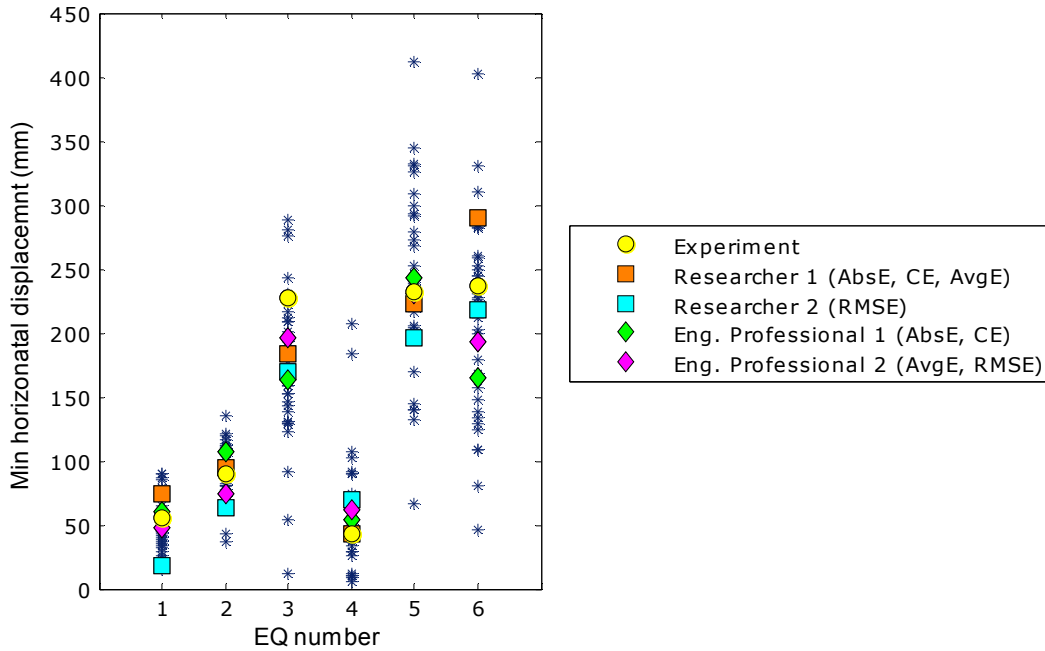


Figure 4.18 Predictions of “Min” displacement at the top of the column versus measured response.

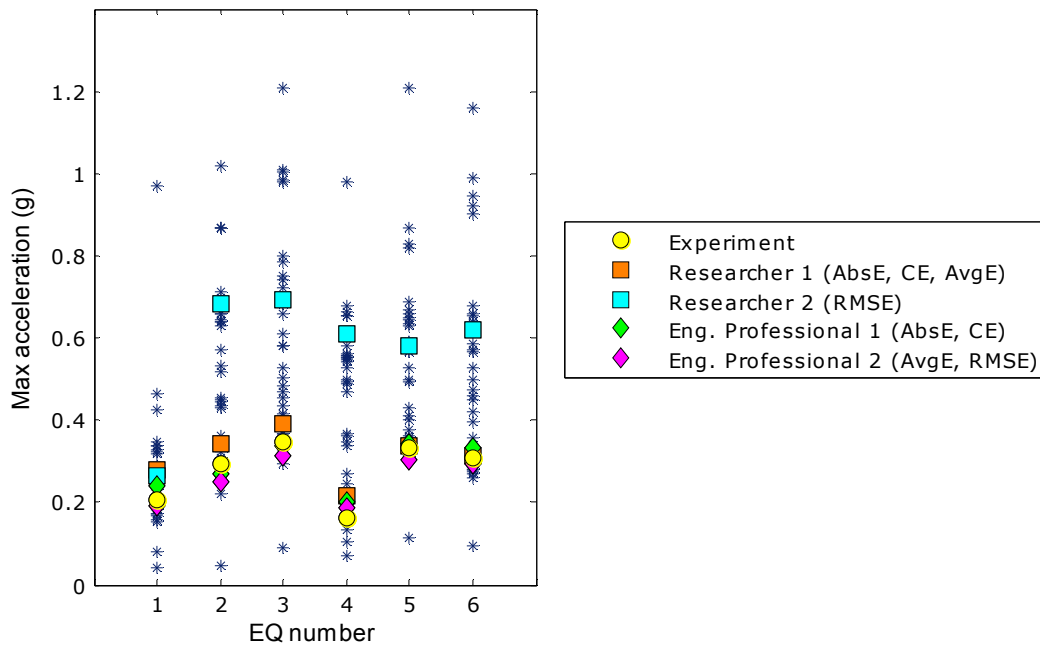


Figure 4.19 Predictions of “Max” horizontal acceleration at the top of the column versus measured response.

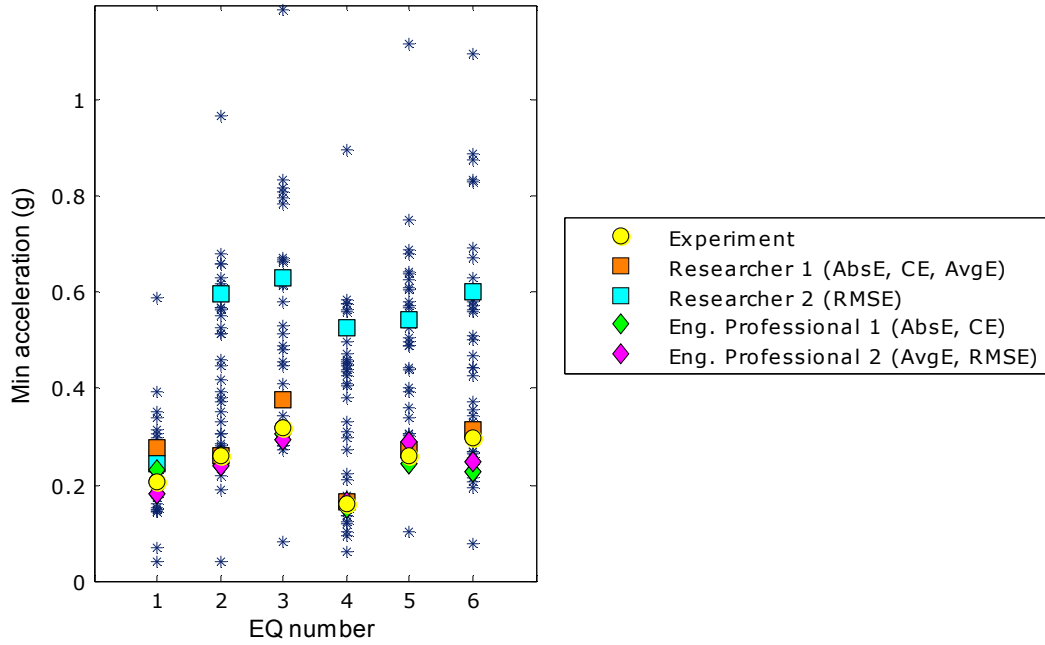


Figure 4.20 Predictions of “Min” horizontal acceleration at the top of the column versus measured response.

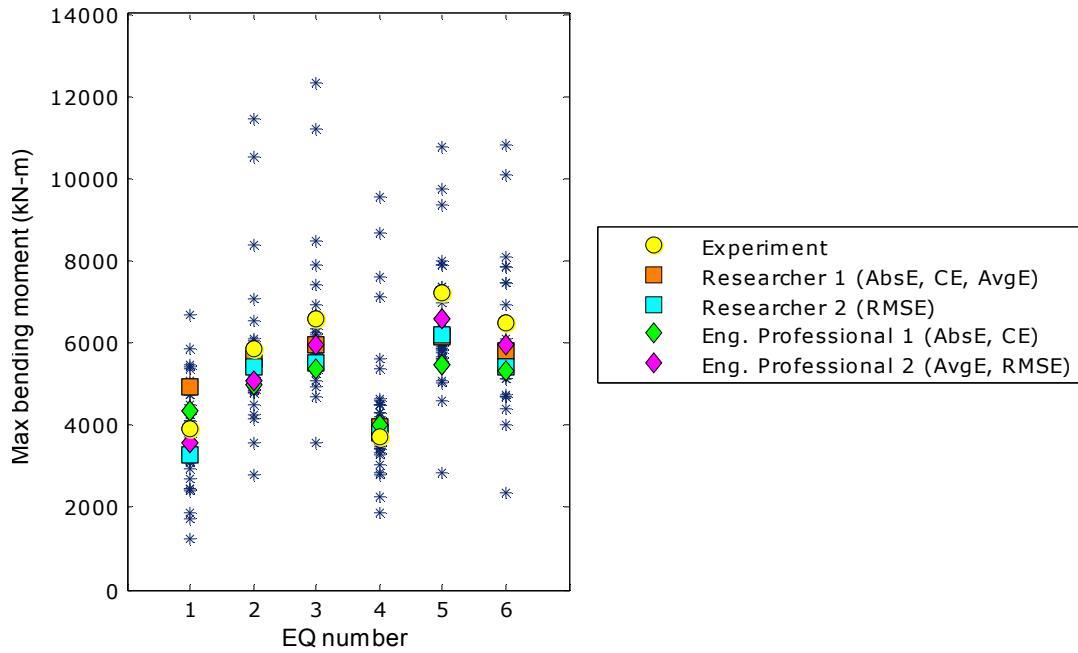


Figure 4.21 Predictions of “Max” bending moment at the base of the column versus measured response.

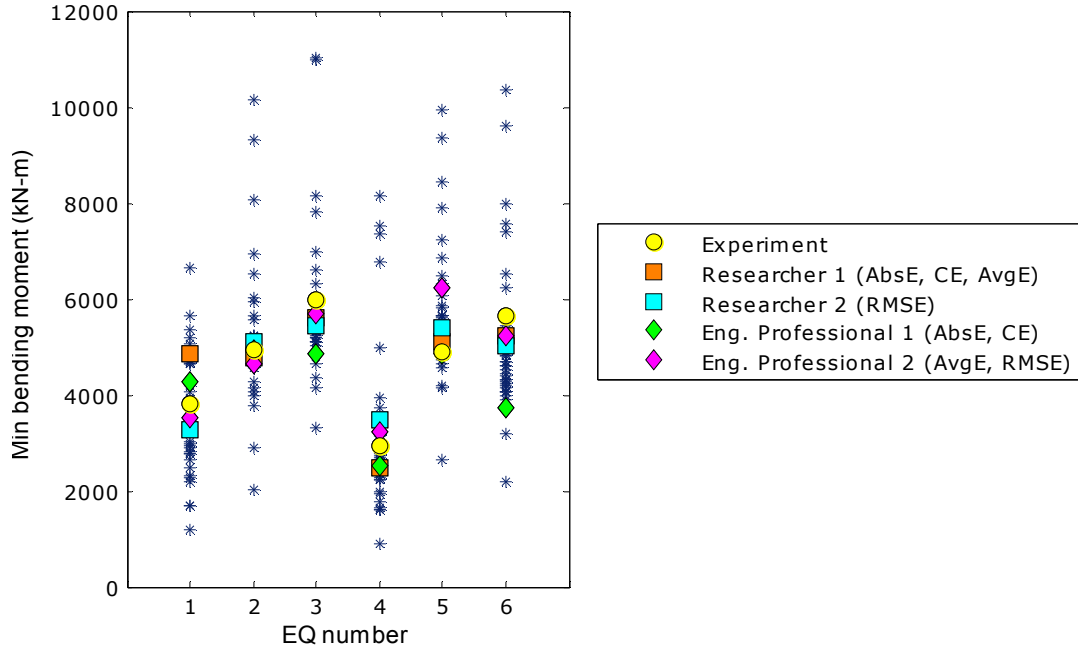


Figure 4.22 Predictions of “Min” bending moment at the base of the column versus measured response.

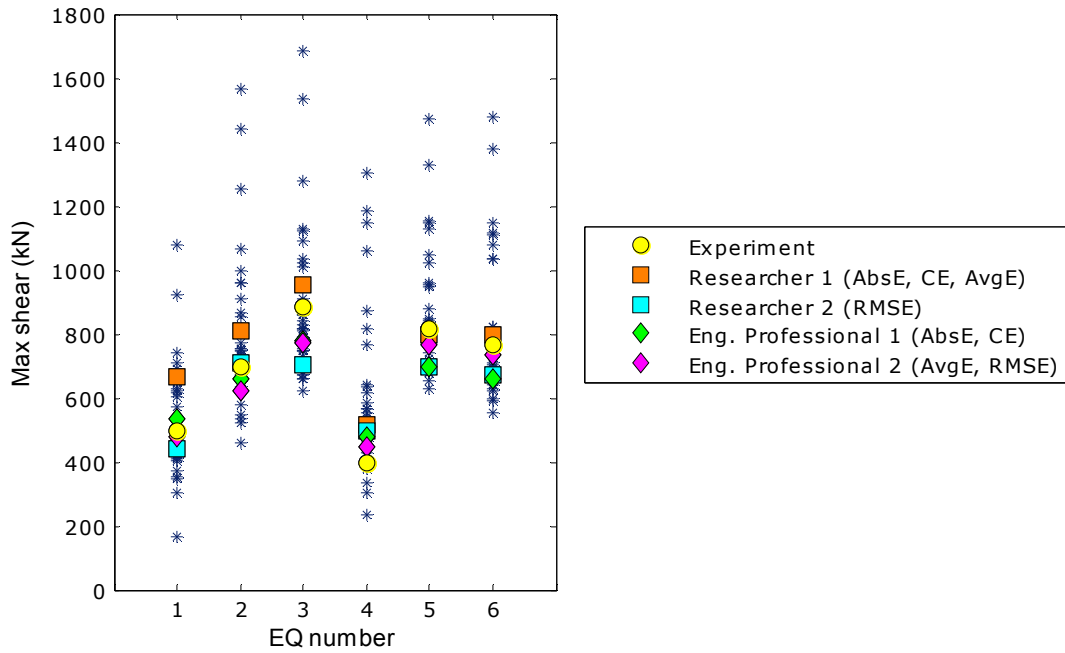


Figure 4.23 Predictions of “Max” shear force at the base of the column versus measured response.

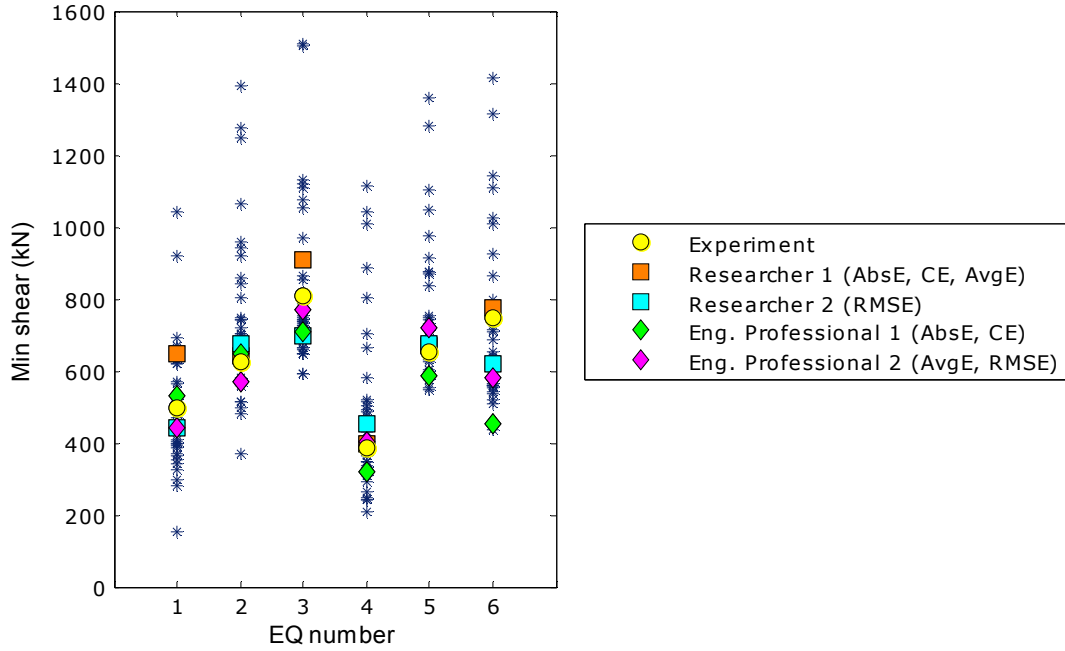


Figure 4.24 Predictions of “Min” shear force at the base of the column versus measured response.

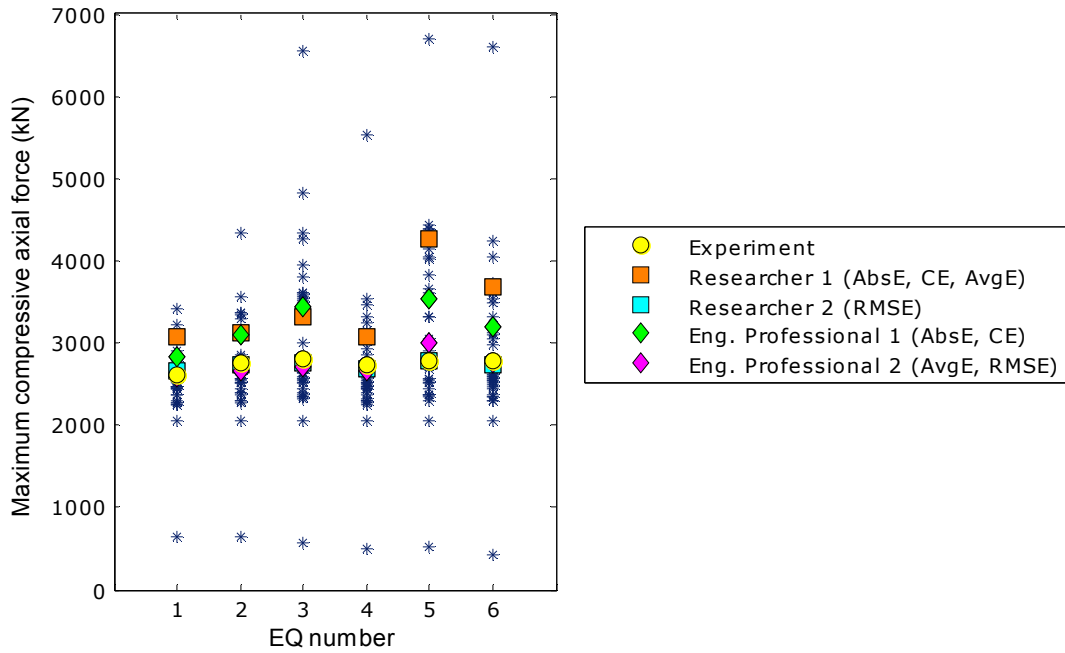


Figure 4.25 Predictions of maximum compressive axial force versus measured response.

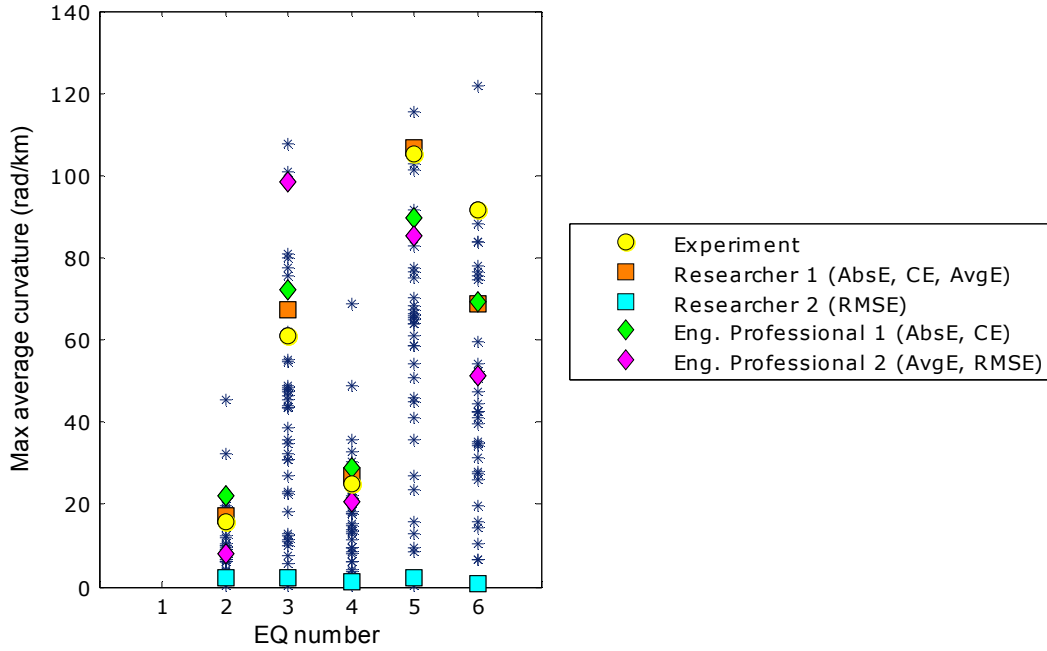


Figure 4.26 Predictions of “Max” average curvature between 51 and 457 mm from the bottom of the column versus measured response.

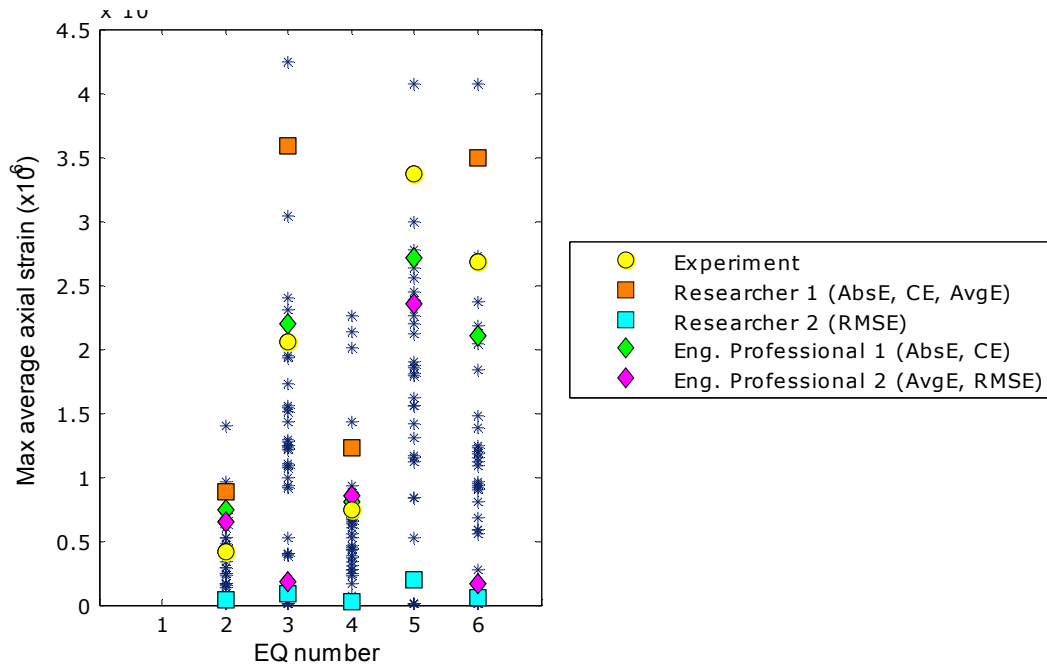


Figure 4.27 Predictions of “Max” average axial strain between 51 and 457 mm from the bottom of the column versus measured response.

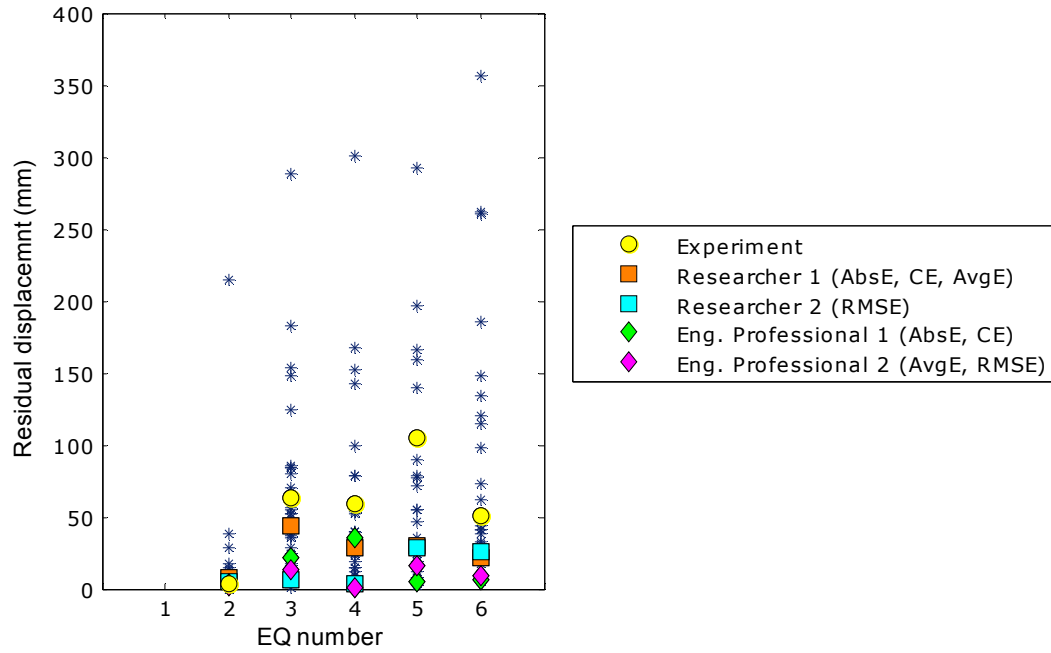


Figure 4.28 Predictions of residual displacement at the top of the column versus measured response.

5 Statistical Analysis of Data

Forty-one participants' predictions of eight response quantities were analyzed according to the six earthquake tests. The following sections summarize the results of these analyses, including: mean and median bias, coefficient of variation (COV), histograms of average error for all predicted quantities over the six ground motions, and histograms that show the increasing error of predicted displacement and acceleration quantities as the test sequence progressed.

5.1 MEAN AND MEDIAN BIAS AND COEFFICIENT OF VARIATIONS FOR CONSIDERED RESPONSE QUANTITIES

The predicted data were statistically analyzed to quantify their variation from the measured responses and to show the dispersion of predicted responses. Figure 5.1 to Figure 5.14 show mean and median bias and COV for each predicted quantity and each earthquake. Bias is a difference between the prediction and the measured response. Designation "Max" in the figures refers to the absolute maximum of the considered response. Designation "Min" refers to the absolute maximum in the opposite direction of "Max". Since "Max" and "Min" are absolute maximums in the two directions, positive bias in the figures means that the analysis results are larger than measured. Table 5.1 gives average COV over all considered earthquakes for different response quantities.

From all required response quantities, the forces at the base of the column were predicted with the best accuracy. The order of increasing accuracy was as follows: compressive axial force, shear, and bending moment. Prediction of displacement at the top of the column was fair. Horizontal acceleration at the top of the column, average curvature at the bottom of the column, average axial strain of the column close to the base, and residual displacement were not predicted with a substantial degree of accuracy (in order of accuracy as listed, with residual displacement being the least accurate). The basic observations derived from statistical analysis are summarized in the following sections.

Table 5.1 Average coefficient of variation (COV) for different response quantities.

	Average COV (%)
Max. displacement at the top of the column	39.0
Min. displacement at the top of the column	38.4
Max. acceleration at the top of the column	47.7
Min. acceleration at the top of the column	46.9
Max. bending moment at the base of the column	27.4
Min. bending moment at the base of the column	31.9
Max. shear force at the base of the column	29.7
Min. shear force at the base of the column	32.4
Max. compressive axial force	25.3
Max. average curvature between 51 and 457 mm from the bottom of the column	62.9
Max. average axial strain between 51 and 457 mm from the bottom of the column	79.2
Residual displacement at the top of the column	152

5.1.1 Relative Lateral Displacement at the Top of the Column

Relative lateral displacement at the top of the column was predicted more accurately for small- and medium-intensity earthquakes (EQ1, EQ2, and EQ4) where the response is fairly linear or only slightly nonlinear compared to high-intensity earthquakes (EQ3, EQ5, and EQ6) [Figure 5.1(b)]. However, the COV is bigger for small- and medium-intensity earthquakes than for high-intensity earthquakes [Figure 5.1(c)].

1. The median bias in predicting the absolute maximum displacement is between 5% and 15% for small and medium intensity earthquakes; however, it is between 21% and 35% for high-intensity earthquakes (Figure 5.1b). For the peak response in the other direction, the median bias is less than 20% for all earthquakes [Figure 5.3(b)].
2. The COV in predicting the absolute maximum displacement for all ground motions is between 26% and 53%, with an average of 38.9% [Figure 5.1(c)]. For the peak response in the other direction, it is between 22% and 69%, with an average of 38.4% [Figure 5.2(c)].

5.1.2 Absolute Acceleration at the Top of the Column

Absolute acceleration at the top of the column (coinciding with the center of mass of the superstructure) was not predicted with a substantial degree of accuracy. EQ4 (a medium-intensity earthquake that simulated an aftershock for EQ3) posed the greatest challenge.

1. The median bias in predicting the absolute maximum acceleration is between 25% and 48% for all earthquakes except EQ4; however, it is 118% for EQ4 [Figure

- 5.3(b)]. For the peak response in the other direction, the median bias is between 18% and 87% for all earthquakes [Figure 5.4(b)].
2. The COV in predicting the absolute maximum acceleration for all ground motions is between 39% and 55%, with an average of 47.7% [Figure 5.3(c)]. For the peak response in the other direction, it is between 38% and 59%, with an average of 46.9% [Figure 5.4(c)].

5.1.3 Bending Moment at the Base of the Column

Bending moment at the base of the column was predicted more accurately for small- and medium-intensity earthquakes (EQ1, EQ2, and EQ4) compared to high-intensity earthquakes (EQ3, EQ5, and EQ6) [Figure 5.5(b)]. However, the COV for predicting bending moment is bigger for small- and medium-intensity earthquakes compared to high-intensity earthquakes [Figure 5.5(c)].

1. The median bias in predicting the absolute maximum bending moment is between 2% and 9% for small- and medium-intensity earthquakes; however, it is between 11% and 15% for high-intensity earthquakes [Figure 5.5(b)]. For the peak response in the other direction, the median bias is between 2% and 8% for small- and medium-intensity earthquakes; however, it is between 8% and 16% for high-intensity earthquakes [Figure 5.6(b)].
2. The COV in predicting the absolute maximum bending moment for all ground motions is between 21% and 30%, with an average of 27.3% [Figure 5.5(c)]. For the peak response in the other direction, it is between 23% and 51%, with an average of 31.9% [Figure 5.6(c)].

5.1.4 Base Shear

Base shear was predicted with a high degree of accuracy for all earthquakes.

1. The median bias in predicting the absolute maximum shear is between 0.5% and 8% for all earthquakes, except EQ4, where it is 27% [Figure 5.7(b)]. For the peak response in the other direction, the median bias is between 2% and 9% for all earthquakes except EQ6, where it is 18% [Figure 5.8(b)].
2. The COV in predicting the absolute maximum shear for all ground motions is between 21% and 44%, with an average of 29.7% [Figure 5.7(c)]. For the peak response in the other direction, it is between 24% and 47%, with an average of 32.4% [Figure 5.8(c)].

5.1.5 Compressive Axial Force

The compressive axial force was predicted with a high degree of accuracy for all earthquakes.

1. The median bias in predicting the maximum compressive axial force is between 2% and 7% for all earthquakes [Figure 5.9(b)].
2. The coefficient of variation in predicting the maximum compressive axial force for all earthquakes is between 15% and 31%, with an average of 25.3% [Figure 5.9(c)].

5.1.6 Maximum Average Curvature between 51 and 254 mm from the Bottom of the Column

The absolute maximum average curvature was predicted over a range of 203 mm (8 in.) at the bottom of the column. Curvatures were measured over a range extending from 51 mm (2 in.) to 254 mm (10 in.) from the bottom of the column. This distance corresponded to one-sixth the column diameter. During tests EQ2, EQ3, and EQ4, major cracks were observed above this region and only minor hairline cracks were observed in this region. The analytical models anticipated major cracks in this region; thus the curvature predictions were significantly larger than measured in this range; see Figure 5.10. Doubling the distance between the measuring points to 406 mm (16 in.) to include major cracks at the bottom of the column improved the accuracy of prediction, but the error was still significant; see Figure 5.11.

1. The median bias in predicting the maximum average curvature over the range of 203 mm (8 in.) at the bottom of the column is 2174%, 155%, 157%, 12%, and 21% for EQ2, EQ3, EQ4, EQ5, and EQ6, respectively; see Figure 5.10(b).
2. The median bias in predicting the maximum average curvature over the range of 406 mm (16 in.) at the bottom of the column is between 23% and 57% for EQ2 through EQ6; see Figure 5.11(b).
3. The COV in predicting the maximum average curvature over the range of 406 mm (16 in.) is between 51% and 69% for EQ2 through 6, with an average of 62.9%; see Figure 5.11(c).

5.1.7 Maximum Average Axial Strain 51 and 254 mm from the Bottom of the Column

The maximum average axial strain in the column measured over the same portion of the column as the maximum average curvature was not predicted with an acceptable degree of accuracy.

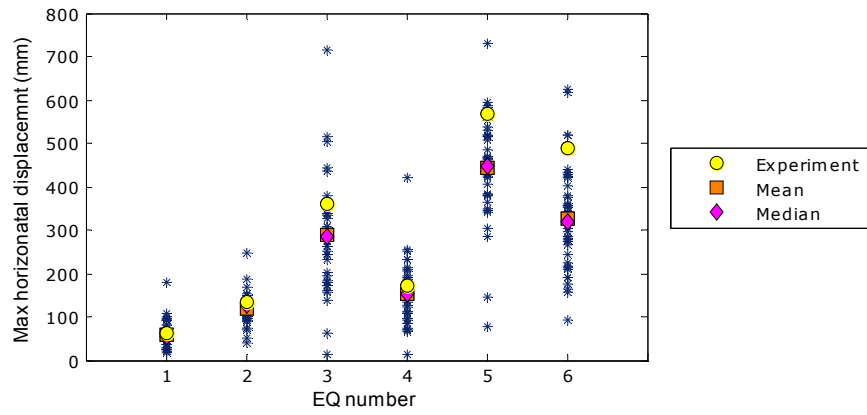
1. The median bias in predicting the maximum average axial strain over the range of 203 mm (8 in.) at the bottom of the column is 305%, 382%, 204%, 4%, and 28% for EQ2, EQ3, EQ4, EQ5, and EQ6, respectively; see Figure 5.12(b).

2. The median bias in predicting the maximum average axial strain over the range of 406 mm (16 in.) at the bottom of the column is between 11% and 58% for EQ2 through EQ6; see Figure 5.13(b).
3. The COV in predicting the maximum average axial strain over the range of 406 mm (16 in.) is between 63% and 90% for EQ2 through EQ6, with an average of 79.2%: see Figure 5.12(c).

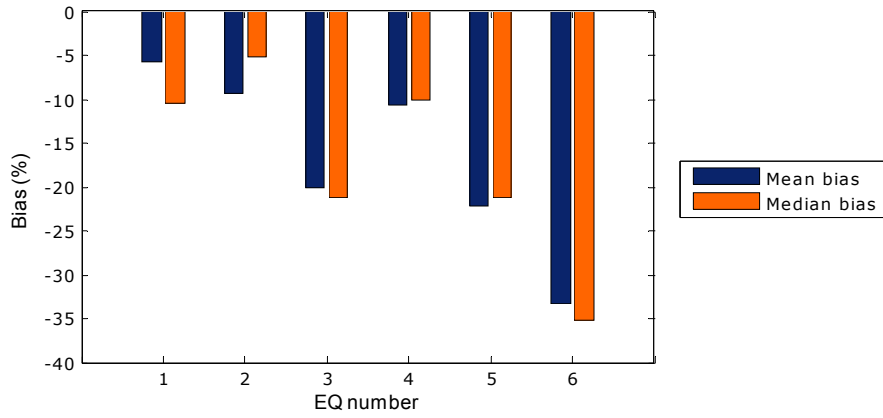
5.1.8 Residual Displacement at the Top of the Column

The residual displacement at the end of each ground motion was not predicted with an acceptable degree of accuracy and had the greatest dispersion compared to all other response quantities.

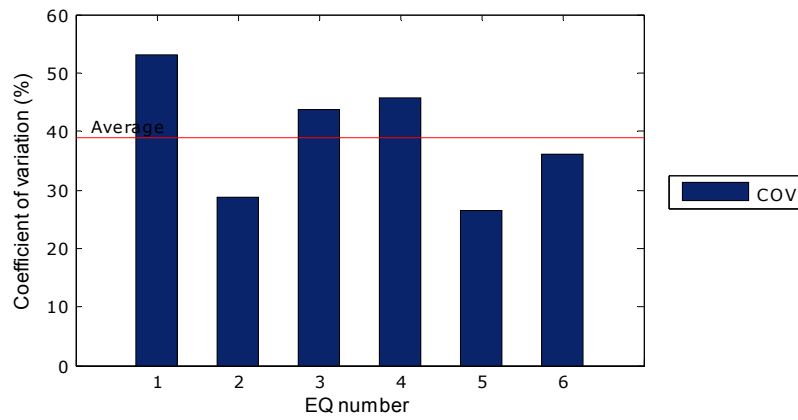
1. The median bias in predicting the residual displacement is between 24% and 75% for EQ2 through EQ6; see Figure 5.14(b).
2. The COV in predicting the residual displacement after EQ2 through EQ6 is between 102% and 277%, with an average of 152%; see Figure 5.14(c). The COV was the greatest for EQ2 (277%); for all other earthquakes; it was in the range from 102% to 127%.



(a)

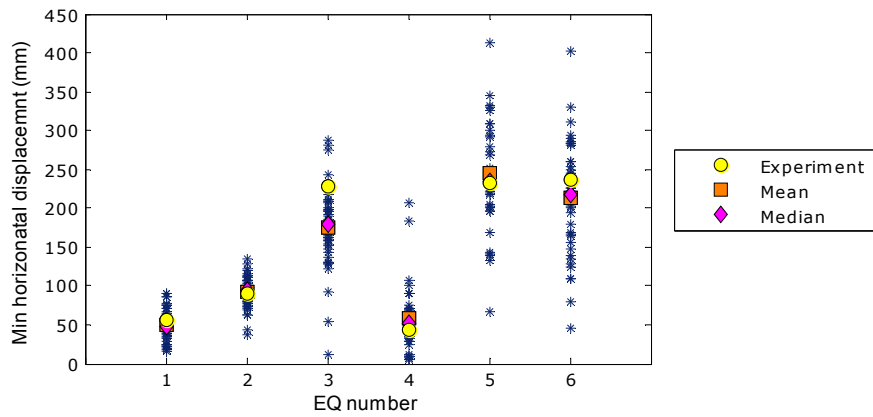


(b)

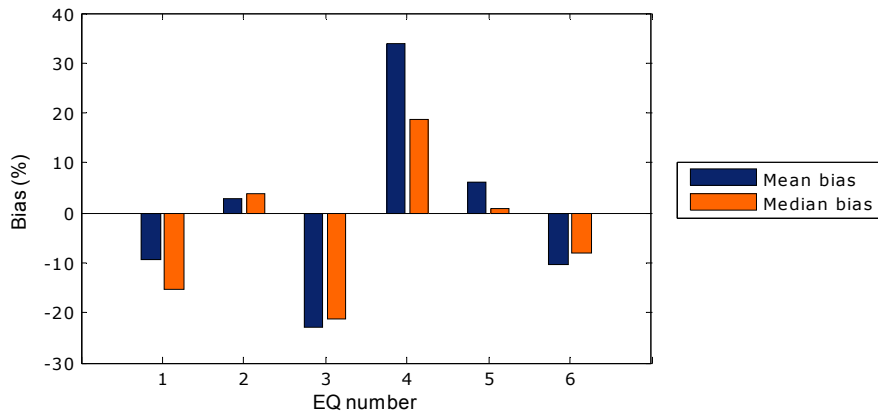


(c)

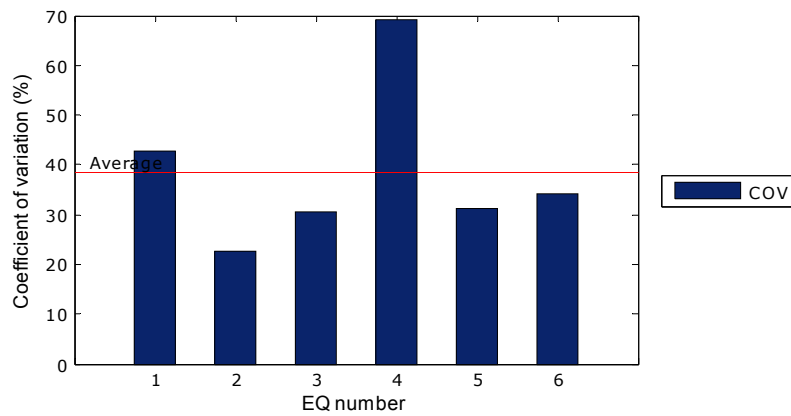
Figure 5.1 Statistical analysis of predictions of “Max” displacements at the top of the column: (a) analytical predictions with measured response, mean, and median marked on the graph; (b) mean and median bias; and (c) coefficient of variation.



(a)

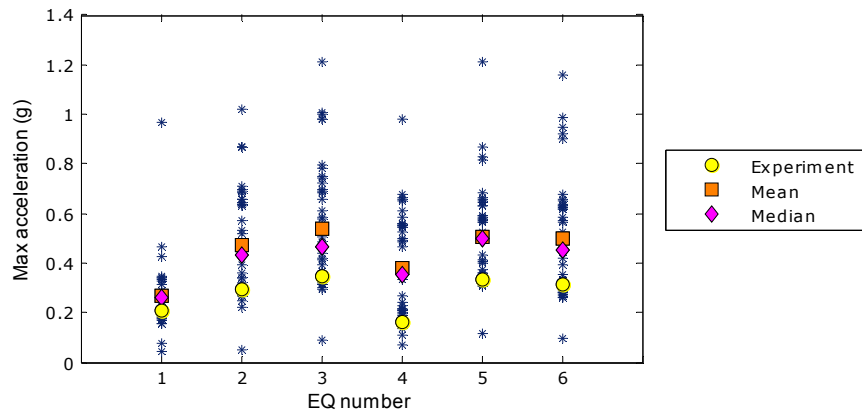


(b)

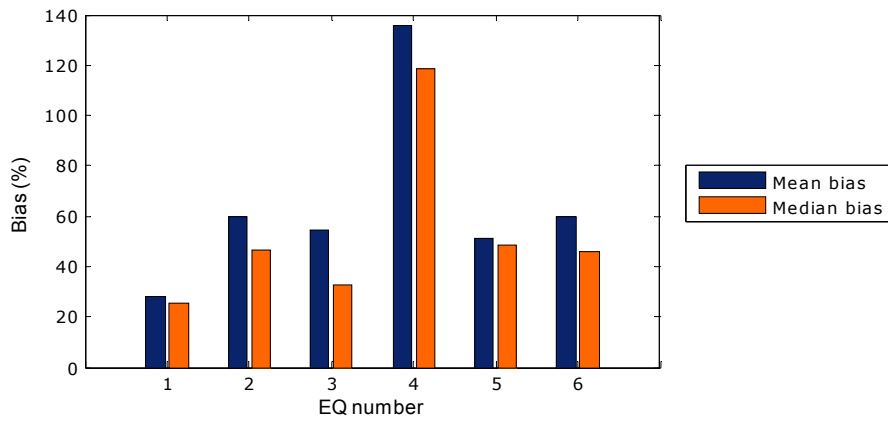


(c)

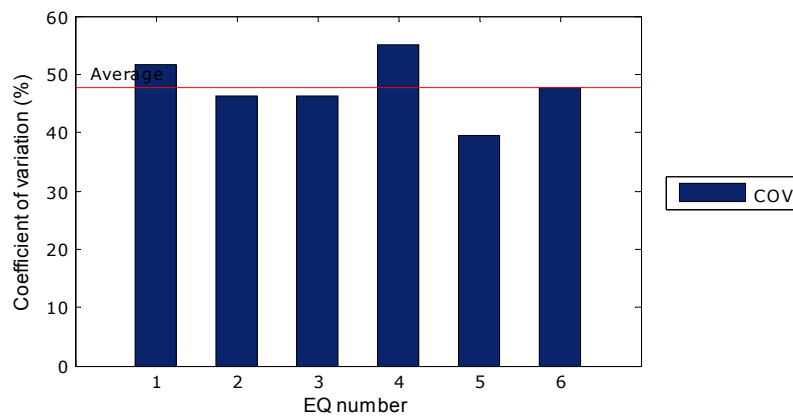
Figure 5.2 Statistical analysis of predictions of “Min” displacements at the top of the column: (a) analytical predictions with measured response, mean, and median marked on the graph; (b) mean and median bias; and (c) coefficient of variation.



(a)

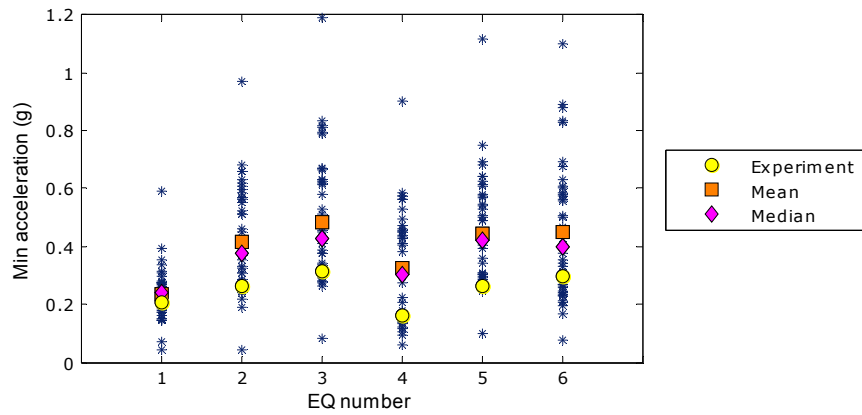


(b)

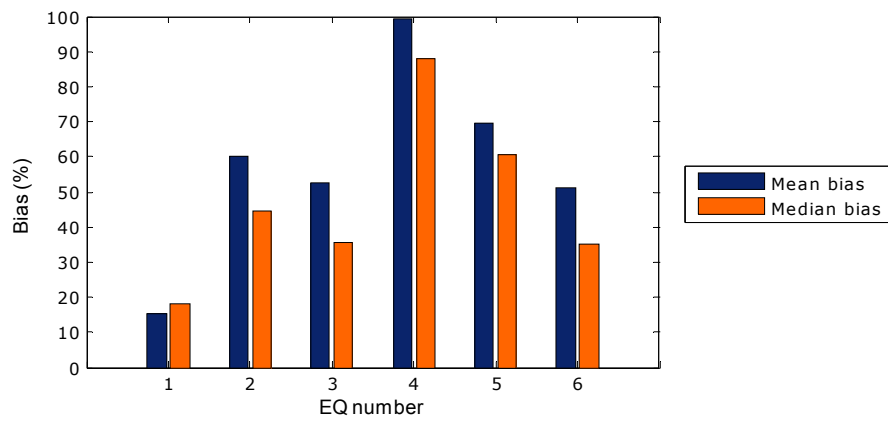


(c)

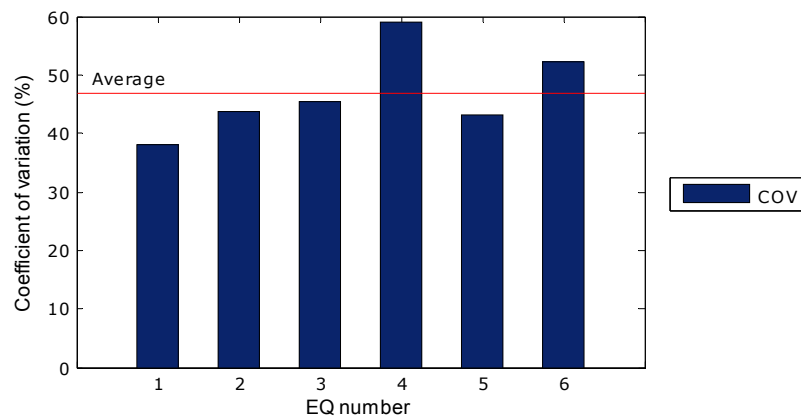
Figure 5.3 Statistical analysis of predictions of “Max” accelerations at the top of the column: (a) analytical predictions with measured response, mean, and median marked on the graph; (b) mean and median bias; and (c) coefficient of variation.



(a)

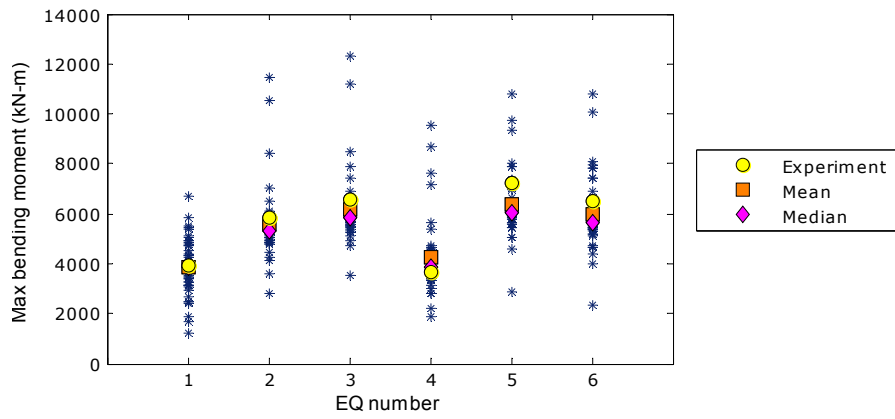


(b)

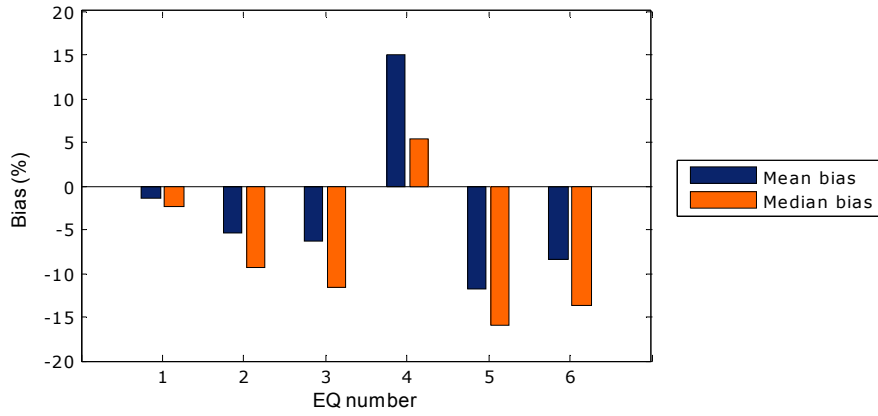


(c)

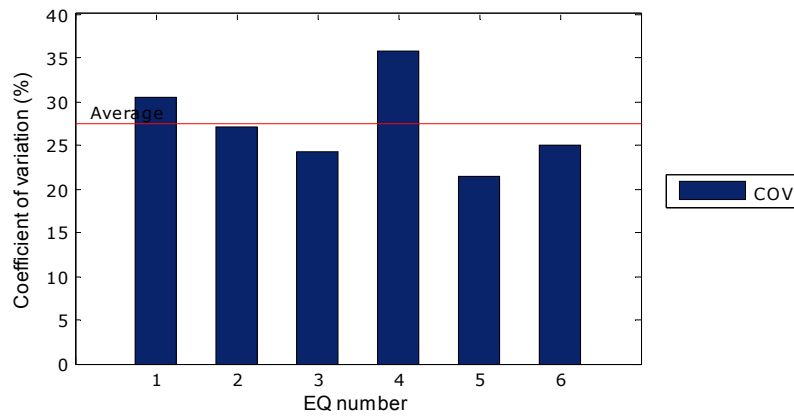
Figure 5.4 Statistical analysis of predictions of “Min” accelerations at the top of the column: (a) analytical predictions with measured response, mean, and median marked on the graph; (b) mean and median bias; and (c) coefficient of variation.



(a)

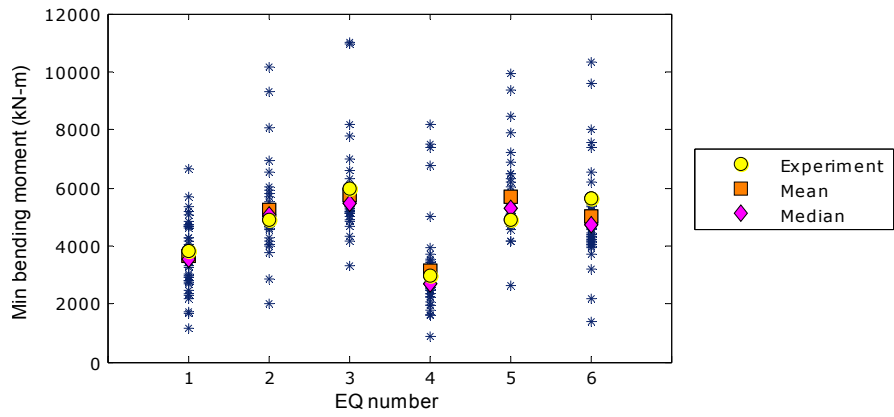


(b)

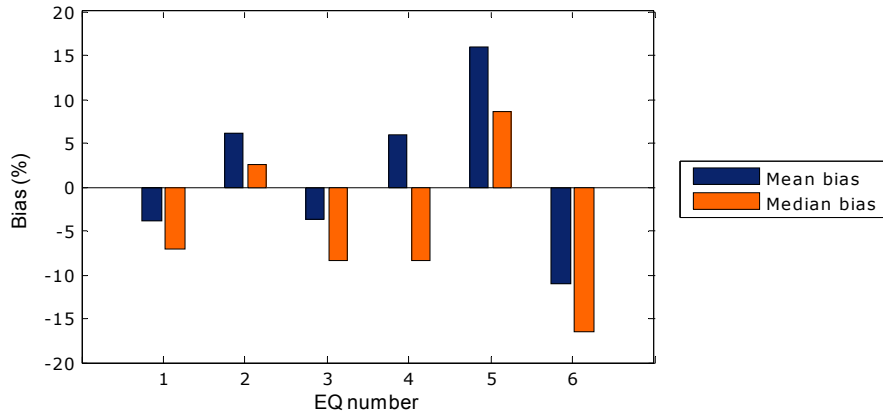


(c)

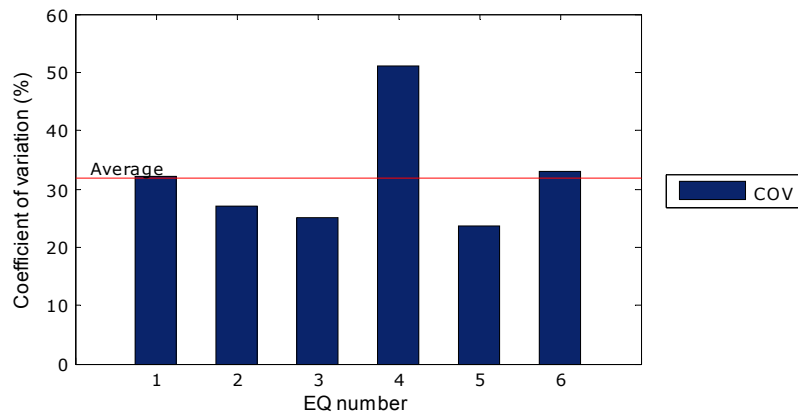
Figure 5.5 Statistical analysis of predictions of “Max” bending moment at the base of the column: (a) analytical predictions with measured response, mean, and median marked on the graph; (b) mean and median bias; and (c) coefficient of variation.



(a)

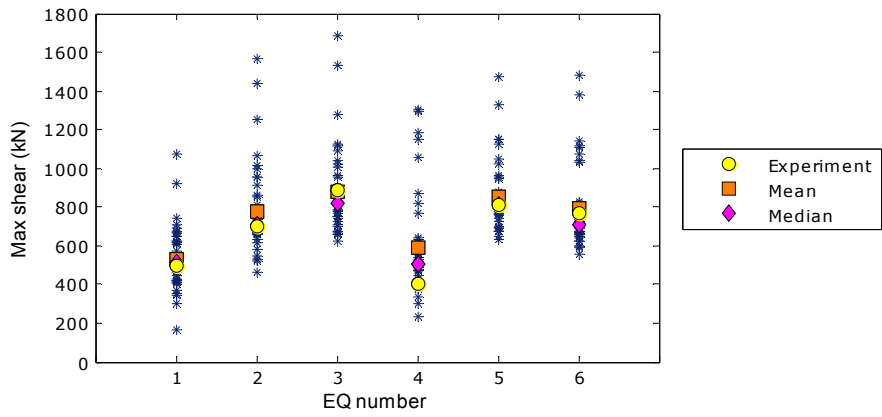


(b)

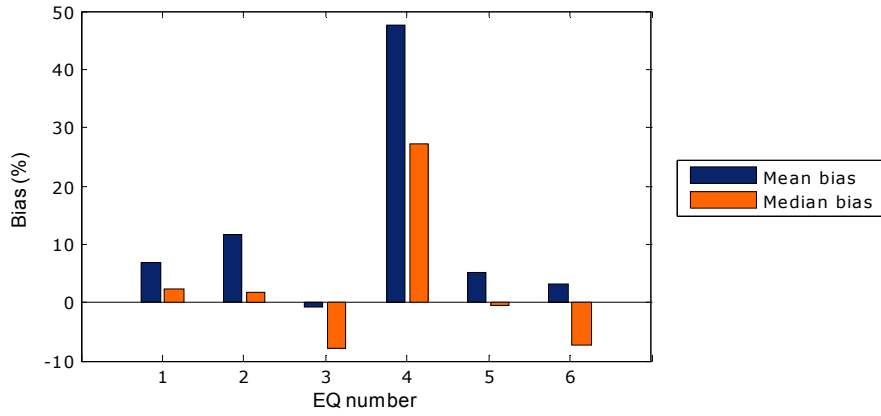


(c)

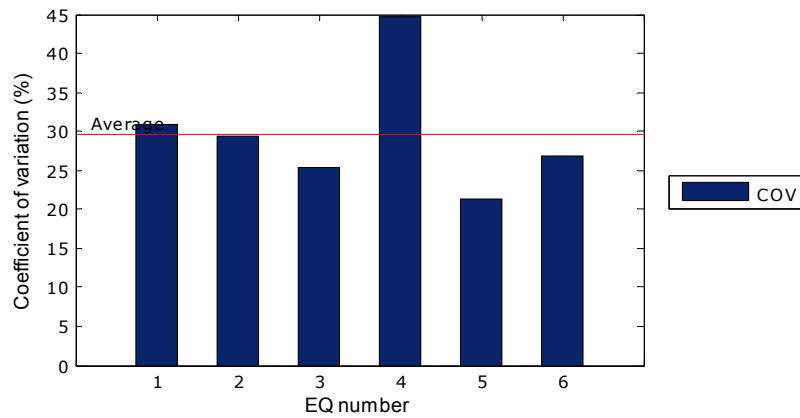
Figure 5.6 Statistical analysis of predictions of “Min” bending moments at the base of the column: (a) analytical predictions with measured response, mean, and median marked on the graph; (b) mean and median bias; and (c) coefficient of variation.



(a)

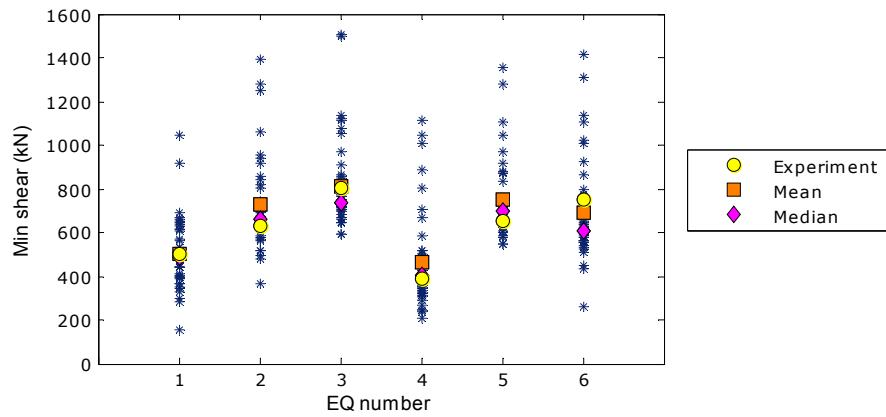


(b)

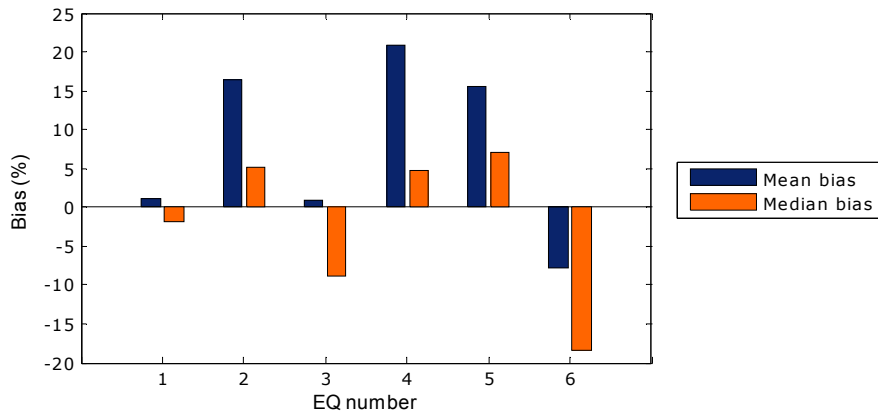


(c)

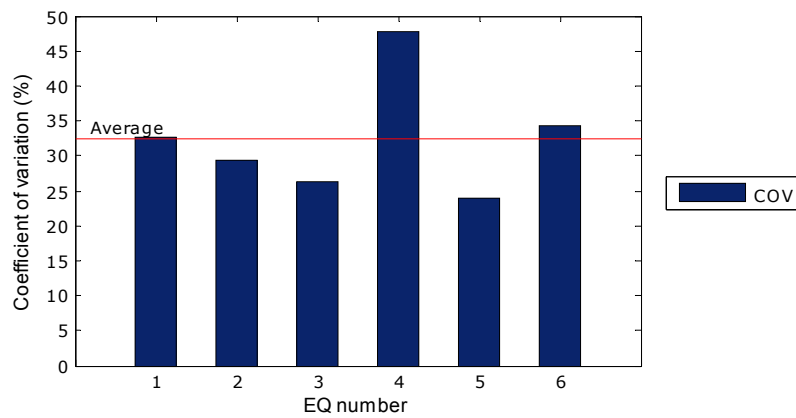
Figure 5.7 Statistical analysis of predictions of “Max” shear at the base of the column: (a) analytical predictions with measured response, mean, and median marked on the graph; (b) mean and median bias; and (c) coefficient of variation.



(a)

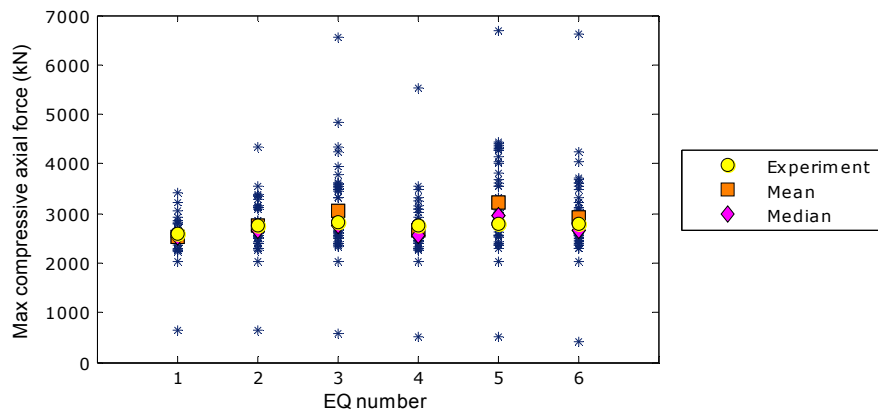


(b)

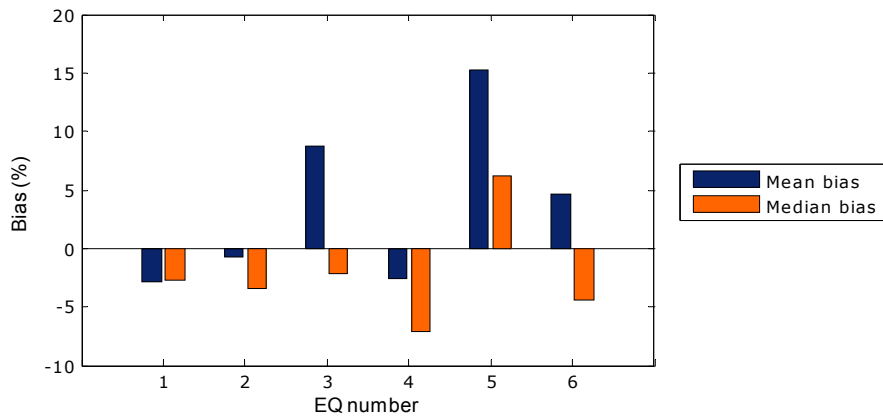


(c)

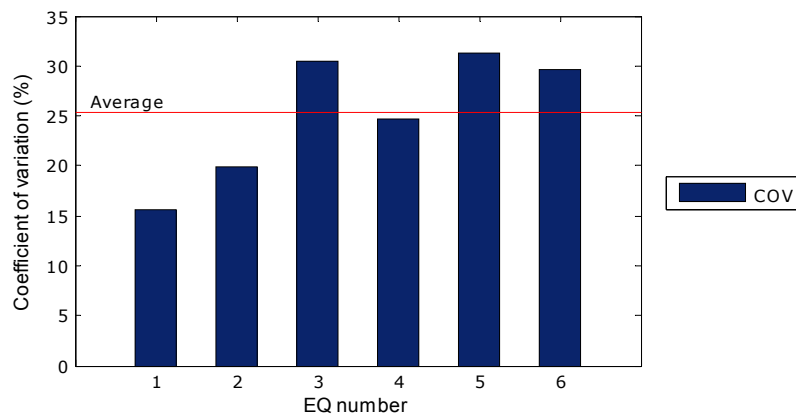
Figure 5.8 Statistical analysis of predictions of “Min” shear at the base of the column: (a) analytical predictions with measured response, with mean and median marked on the graph; (b) mean and median bias; and (c) coefficient of variation.



(a)

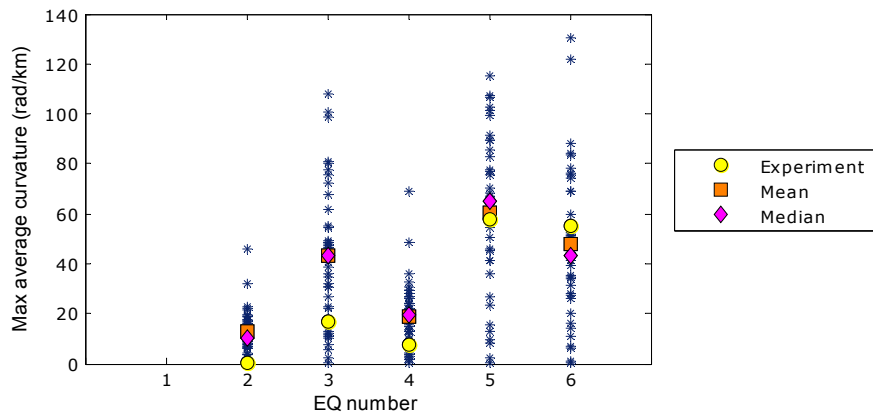


(b)

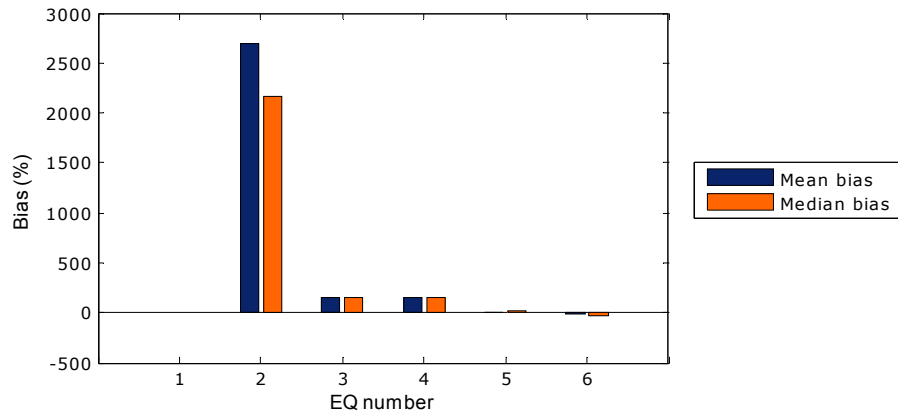


(c)

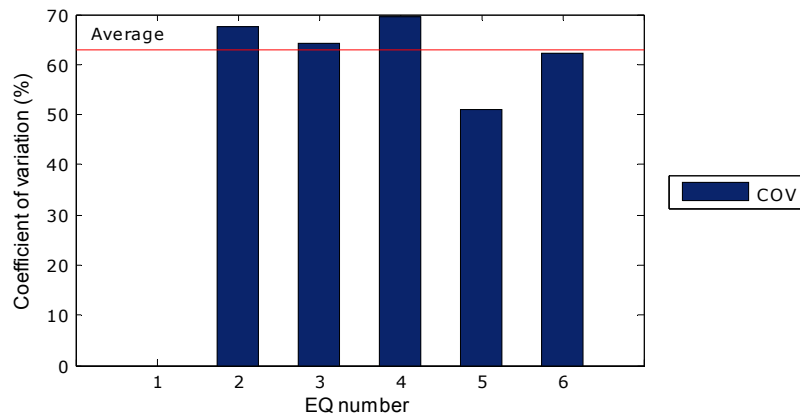
Figure 5.9 Statistical analysis of predictions of maximum compressive axial force: (a) analytical predictions with measured response, with mean and median marked on the graph; (b) mean and median bias; and (c) coefficient of variation.



(a)

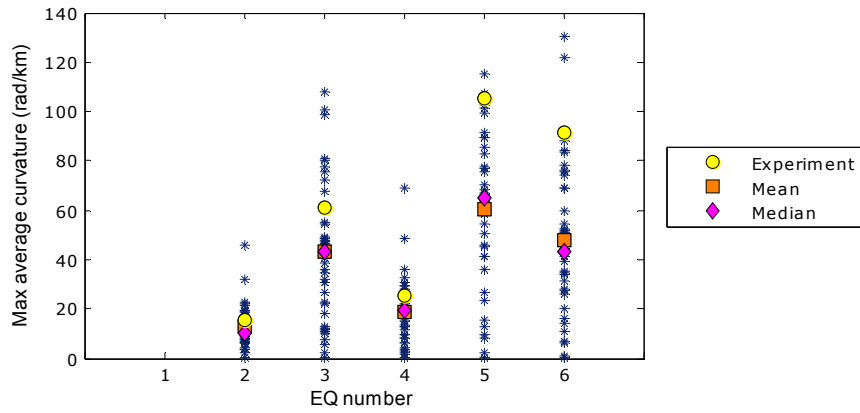


(b)

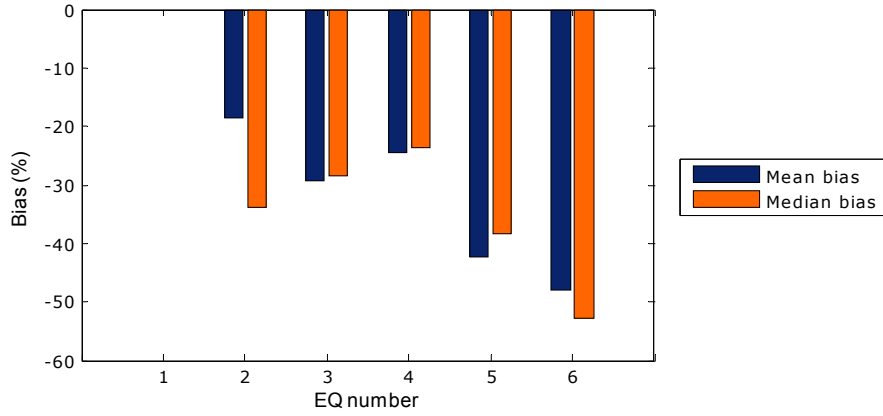


(c)

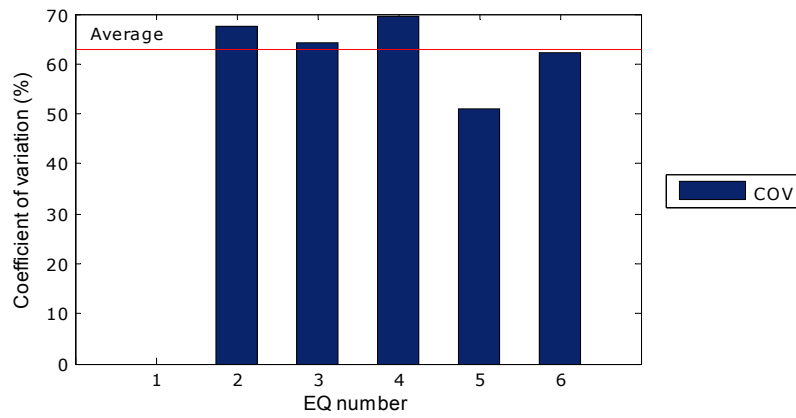
Figure 5.10 Statistical analysis of predictions of “Max” average curvature (between 51 and 254 mm from the bottom of the column): (a) analytical predictions and measured response; (b) mean and median bias; and (c) coefficient of variation.



(a)

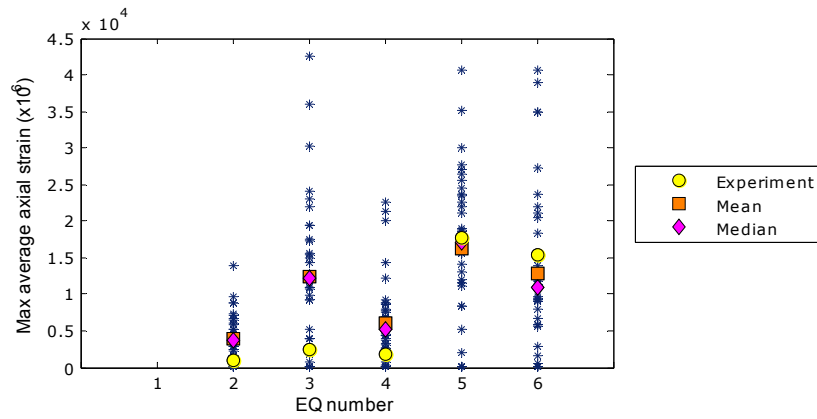


(b)

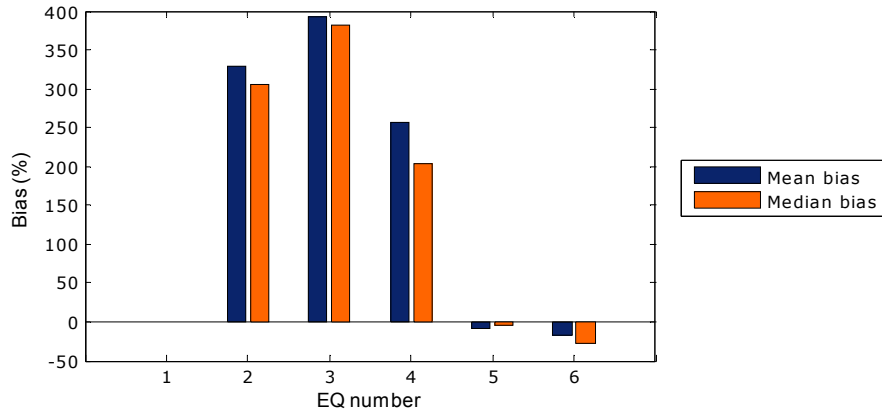


(c)

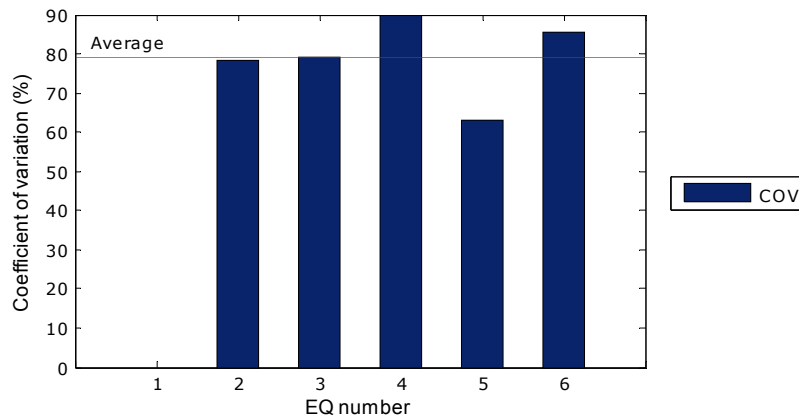
Figure 5.11 Statistical analysis of predictions of “Max” average curvature (between 51 and 457 mm from the bottom of the column): (a) analytical predictions and measured response; (b) mean and median bias; and (c) coefficient of variation.



(a)

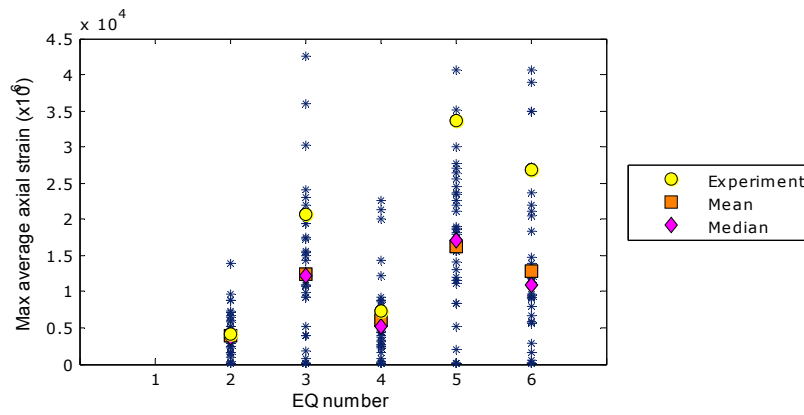


(b)

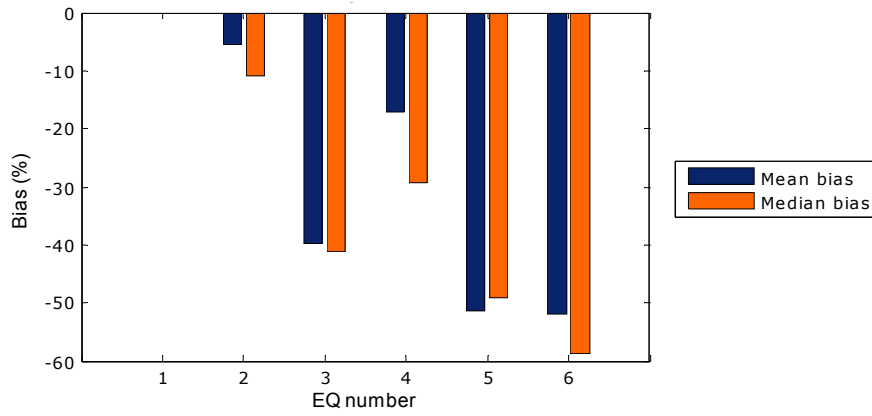


(c)

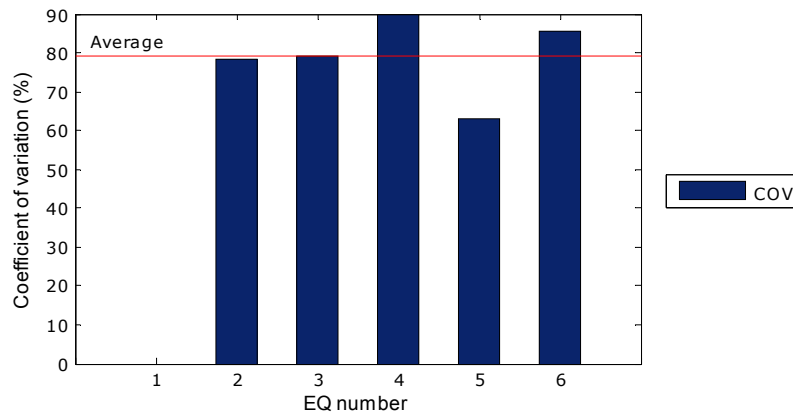
Figure 5.12 Statistical analysis of predictions of “Max” average axial strain (between 51 and 254 mm from the bottom of the column): (a) analytical predictions and measured response; (b) mean and median bias; and (c) coefficient of variation.



(a)

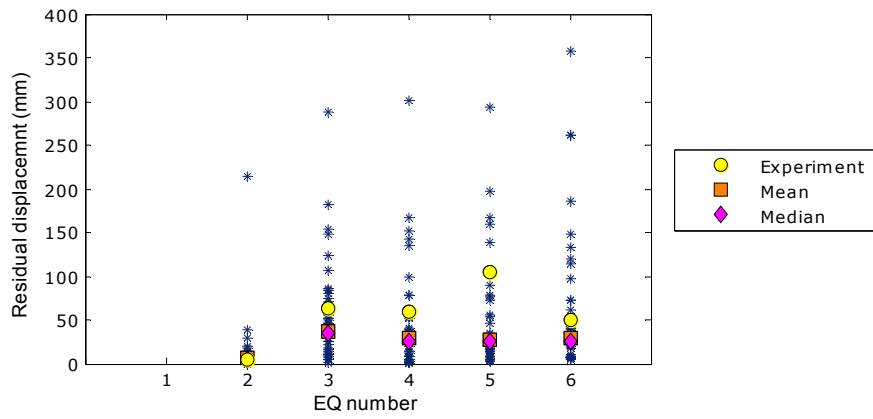


(b)

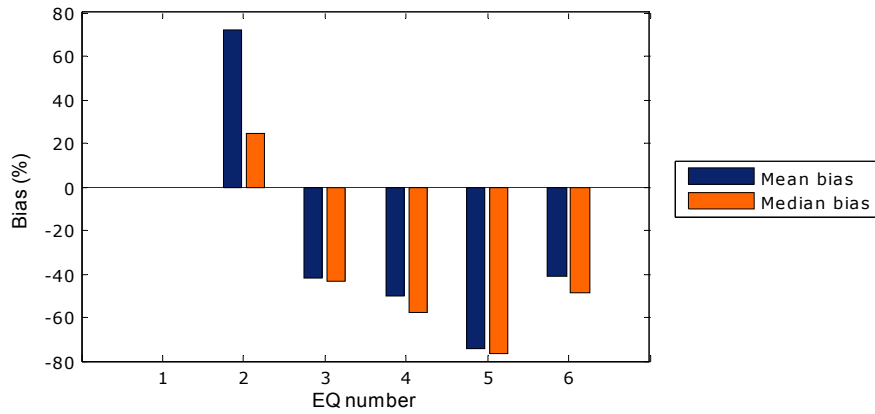


(c)

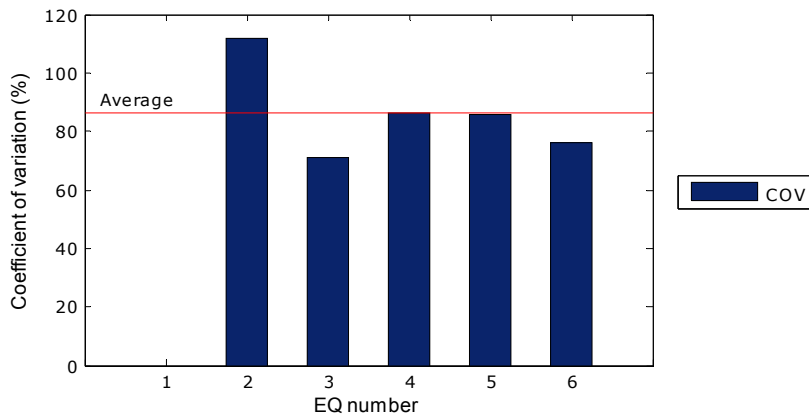
Figure 5.13 Statistical analysis of predictions of “Max” average axial strain (between 51 and 457 mm from the bottom of the column): (a) analytical predictions and measured response; (b) mean and median bias; and (c) coefficient of variation.



(a)



(b)



(c)

Figure 5.14 Statistical analysis of predictions of residual displacements at the top of the column: (a) analytical predictions with measured response, with mean and median marked on the graph; (b) mean and median bias; and (c) coefficient of variation.

5.2 DISTRIBUTIONS OF AVERAGE ERROR IN PREDICTION OF CONTEXT-SPECIFIED RESPONSE QUANTITIES

Figure 5.15 to Figure 5.22 gives the lognormal distribution of error in predicting the absolute maximum displacement, acceleration, bending moment, shear, axial force, average curvature, average axial strain, and residual displacement. The error is quantified by average error of a predicted response quantity over a set of earthquakes and is calculated as follows:

$$AvgErrRC = \frac{1}{j} \sum_{i=1}^j abs \left[\left(R_a - R_{exp} \right) / R_{exp} \right] \quad (5.1)$$

where j is the number of earthquakes for one predicted response quantity (5 or 6), R_a is analytically predicted response, and R_{exp} is a response measured from the experiment. To present the results in percentages, the average error calculated by Equation (5.1) is multiplied by 100. The Kolmogorov-Smirnov test with the significant level of 0.05 was used to verify that the lognormal distribution provides good representation of the data. The median (θ) and the standard deviation of natural logarithm of the average error (β , referred as a dispersion), are shown on the plots for each response quantity and are also given in Table 5.2.

The shear and bending moment at the base of the column were predicted with the best degree of accuracy. The order of increasing accuracy was as follows: shear (median of the average error over six earthquakes (θ) was 18.3%), bending moment ($\theta = 16.3\%$), and compressive axial force ($\theta = 12.2\%$). The prediction of the lateral displacement at the top of the column was fair ($\theta = 25.6\%$). Horizontal acceleration at the top of the column ($\theta = 39.4\%$) and average curvature at the bottom of the column ($\theta = 39.6\%$) were not predicted with an acceptable degree of accuracy. The average axial strain of the column close to the base ($\theta = 54.4\%$) and residual displacement ($\theta = 73.9\%$) were the quantities that proved to be the most difficult to predict. The dispersion of the average error was high for all response quantities, ranging from 0.43 for bending moment to 1.08 for acceleration.

Table 5.2 Median and dispersion (β) of the average error for different response quantities

	Median (%)	β
Max. displacement at the top of the column	25.6	0.52
Max. acceleration at the top of the column	39.4	1.08
Max. bending moment at the base of the column	16.3	0.43
Max. shear force at the base of the column	18.3	0.63
Max. compressive axial force	12.2	0.79
Max. average curvature between 51 and 457 mm from the bottom of the column	39.6	0.53
Max. average axial strain between 51 and 457 mm from the bottom of the column	54.4	0.65
Residual displacement at the top of the column	73.9	0.48

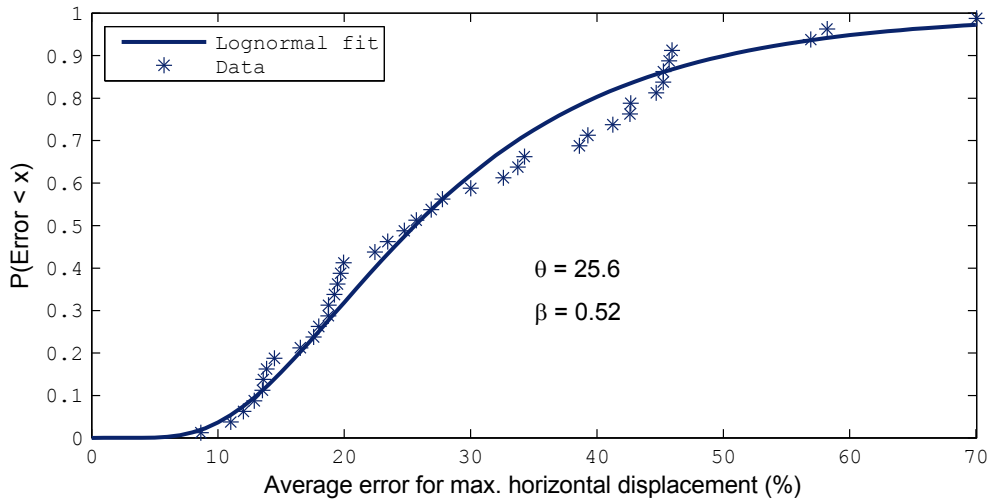


Figure 5.15 Lognormal distribution of average error in predicting absolute maximum horizontal displacement at the top of the column.

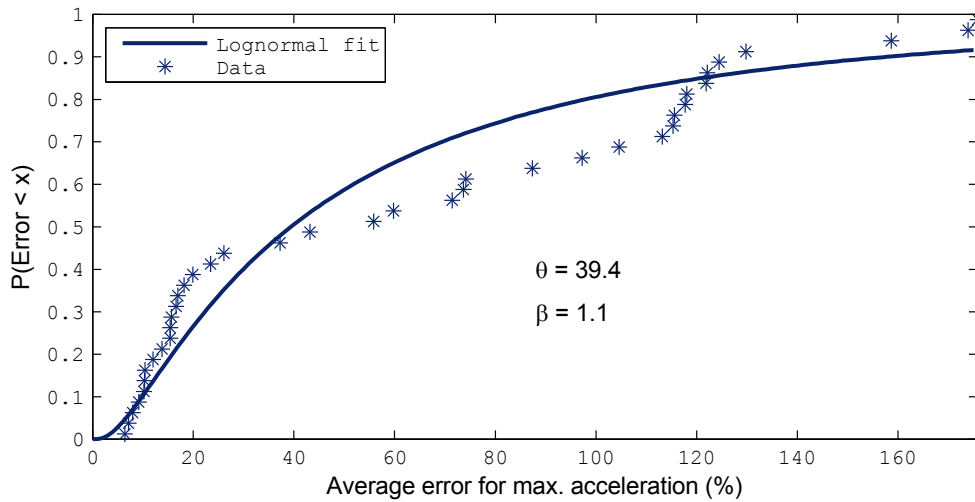


Figure 5.16 Lognormal distribution of average error in predicting absolute maximum horizontal acceleration at the top of the column.

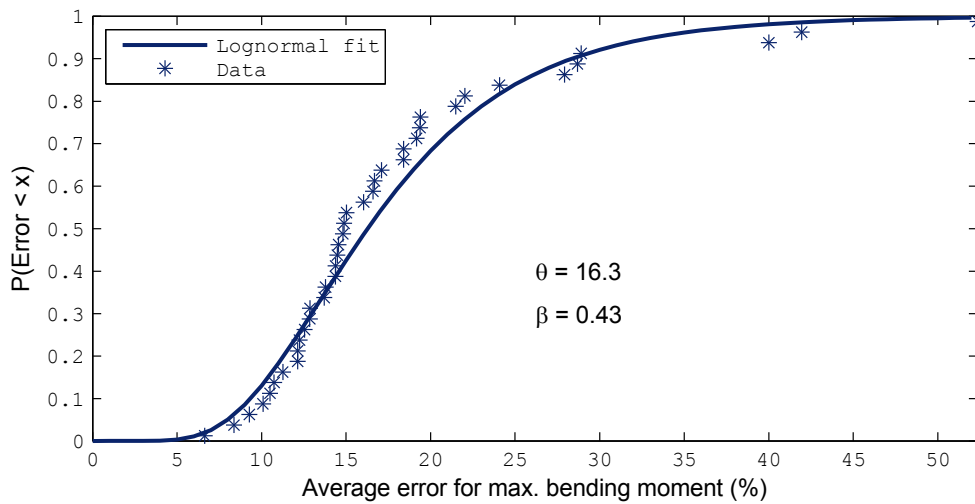


Figure 5.17 Lognormal distribution of average error in predicting absolute maximum bending moment at the base of the column.

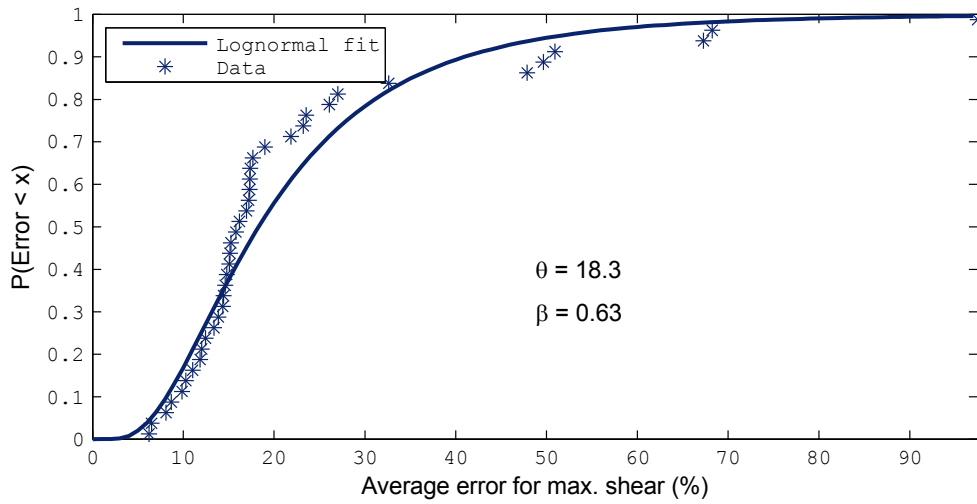


Figure 5.18 Lognormal distribution of average error in predicting maximum shear at the base of the column.

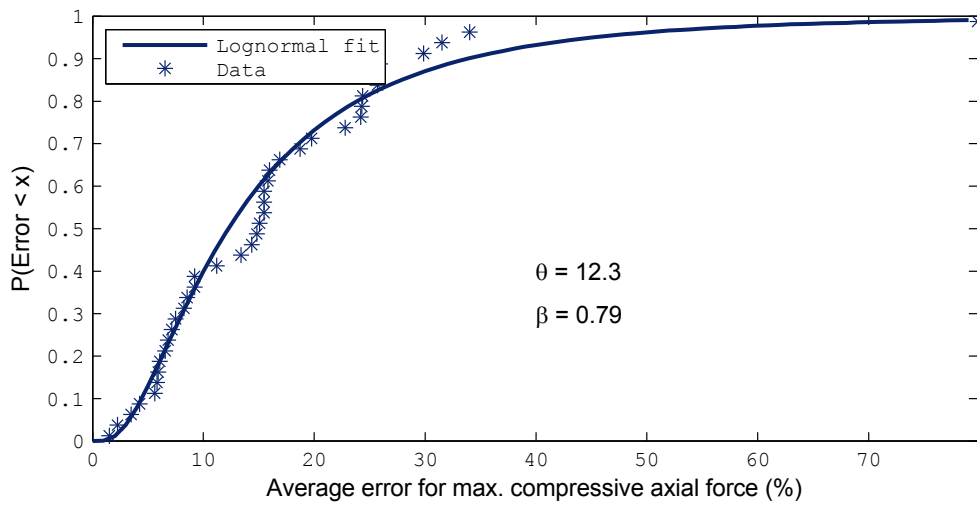


Figure 5.19 Lognormal distribution of average error in predicting maximum compressive axial force.

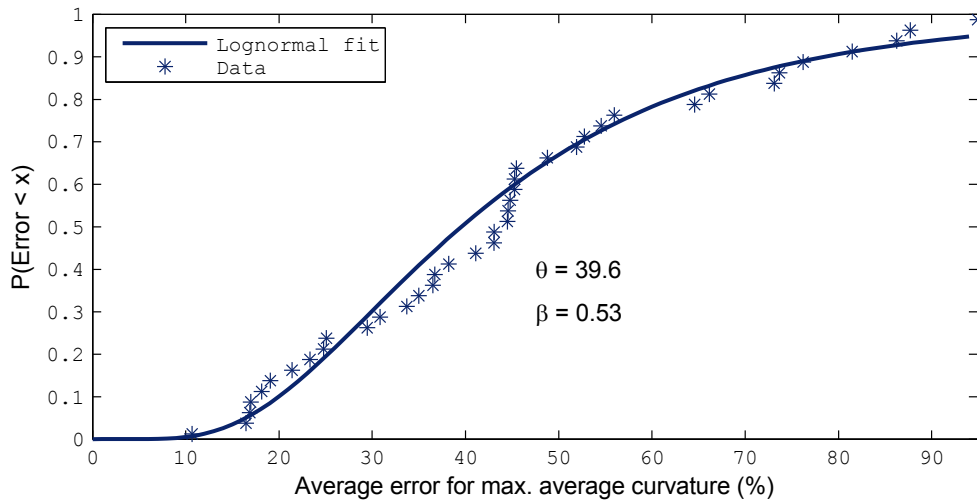


Figure 5.20 Lognormal distribution of average error in predicting maximum average curvature between 51 and 457 mm from the bottom of the column.

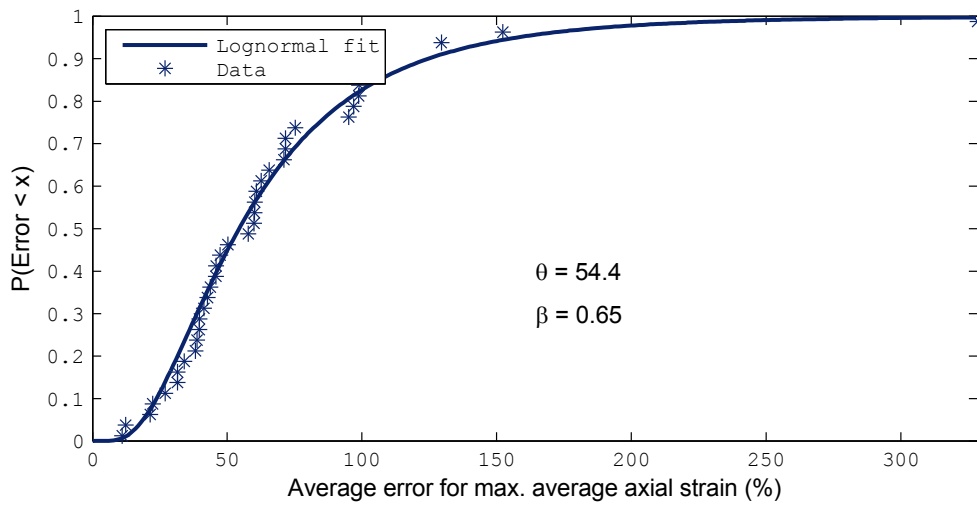


Figure 5.21 Lognormal distribution of average error in predicting maximum average axial strain between 51 and 457 mm from the bottom of the column.

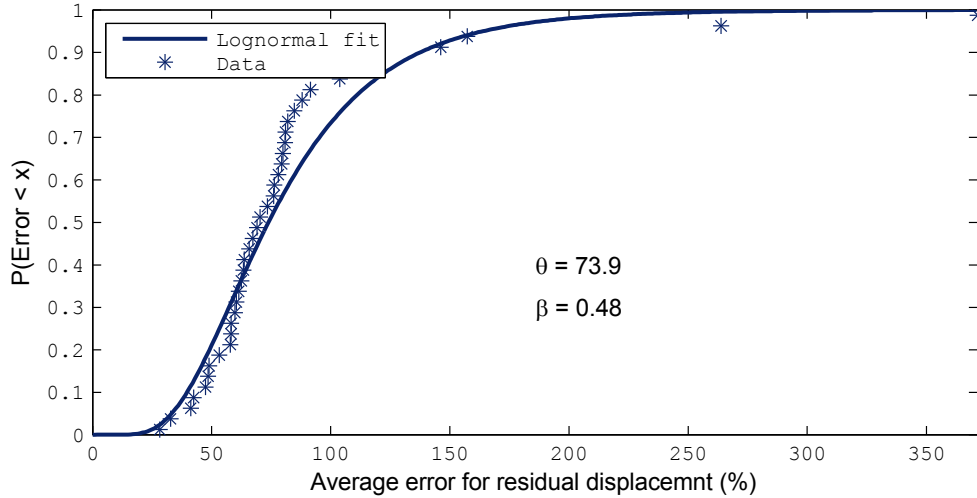


Figure 5.22 Lognormal distribution of average error in predicting residual displacement at the top of the column.

5.3 ERROR AS A FUNCTION OF DAMAGE STATE OF COLUMN AFTER AN EARTHQUAKE

Currently, lateral displacements and accelerations are the most used engineering demand parameters (EDPs) in the framework of PBEE analysis. Therefore, it is important to identify the distribution of error in predicting these response quantities over a range of earthquakes and for different damage states. The damage state of the column after each earthquake is described in Section 0.

The distribution of error in predicting a response quantity is presented in two formats: as cumulative error and as average error over a set of earthquakes. In both types of plots the error was disaggregated to show the contribution of each set of earthquakes to the cumulative or average error. Cumulative error and average error are calculated using Equations (5.2) and (5.3), respectively:

$$CumErr = \sum_{i=1}^n abs \left[\frac{(R_a - R_{exp})}{R_{exp}} \right] \quad (5.2)$$

$$AvgErrRC = \frac{1}{n} \sum_{i=1}^n abs \left[\frac{(R_a - R_{exp})}{R_{exp}} \right] \quad (5.3)$$

where n is the number of earthquakes considered, R_a is the analytically predicted response, and R_{exp} is a measured response.

Figure 5.23 shows the cumulative error [Equation (5.2)] in predicting the maximum horizontal displacement. The error in predicting the maximum displacement for EQ1, where the column response was only slightly nonlinear due to cracking of the concrete, has the largest contribution to the total error. The likely source for this large error is poor modeling of the elastic

modulus of concrete, which could have been derived from the measured concrete stress–strain relationships; instead, the contestants probably calculated it using standard equations.

Test EQ2 initiated nonlinear deformation of the column. The majority of contestants predicted the maximum displacement with significantly greater accuracy compared to those predictions for EQ1.

Test EQ3, the design-level earthquake, initiated spalling of concrete cover and had a residual drift ratio of -0.87%. The majority of contestants had a greater margin of error in predictions of the maximum displacement when compared to predictions for EQ2.

Test EQ4 was a repeat of EQ2, which enlarged the spalled region of concrete cover. The margin of error in predicting the maximum displacement was comparable to the margin of error found for predictions for EQ3.

Test EQ5 induced the most extensive damage resulting in column softening response [Figure 3.3(e)] and a residual drift ratio of 1.43%. The majority of contestants predicted it with smaller error relative to the other earthquakes. Note: this is an artifact because of the poorly predicted negative residual drift in EQ4 (median bias was approximately 50% and COV was approximately 110%) and the inability of models to capture softening response. Although the column started from a drift ratio of -0.81% and achieved a maximum drift of 7.78%, many models started from smaller values of negative residual drift (closer to zero) and had smaller overall drift due to their inability to capture the softening response. This resulted in a good prediction of the maximum drift but lacked fidelity of the true response.

Test EQ6 was a repeat of EQ3. All contestants predicted it with large errors. The reasons are poor prediction of positive residual drift in EQ5 (the median bias was approximately 75% and the COV was approximately 110%) and the models' inability to capture the softening response. Although the column started from a drift ratio of 1.43% and achieved maximum of 6.69%, the models started from smaller values of positive residual drift (closer to zero) and had smaller overall drift due to their inability to capture the softening response; this resulted in significant errors in predicting the maximum drift.

Figure 5.24 shows the average error [Equation (5.3)] in predicting the maximum horizontal displacement considering different numbers of earthquakes. The designation “n” on the plot represents the number of earthquakes considered when calculating the average error. Except for the ten best predictions (~25% of participants), the error in predicting the maximum displacement due to EQ1 was significantly greater than for any other earthquake.

Figure 5.25 shows the cumulative error for maximum horizontal acceleration, with contributions from each earthquake marked on the plots. For the first 14 (33%) contestants, the cumulative error increased almost linearly from 40 to 100%. From then on, the increase in the cumulative error was rapid. The worst prediction reached a cumulative error of almost 1200%. The maximum acceleration after the EQ4, which simulated an aftershock, was the most difficult to predict, while the best prediction was achieved for EQ1 (elastic column response). This can also be observed from Figure 5.26, which shows the average error in predicting the maximum horizontal acceleration considering different number of earthquakes.

The presented data indicate the difficulty in predicting the maximum displacement of the column in the following cases: (1) in the elastic range of behavior; (2) for significant damage that results in column softening response; and (3) if residual drifts are present in the column. Although it was difficult to predict displacement in the elastic range of behavior, most of the contestants successfully predicted the maximum acceleration of the column in that range. However, for earthquakes that induced nonlinear deformations in the column, the error in predicting horizontal acceleration increased significantly for the majority of contestants.

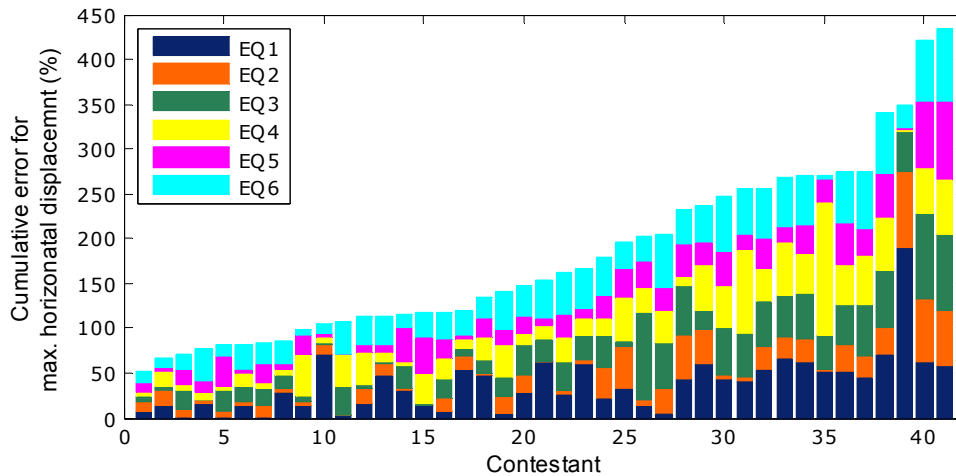


Figure 5.23 Cumulative error over six earthquakes in predicting maximum horizontal displacement at the top of the column.

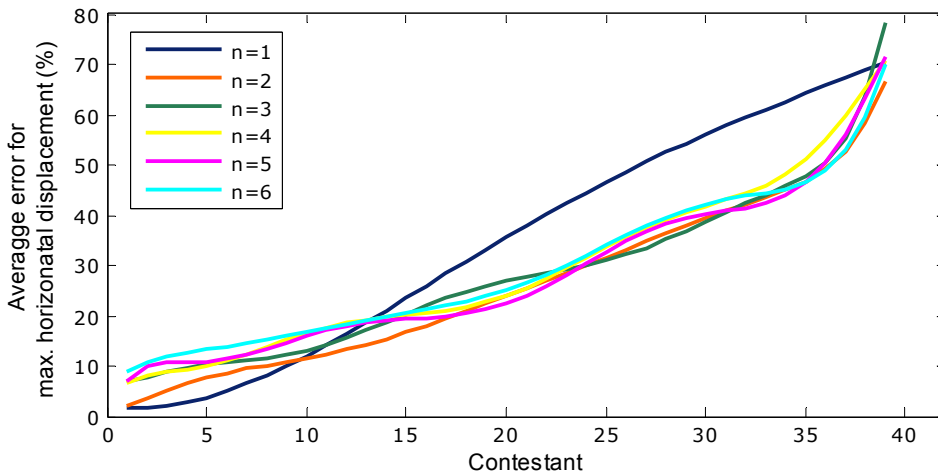
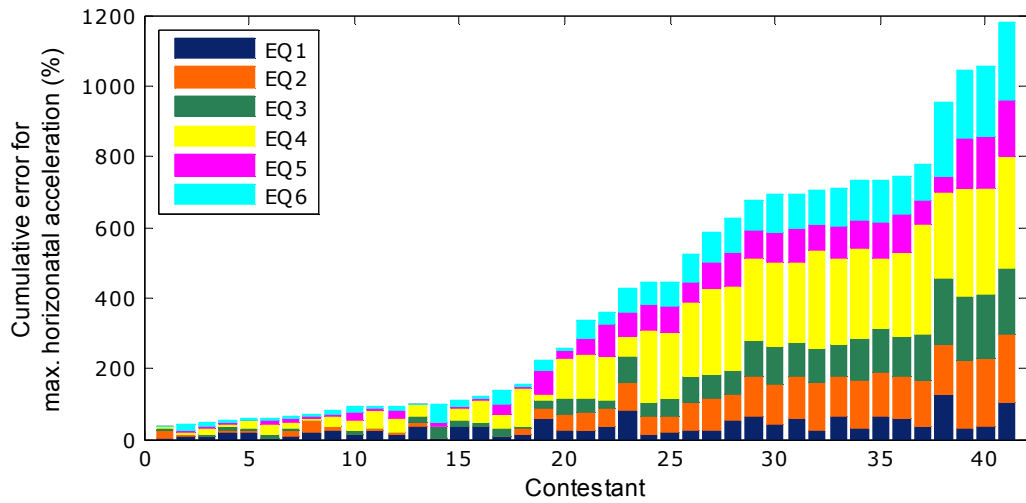
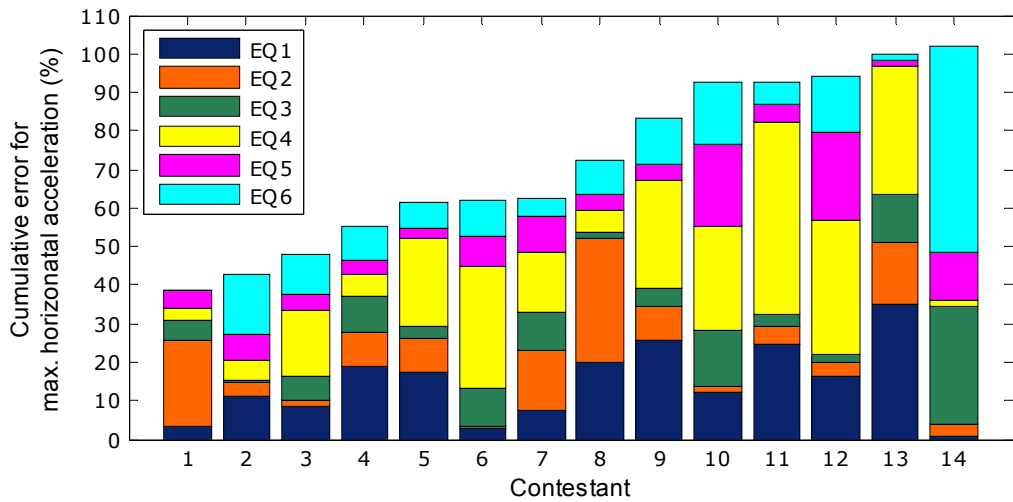


Figure 5.24 Average error in predicting maximum horizontal displacement at the top of the column considering different numbers of earthquakes (“n” represents number of considered earthquakes).



(a)



(b)

Figure 5.25 Cumulative error over six earthquakes in predicting maximum horizontal acceleration at the top of the column: (a) all contestants, and (b) the best 14 contestants.

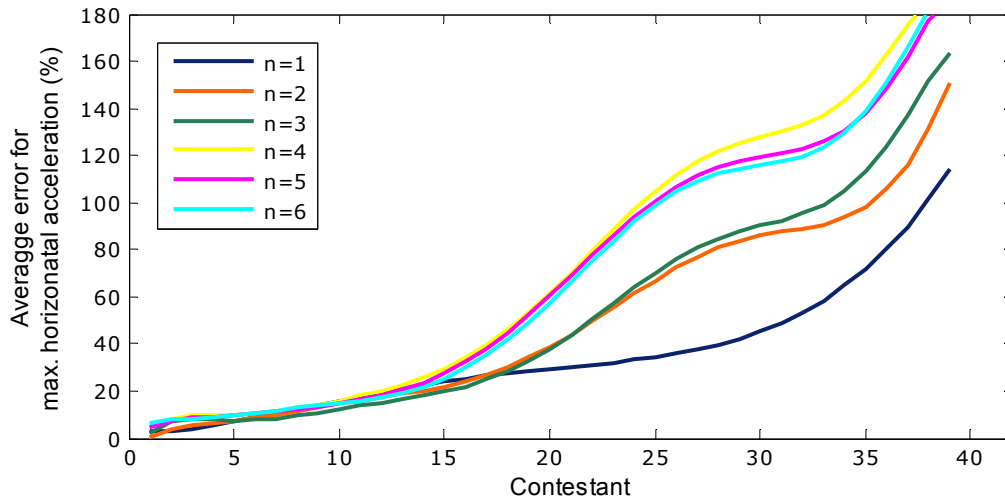


Figure 5.26 Average error in predicting maximum horizontal acceleration at the top of the column considering different numbers of earthquakes (“n” represents number of considered earthquakes).

6 Comparison of Numerical Models of Bridge Column

To enhance understanding of different modeling parameters on the accuracy of predictions, a questionnaire was sent to all participants. The questionnaire contained questions related to the following: software used for numerical simulations, model description (e.g., type of element, number of elements), mass and damping formulation, integration scheme, and output acceleration data signal processing. Twenty-five participants returned the questionnaire; their responses are presented in Appendix A. Each questionnaire has a number assigned to it that designates a contestant/team.

To study the accuracy of different models as a function of the element type used for modeling the bridge column, the questionnaire was divided into four groups. These four groups are labeled by the names of element types: force-based beam-column element (FB), displacement-based beam-column element (DB), beam-column element with distributed plastic hinges (DPH), and beam-column element with concentrated plastic hinges (CPH).

Figure 6.1 to Figure 6.12 show the average error over all earthquakes [calculated using Equation (5.1)] considering the requested response quantities (displacement, acceleration, bending moment, shear, axial force, curvature, axial strain, and residual displacement).

$$AvgErrRC = \frac{1}{j} \sum_{i=1}^j abs \left[\frac{(R_a - R_{exp})}{R_{exp}} \right] \quad (5.1)$$

The average errors are marked with different colors based on the element type used by a contestant. For one type of element, the contestants are ordered based on cumulative error over all response quantities, from smallest to highest. A contestant that used force based elements to model the column had the smallest overall cumulative error. However, the best predictions using other types of elements exhibited a comparable level of accuracy, demonstrating that a high level of accuracy can be achieved utilizing relatively simple numerical elements.

In addition, it was of interest to:

- identify a good damping model
- characterize the effect of rotational mass on the accuracy of the predictions

- define the optimal number of elements for FB and DB elements

Unfortunately, none of these modeling parameters could be extracted from the collected data as each model was too unique; these modeling properties had different weights within different models. For example, Contestants 1 and 7 used the same damping model and damping ratio, and yet had greatly different predictions. A comprehensive analytical study is needed to address these issues.

Although some of the contestants that utilized force-based beam-column elements to model the column predicted maximum horizontal acceleration at the top of the column (coinciding with the center of mass of the superstructure) with a good accuracy, most predicted maximum acceleration with enormously large average error (100–200%); see Figures 6.3 and 6.4). The reasons for such large errors need to be understood to prevent such false predictions from happening. Additionally, as shown in Figure 6.9, one contestant predicted the maximum compression force in the column with an average error of about 160%. The reason for this is probably a wrong estimate of the gravity load on the column. Such a case points out a lack of quality control that is unacceptable for the engineering profession.

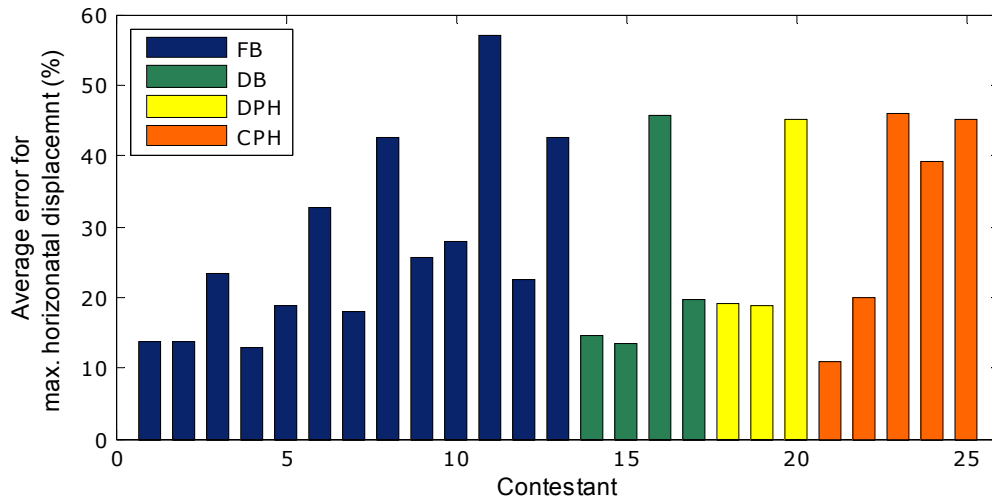


Figure 6.1 Average error over 6 earthquakes in predicting maximum horizontal displacement at the top of the column using four different element types: force based element (FB), displacement based element (DB), beam with distributed plastic hinges (DPH), and beam with concentrated plastic hinges (CPH).

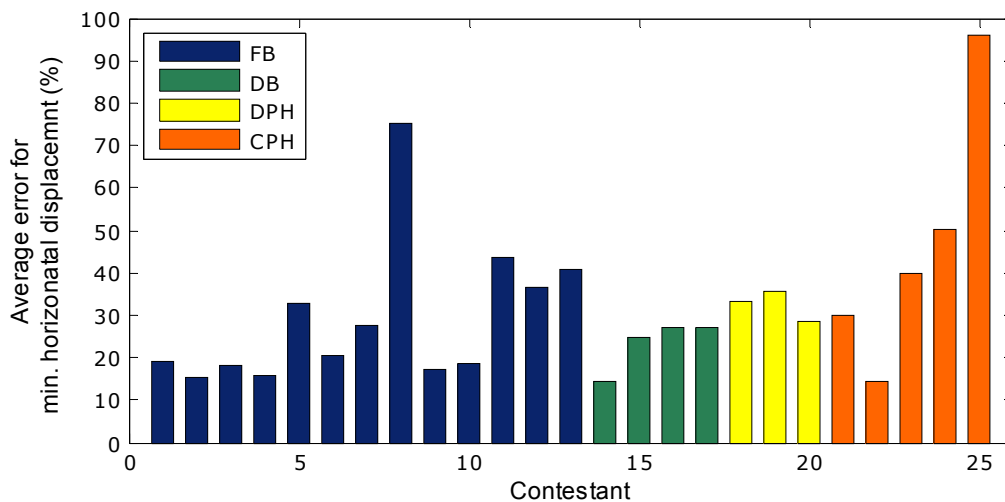


Figure 6.2 Average error over six earthquakes in predicting minimum horizontal displacement at the top of the column using four different element types: force based element (FB), displacement based element (DB), beam with distributed plastic hinges (DPH), and beam with concentrated plastic hinges (CPH).

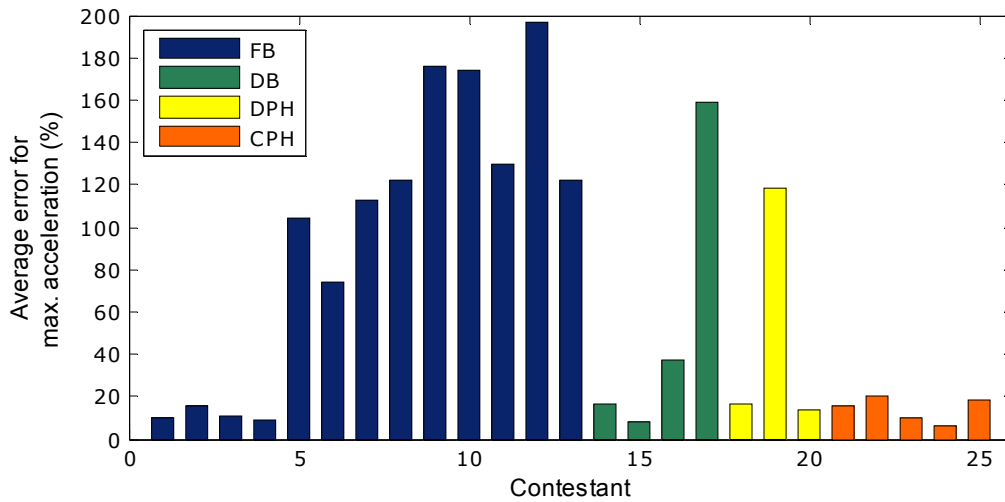


Figure 6.3 Average error over six earthquakes in predicting maximum horizontal acceleration at the top of the column using four different element types: force based element (FB), displacement based element (DB), beam with distributed plastic hinges (DPH), and beam with concentrated plastic hinges (CPH).

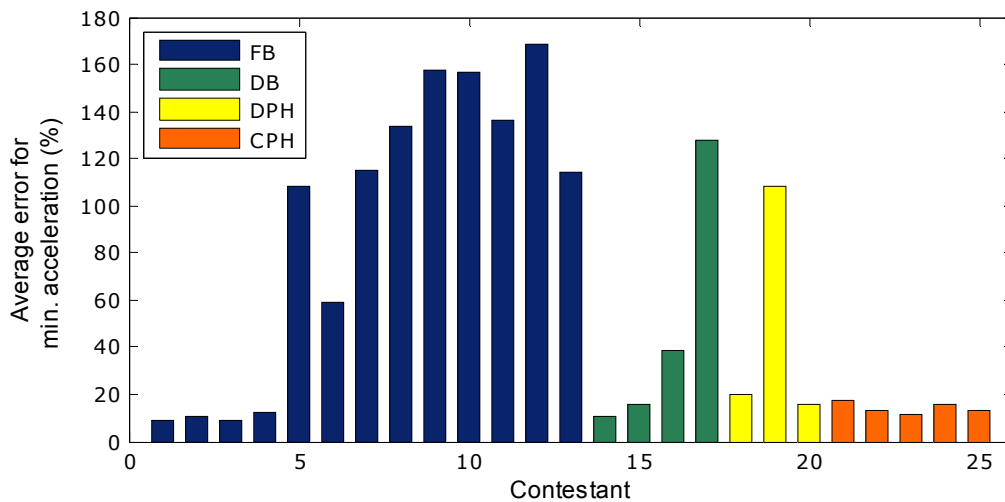


Figure 6.4 Average error over six earthquakes in predicting minimum horizontal acceleration at the top of the column using four different element types: force based element (FB), displacement based element (DB), beam with distributed plastic hinges (DPH), and beam with concentrated plastic hinges (CPH).

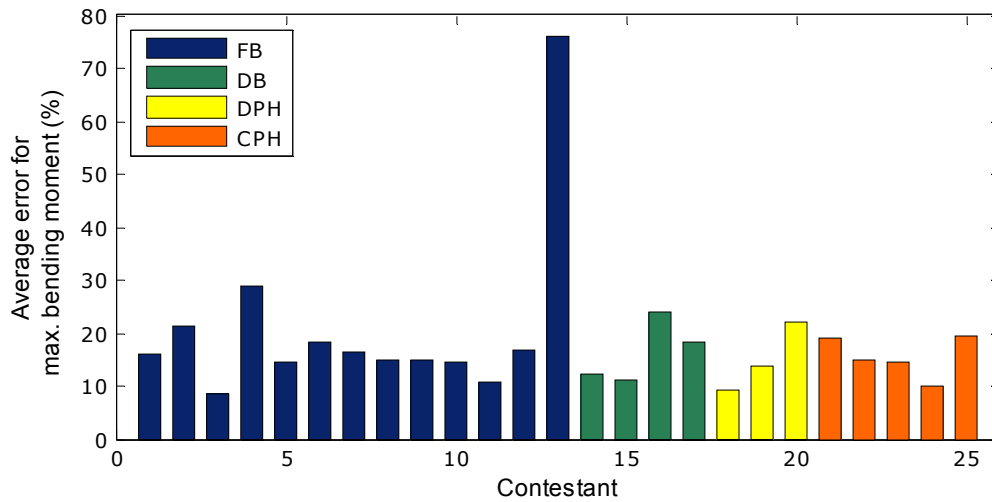


Figure 6.5 Average error over six earthquakes in predicting maximum bending moment at the base of the column using four different element types: force based element (FB), displacement based element (DB), beam with distributed plastic hinges (DPH), and beam with concentrated plastic hinges (CPH).

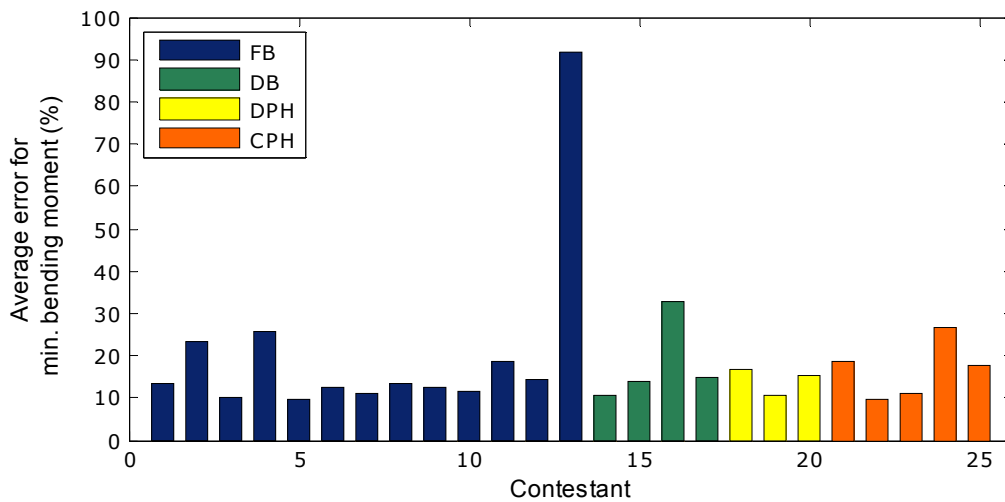


Figure 6.6 Average error over six earthquakes in predicting minimum bending moment at the base of the column using four different element types: force based element (FB), displacement based element (DB), beam with distributed plastic hinges (DPH), and beam with concentrated plastic hinges (CPH).

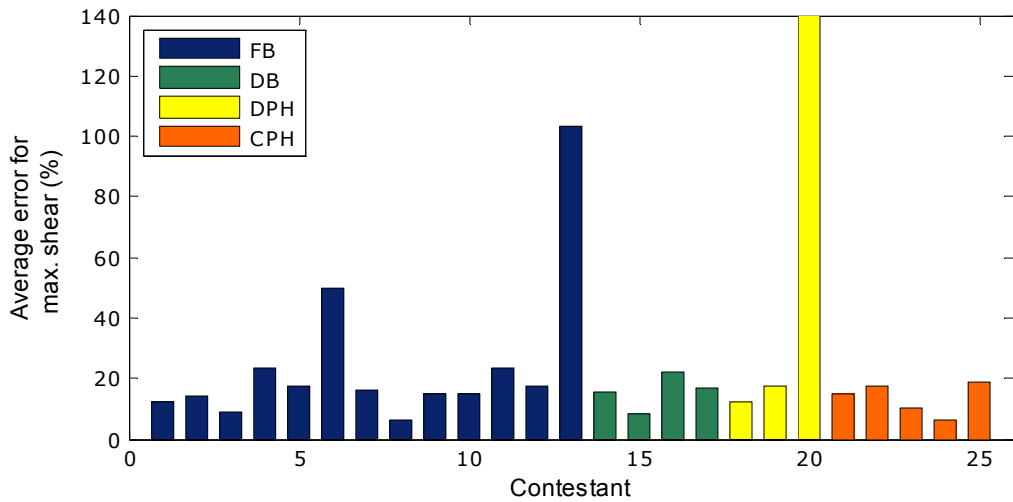


Figure 6.7 Average error over six earthquakes in predicting maximum shear at the base of the column using four different element types: force based element (FB), displacement based element (DB), beam with distributed plastic hinges (DPH), and beam with concentrated plastic hinges (CPH).

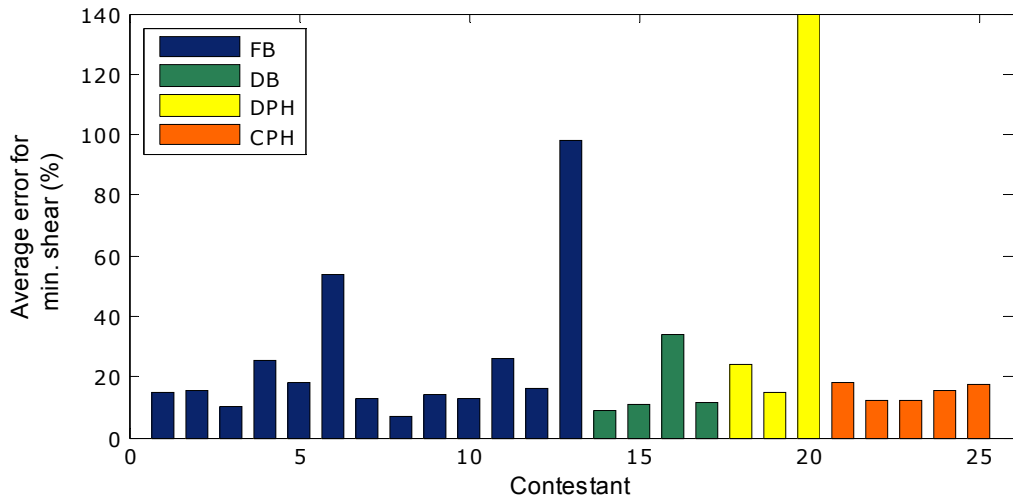


Figure 6.8 Average error over six earthquakes in predicting minimum shear at the base of the column using four different element types: force based element (FB), displacement based element (DB), beam with distributed plastic hinges (DPH), and beam with concentrated plastic hinges (CPH).

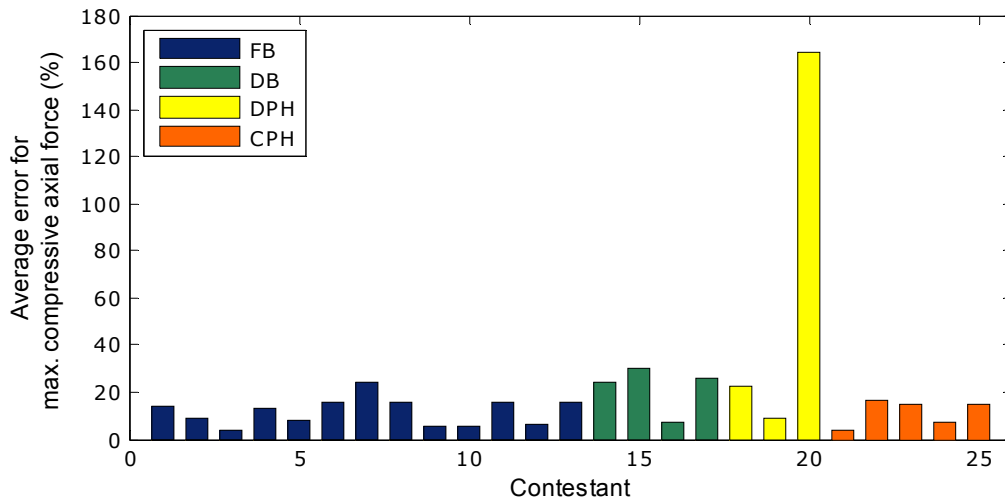


Figure 6.9 Average error over six earthquakes in predicting maximum compressive axial force using four different element types: force based element (FB), displacement based element (DB), beam with distributed plastic hinges (DPH), and beam with concentrated plastic hinges (CPH).

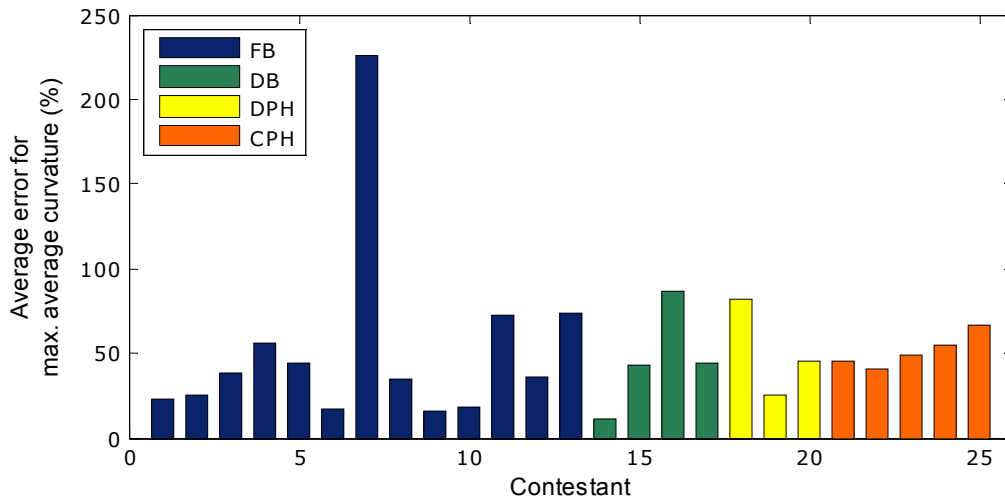


Figure 6.10 Average error over six earthquakes in predicting maximum average curvature between 51 and 457 mm from the bottom of the column using four different element types: force based element (FB), displacement based element (DB), beam with distributed plastic hinges (DPH), and beam with concentrated plastic hinges (CPH).

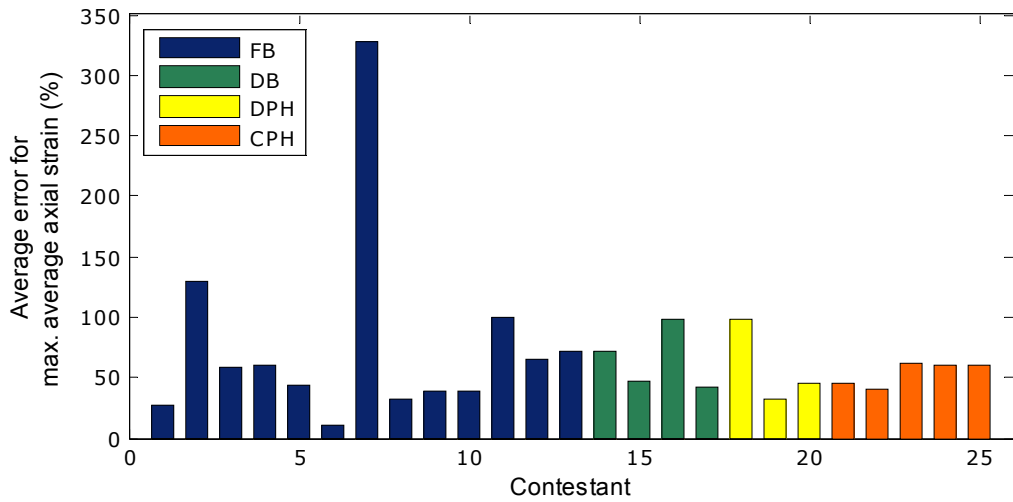


Figure 6.11 Average error over six earthquakes in predicting maximum average axial strain between 51 and 457 mm from the bottom of the column using four different element types: force based element (FB), displacement based element (DB), beam with distributed plastic hinges (DPH), and beam with concentrated plastic hinges (CPH).

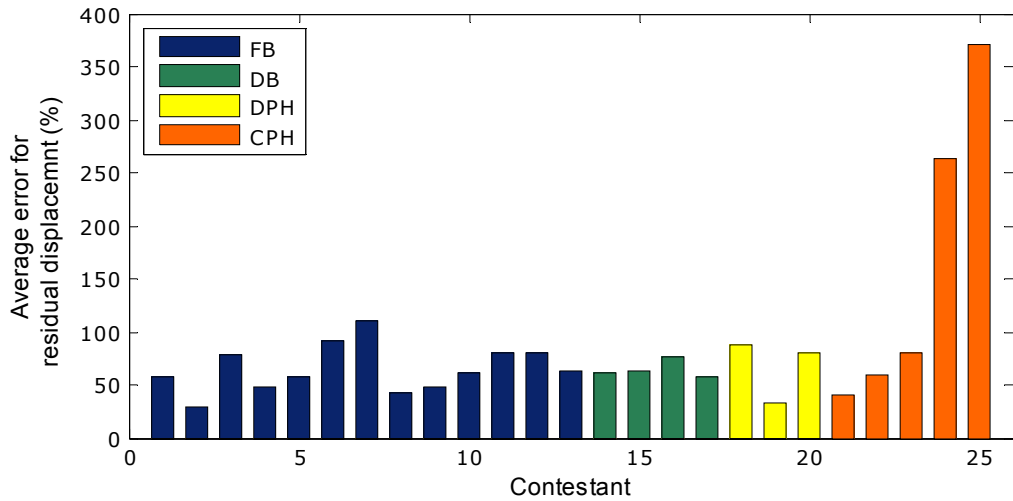


Figure 6.12 Average error over six earthquakes in predicting residual displacement at the top of the column using four different element types: force based element (FB), displacement based element (DB), beam with distributed plastic hinges (DPH), and beam with concentrated plastic hinges (CPH).

7 Summary and Conclusions

Based on the analysis of forty-one predictions of a bridge column peak responses subjected to six consecutive earthquakes, the following conclusions are drawn:

1. The forces at the base of the column were predicted with the best accuracy. The order of increasing accuracy was as follows: shear [median of the average error over six earthquakes (θ) was 18.3%], bending moment ($\theta = 16.3\%$), and compressive axial force ($\theta = 12.2\%$). The prediction of displacement at the top of the column was fair ($\theta = 25.6\%$). Horizontal acceleration at the top of the column ($\theta = 39.4\%$) and average curvature at the bottom of the column ($\theta = 39.6\%$) were not predicted with an acceptable degree of accuracy. The hardest parameter to predict was the average axial strain of the column close to the base ($\theta = 54.4\%$) and residual displacement ($\theta = 73.9\%$).
2. The dispersion in predicting each of the considered response quantities after each of the earthquakes was high. The average coefficient of variation (COV) over six earthquakes was the smallest and approximately (a) 30% for the forces at the base of the column, (b) 39% for displacements, (c) 47% for accelerations, (d) 63% for curvature, (e) 80% for axial strain of the column, and (f) more than 100% for residual displacement. Because some of the predictions were several magnitudes different than the measured response, it is suspected that some errors were not only due to false modeling assumptions, but also due to wrong unit conversions.
3. Horizontal peak displacement of the column was predicted with higher accuracy if the column sustained moderate amounts of damage than if it had minor or significant damage. The error in predicting the peak displacement for earthquake that displaced column within its elastic range had the largest contribution to the total error. The likely source for this large error was poor modeling of the elastic modulus of concrete. The error was also large if residual displacements and significant damage that resulted in a column softening response were induced by the set of earthquakes.
4. Horizontal peak accelerations were best predicted if the column was displaced within the elastic range of behavior. For the earthquakes that induced nonlinear deformations in the column, the error in predicting horizontal acceleration increased significantly for the majority of contestants.

The announced winners predicted well most of the column responses; however, some of the predictions were greatly inaccurate. To identify the winner, the four best predictions were awarded with 8, 5, 3, and 1 points (8 for the best prediction) for each of 69 entries, all points were then totaled, and the team with the greatest total was declared a winner. The same weight was given to each response quantity. Giving points to only four best predictions and not penalizing poor predictions have possibly skewed the results. To identify the winner with consistent predictions across all considered response quantities, different scoring schemes were analyzed. The cumulative error method, which is based on summation of errors in predicting each response quantity and is percentage rather than point-based, proved to be very effective in identifying the analytical model that predicted all response quantities with great accuracy.

The properties of submitted models were also studied to enhance understanding of different modeling parameters on the accuracy of predictions. It was observed that the comparable level of accuracy could be achieved if the column was modeled with complex force-based fiber beam-column elements and simpler beam-column element with concentrated plastic hinges. An attempt was also made to: (1) identify a good damping model, (2) characterize the effect of rotational mass on the accuracy of the predictions, and (3) define the optimal number of elements for FB and DB elements. None of this could be extracted from the collected data as each model was unique; therefore, these modeling properties had different weights within different models.

The results of this blind prediction contest provide data regarding the modeling uncertainty of modern bridge columns for use within performance-based earthquake evaluations. More than anything, these results stress the need for a comprehensive analytical study with the goal of producing guidelines to reduce the uncertainty in the modeling of bridge columns

Blind prediction contests provide (1) very useful information regarding areas where current numerical models might be improved, and (2) quantitative data regarding the uncertainty of analytical models for use in performance-based earthquake evaluations. Such blind prediction contest should be encouraged for other experimental tests.

REFERENCES

- ATC (1996). *Seismic Evaluation and Retrofit of Concrete Buildings*, ATC-40, Report No. SSC 96-01, Applied Technology Council, Redwood City, CA.
- Caltrans (2004). *Bridge Design Specifications*, California Department of Transportation, Sacramento, CA.
- Caltrans (2006). *Seismic Design Criteria*, California Department of Transportation, Sacramento, CA.
- Cornell C.A., Krawinkler H. (2000). Progress and challenges in seismic performance assessment, *PEER Center News*, Spring, 3(2).
- FEMA (1997). *NEHRP Recommended Provisions for the Seismic Regulations for new Buildings and other Structures*, Report No. FEMA-302, Federal Emergency Management Agency, Washington D.C.
- FEMA (2000a). *Prestandard and Commentary for the Seismic Rehabilitation of Buildings*, Report No. FEMA-356, Federal Emergency Management Agency, Washington D.C.
- FEMA (2000b). *Recommended Seismic Design Criteria for New Steel Moment-Frame Buildings*, Report No. FEMA-350, Federal Emergency Management Agency, Washington D.C.
- Krawinkler H. (1999). Challenges and progress in performance-based earthquake engineering, *Proceedings, International Seminar on Seismic Engineering for Tomorrow*, Tokyo, Japan.
- NEES (2010). NEES @ UC San Diego – Shake Table Specifications, <http://nees.ucsd.edu/facilities/shake-table.shtml>, (accessed October 2010).
- PEER (2007). PEER strong motion database: Introduction, Pacific Earthquake Engineering Research Center, Berkeley, CA, <http://peer.berkeley.edu/smcat/> (accessed July 2010).
- Schoettler M.J., Restrepo J.I., Guerrini G., Duck D.E., Carrea F. (2014). A full-scale, single-column bridge bent tested by shake-table excitation, *PEER Report No. 2015/02*, Pacific Earthquake Engineering Research Center, University of California, Berkeley, CA.
- SEAOC (1995). *Vision 2000 – A Framework for Performance Based Earthquake Engineering*, Vol. 1, Structural Engineers Association of California, Sacramento, CA.

Appendix A Questionnaires



Concrete Column Blind Prediction Contest 2010



Questionnaire - Contestant/Team #1

1	Nonlinear Analysis Program used (select program from drop down menu in cell C9)	OpenSees	Other:	
2	Model Description - Column modeling (type of element)	Force based beam-column	Other:	
3	Model Description - Column cross section discretization	Force-based fibers		
4	Model Description - Column vertical discretization	13 nodes		
5	Model Description - Strain penetration i.e. longitudinal bar bond-slip in footing (explain if answer is yes)	No	Explanation:	
6	Model Description - Material strain rate effect (explain if answer is yes)	No	Explanation:	
7	Model Description - Additional Information (optional)	The concrete constitutive model is Concrete 02 (unconfined concrete calibrated from provided test results (18 fibers in circular dir, 3 fibers in radial dir), confined concrete calculated after Mander (18 fibers in circular dir, 21 fibers in radial dir); the steel constitutive model is Reinforcing Steel of OpenSees (the properties are calibrated from the provided tests, the reinforcing steel material was wrapped with a MinMax material). The number of Gauss integration points of the force-based beam column element are 5. The element has a mass density of 0.00043167 kip-sec ² /in ³		
8	Mass block formulation	Lumped	Other:	
9	Inertial block mass discretization (answer if masses were lumped)	Lumped on 3DOFs	Other:	
10	Mass of inertial block (if mass was subdivided then show the sum of the masses)	234.5	kN-sec ² / m	
11	Rotational mass (only if calculated and applied to the rotary degree of freedom)	1057	kN-m-sec ²	
12	Damping model	Rayleigh - tangenl stiffness	Other:	
12a	Damping ratio 1	2	(%)	
12b	Corresponding frequency for damping ratio 1	1.13	Hz	
12c	Damping ratio 2	n/a	(%)	
12d	Corresponding frequency for damping ratio 2	n/a	Hz	
13	Were damping forces included in the calculation of forces M, V and P?	Yes		
14	Integration scheme	Newmark Method	Other:	Variable transient analysis with dtMin = 1e-6 and dtMax=0.00390625 and 10 iterations
15	Integration time-step	0.00390625	sec	
16	Type of analysis	Large-displacement theory		
17	Output acceleration data signal processing	Butterworth	Other:	
17a	Filter order (answer only if data was filtered)	4		
17b	Filter low-pass corner frequency (answer only if data was filtered)		Hz	
17c	Filter high-pass corner frequency (answer only if data was filtered)	0.1	Hz	
18	What was the greatest challenge/switch you came across while modeling and analyzing the column?	Choosing the damping model and the damping ratios		



Concrete Column Blind Prediction Contest 2010



Questionnaire - Contestant/Team #2

1	Nonlinear Analysis Program used (select program from drop down menu in cell C9)	Other (specify)	Other:	Seismostruct
2	Model Description - Column modeling (type of element)	Force based beam-column	Other:	
3	Model Description - Column cross section discretization	Force-based fibers		
4	Model Description - Column vertical discretization	11+ nodes		
5	Model Description - Strain penetration i.e. longitudinal bar bond-slip in footing (explain if answer is yes)	No	Explanation:	
6	Model Description - Material strain rate effect (explain if answer is yes)	No	Explanation:	
7	Model Description - Additional Information (optional)	Concrete constitutive law follows Mander et al. [1988], including the confinement effects as proposed therein, with cyclic rules as suggested by Martinez-Rueda and Elnashai [1997]; Steel constitutive law follows Menegotto and Pinto [1973], combined with the isotropic hardening rules proposed by Fillipou et al. [1983]. Longitudinal rebar buckling was not considered. The pier footing was also modeled as a linear elastic element, with a slightly reduced Young Modulus.		
8	Mass block formulation	Lumped	Other:	
9	Inertial block mass discretization (answer if masses were lumped)	Lumped on Hor and Ver DOFs only	Other:	
10	Mass of inertial block (if mass was subdivided then show the sum of the masses)	236.149	kN-sec ² / m	
11	Rotational mass (only if calculated and applied to the rotary degree of freedom)		kN-m-sec ²	
12	Damping model	Rayleigh - mass & tangenl stiffness	Other:	
12a	Damping ratio 1	1	(%)	
12b	Corresponding frequency for damping ratio 1	1.4708	Hz	
12c	Damping ratio 2	1	(%)	
12d	Corresponding frequency for damping ratio 2	0.6667	Hz	
13	Were damping forces included in the calculation of forces M, V and P?	No		
14	Integration scheme	Hilber-Hughes-Taylor Method	Other:	
15	Integration time-step	0.05	sec	
16	Type of analysis	Small-displacement theory		
17	Output acceleration data signal processing	None	Other:	
17a	Filter order (answer only if data was filtered)			
17b	Filter low-pass corner frequency (answer only if data was filtered)		Hz	
17c	Filter high-pass corner frequency (answer only if data was filtered)		Hz	
18	What was the greatest challenge/switch you came across while modeling and analyzing the column?	It probably was deciding how to set up the damping scheme. Which damping model to employ, which damping ratios to use, reporting to which frequencies... In fact, several things in respect to damping came as quite unclear choices. Led by team members' experience, of course, but regardless, every such option recognizes not only scientific insight as also an educated guess.		



Questionnaire - Contestant/Team #3

1	Nonlinear Analysis Program used (select program from drop down menu in cell C9)	Other (specify)	Other:	SeismoStruct
2	Model Description - Column modeling (type of element)	Force based beam-column	Other:	
3	Model Description - Column cross section discretization	Force-based fibers		
4	Model Description - Column vertical discretization	2 nodes		
5	Model Description - Strain penetration i.e. longitudinal bar bond-slip in footing (explain if answer is yes)	No	Explanation:	
6	Model Description - Material strain rate effect (explain if answer is yes)	No	Explanation:	
7	Model Description - Additional Information (optional)	Steel material used Menegotto-Pinto stress-strain relationship with isotropic hardening and Monti-Nuti buckling. Concrete cover material was a trilinear model with spalling. Core concrete used a Mander model with constant confinement, with confinement ratio calculated per Mander.		
8	Mass block formulation	Lumped	Other:	
9	Inertial block mass discretization (answer if masses were lumped)	Lumped on 3DOFs	Other:	
10	Mass of inertial block (if mass was subdivided then show the sum of the masses)	234.5	kN-sec ² / m	
11	Rotational mass (only if calculated and applied to the rotary degree of freedom)	1056.2	kN-m-sec ²	
12	Damping model	Rayleigh - tangenl stiffness	Other:	
12a	Damping ratio 1	1	(%)	
12b	Corresponding frequency for damping ratio 1	1.25	Hz	
12c	Damping ratio 2		(%)	
12d	Corresponding frequency for damping ratio 2		Hz	
13	Were damping forces included in the calculation of forces M, V and P?	No		
14	Integration scheme	Hilber-Hughes-Taylor Method	Other:	
15	Integration time-step	0.01	sec	
16	Type of analysis	Large-displacement theory		
17	Output acceleration data signal processing	Butterworth	Other:	
17a	Filter order (answer only if data was filtered)	4		
17b	Filter low-pass corner frequency (answer only if data was filtered)		Hz	
17c	Filter high-pass corner frequency (answer only if data was filtered)	0.1	Hz	
18	What was the greatest challenge/switch you came across while modeling and analyzing the column?			



Concrete Column Blind Prediction Contest 2010



Questionnaire - Contestant/Team #4

1	Nonlinear Analysis Program used (select program from drop down menu in cell C9)	OpenSees	Other:	
2	Model Description - Column modeling (type of element)	Force based beam-column	Other:	
3	Model Description - Column cross section discretization	Force-based fibers		
4	Model Description - Column vertical discretization	4 nodes		
5	Model Description - Strain penetration i.e. longitudinal bar bond-slip in footing (explain if answer is yes)	Yes	Explanation:	Priestley, Calvi, Kowalsky (2007) equation for strain penetration is used in a fiber finite element inside the foundation.
	Model Description - Material strain rate effect (explain if answer is yes)	No	Explanation:	
7	Model Description - Additional Information (optional)	Material Modeling. For reinforced concrete: Mander et al. (1988) constitutive law. For steel: Giuffre, Menegotto, Pinto (1973) constitutive law. Element properties: P-delta effects, fatigue model: Uriz, Mahin (2007).		
8	Mass block formulation	Lumped	Other:	
9	Inertial block mass discretization (answer if masses were lumped)	Other	Other:	Horizontal and rotational DOF at the top of the column
10	Mass of inertial block (if mass was subdivided then show the sum of the masses)	238		kN-sec ² / m
11	Rotational mass (only if calculated and applied to the rotary degree of freedom)	797		kN-m-sec ²
12	Damping model	Rayleigh - mass & initial stiffness	Other:	
12a	Damping ratio 1	3		(%)
12b	Corresponding frequency for damping ratio 1	1		Hz
12c	Damping ratio 2	3		(%)
12d	Corresponding frequency for damping ratio 2	5		Hz
13	Were damping forces included in the calculation of forces M, V and P?	No		
14	Integration scheme	Newmark Method	Other:	
15	Integration time-step	0.003906		sec
16	Type of analysis	Approximate P-Delta effects		
17	Output acceleration data signal processing	None	Other:	
17a	Filter order (answer only if data was filtered)			
17b	Filter low-pass corner frequency (answer only if data was filtered)			Hz
17c	Filter high-pass corner frequency (answer only if data was filtered)			Hz
18	What was the greatest challenge/switch you came across while modeling and analyzing the column?	The Fiber Finite Element Model (FFEM) was obtained calibrating response parameters of 30 columns laboratory tested under lateral reversible and increasing displacements by several authors and recalibrated to simulate the responses of two columns shake table tested by Hachem, Mahin, Moehle (2003). The FFEM was used for the contest.		



Questionnaire - Contestant/Team #5

1	Nonlinear Analysis Program used (select program from drop down menu in cell C9)	OpenSees	Other:	
2	Model Description - Column modeling (type of element)	Force based beam-column	Other:	
3	Model Description - Column cross section discretization	Force-based fibers		
4	Model Description - Column vertical discretization	3 nodes		
5	Model Description - Strain penetration i.e. longitudinal bar bond-slip in footing (explain if answer is yes)	Yes	Explanation:	
6	Model Description - Material strain rate effect (explain if answer is yes)	No	Explanation:	
7	Model Description - Additional Information (optional)	The concrete constitutive model was concrete02 and the steel constitutive model was steel02. No buckling was included in the steel model.		
8	Mass block formulation	Lumped	Other:	
9	Inertial block mass discretization (answer if masses were lumped)	Lumped on 3DOFs	Other:	
10	Mass of inertial block (if mass was subdivided then show the sum of the masses)	243.5	kN-sec ² / m	
11	Rotational mass (only if calculated and applied to the rotary degree of freedom)	755.1	kN-m-sec ²	
12	Damping model	Other	Other:	No damping/zero damping
12a	Damping ratio 1	0	(%)	
12b	Corresponding frequency for damping ratio 1		Hz	
12c	Damping ratio 2		(%)	
12d	Corresponding frequency for damping ratio 2		Hz	
13	Were damping forces included in the calculation of forces M, V and P?	No		
14	Integration scheme	Newmark Method	Other:	
15	Integration time-step	0.003906	sec	
16	Type of analysis	Approximate P-Delta effects		
17	Output acceleration data signal processing	None	Other:	
17a	Filter order (answer only if data was filtered)			
17b	Filter low-pass corner frequency (answer only if data was filtered)		Hz	
17c	Filter high-pass corner frequency (answer only if data was filtered)		Hz	
18	What was the greatest challenge/switch you came across while modeling and analyzing the column?	Strain Penetration Effect		



Concrete Column Blind Prediction Contest 2010



Questionnaire - Contestant/Team #6

1	Nonlinear Analysis Program used (select program from drop down menu in cell C9)	OpenSees	Other:	
2	Model Description - Column modeling (type of element)	Force based beam-column	Other:	
3	Model Description - Column cross section discretization	Force-based fibers		
4	Model Description - Column vertical discretization	6 nodes		
5	Model Description - Strain penetration i.e. longitudinal bar bond-slip in footing (explain if answer is yes)	Yes	Explanation:	Zero-length element with bar bond-slip to model strain penetration
6	Model Description - Material strain rate effect (explain if answer is yes)	Yes	Explanation:	
7	Model Description - Additional Information (optional)	uniaxial material: Concrete02 for cover and core concrete matching the result from the specimen test. Reinforcing steel material with Dhakal and Maekawa (2002) buckling model.		
8	Mass block formulation	Lumped	Other:	
9	Inertial block mass discretization (answer if masses were lumped)	Lumped on Hor and Ver DOFs only	Other:	
10	Mass of inertial block (if mass was subdivided then show the sum of the masses)	237.9		kN-sec ² / m
11	Rotational mass (only if calculated and applied to the rotary degree of freedom)			kN-m-sec ²
12	Damping model	Rayleigh - mass & initial stiffness	Other:	
12a	Damping ratio 1	5		(%)
12b	Corresponding frequency for damping ratio 1	0.86		Hz
12c	Damping ratio 2			(%)
12d	Corresponding frequency for damping ratio 2			Hz
13	Were damping forces included in the calculation of forces M, V and P?	No		
14	Integration scheme	Newmark Method	Other:	
15	Integration time-step	1/256		sec
16	Type of analysis	Approximate P-Delta effects		
17	Output acceleration data signal processing	None	Other:	
17a	Filter order (answer only if data was filtered)			
17b	Filter low-pass corner frequency (answer only if data was filtered)			Hz
17c	Filter high-pass corner frequency (answer only if data was filtered)			Hz
18	What was the greatest challenge/switch you came across while modeling and analyzing the column?	Accurately fitting the model to the material result, and guessing the concrete properties the day of the test. Checking the result with my estimation and understanding where I could improve in my future models and assumptions.		



Concrete Column Blind Prediction Contest 2010



Questionnaire - Contestant/Team #7

1	Nonlinear Analysis Program used (select program from drop down menu in cell C9)	OpenSees	Other:	Seismostruct
2	Model Description - Column modeling (type of element)	Force based beam-column	Other:	
3	Model Description - Column cross section discretization	Force-based fibers		
4	Model Description - Column vertical discretization	4 nodes		
5	Model Description - Strain penetration i.e. longitudinal bar bond-slip in footing (explain if answer is yes)	Yes	Explanation:	OpenSees has a model to include this. Default values were used
6	Model Description - Material strain rate effect (explain if answer is yes)	No	Explanation:	
7	Model Description - Additional Information (optional)	The model consisted of two beam column element. The element at the base was introduced to obtain the curvatures at the specific location requested. One zero length element was included at the base to model the strain penetration. The mass was lumped at the top node.		
8	Mass block formulation	Lumped	Other:	
9	Inertial block mass discretization (answer if masses were lumped)	Lumped on 3DOFs	Other:	
10	Mass of inertial block (if mass was subdivided then show the sum of the masses)	229.08		kN-sec ² / m
11	Rotational mass (only if calculated and applied to the rotary degree of freedom)	0		kN-m-sec ²
12	Damping model	Rayleigh - tangenl stiffness	Other:	
12a	Damping ratio 1	2		(%)
12b	Corresponding frequency for damping ratio 1	1.77		Hz
12c	Damping ratio 2			(%)
12d	Corresponding frequency for damping ratio 2			Hz
13	Were damping forces included in the calculation of forces M, V and P?	No		
14	Integration scheme	Newmark Method	Other:	
15	Integration time-step	0.005		sec
16	Type of analysis	Small-displacement theory		
17	Output acceleration data signal processing	None	Other:	
17a	Filter order (answer only if data was filtered)			
17b	Filter low-pass corner frequency (answer only if data was filtered)			Hz
17c	Filter high-pass corner frequency (answer only if data was filtered)			Hz
18	What was the greatest challenge/switch you came across while modeling and analyzing the column?	Selection of concrete model and introduction of the strain penetration element at the base. The location of the nodes of the elements was tricky so that one integration point would coincide with a specific location where curvature was requested		



Concrete Column Blind Prediction Contest 2010



Questionnaire - Contestant/Team #8

1	Nonlinear Analysis Program used (select program from drop down menu in cell C9)	Other (specify)	Other:	Engineer's Studio
2	Model Description - Column modeling (type of element)	Force based beam-column	Other:	
3	Model Description - Column cross section discretization	Force-based fibers		
4	Model Description - Column vertical discretization	2 nodes		
5	Model Description - Strain penetration i.e. longitudinal bar bond-slip in footing (explain if answer is yes)	No	Explanation:	
6	Model Description - Material strain rate effect (explain if answer is yes)	No	Explanation:	
7	Model Description - Additional Information (optional)			
8	Mass block formulation	Distributed	Other:	
9	Inertial block mass discretization (answer if masses were lumped)	Lumped on 3DOFs	Other:	
10	Mass of inertial block (if mass was subdivided then show the sum of the masses)	227.775		
11	Rotational mass (only if calculated and applied to the rotary degree of freedom)	653.96		
12	Damping model	Other	Other:	Only considering Hysteresis Damping for Columns
12a	Damping ratio 1			
12b	Corresponding frequency for damping ratio 1			
12c	Damping ratio 2			
12d	Corresponding frequency for damping ratio 2			
13	Were damping forces included in the calculation of forces M, V and P?	Yes		
14	Integration scheme	Newmark Method	Other:	
15	Integration time-step	1/256		
16	Type of analysis	Large-displacement theory		
17	Output acceleration data signal processing	None	Other:	
17a	Filter order (answer only if data was filtered)			
17b	Filter low-pass corner frequency (answer only if data was filtered)			
17c	Filter high-pass corner frequency (answer only if data was filtered)			
18	What was the greatest challenge/switch you came across while modeling and analyzing the column?	Unit system and American materials properties		



Concrete Column Blind Prediction Contest 2010



Questionnaire - Contestant/Team #9

1	Nonlinear Analysis Program used (select program from drop down menu in cell C9)	OpenSees	Other:	
2	Model Description - Column modeling (type of element)	Force based beam-column	Other:	
3	Model Description - Column cross section discretization	Force-based fibers		
4	Model Description - Column vertical discretization	4 nodes		
5	Model Description - Strain penetration i.e. longitudinal bar bond-slip in footing (explain if answer is yes)	No	Explanation:	
6	Model Description - Material strain rate effect (explain if answer is yes)	No	Explanation:	
7	Model Description - Additional Information (optional)	The concrete constitutive model is Concrete 02 of Opensees; the steel constitutive model is Steel 02 of Opensees. The number of Gauss integration points of the force-based beam column element are 4.		
8	Mass block formulation	Distributed	Other:	
9	Inertial block mass discretization (answer if masses were lumped)	Lumped on Hor DOF only	Other:	
10	Mass of inertial block (if mass was subdivided then show the sum of the masses)	233.35		kN-sec ² / m
11	Rotational mass (only if calculated and applied to the rotary degree of freedom)	0		kN-m-sec ²
12	Damping model	Rayleigh - mass & tangen stiffness	Other:	
12a	Damping ratio 1	0.3		(%)
12b	Corresponding frequency for damping ratio 1	1.608		Hz
12c	Damping ratio 2	1.2		(%)
12d	Corresponding frequency for damping ratio 2	2.008		Hz
13	Were damping forces included in the calculation of forces M, V and P?	No		
14	Integration scheme	Newmark Method	Other:	
15	Integration time-step	0.00389		sec
16	Type of analysis	Large-displacement theory		
17	Output acceleration data signal processing	None	Other:	
17a	Filter order (answer only if data was filtered)			
17b	Filter low-pass corner frequency (answer only if data was filtered)			Hz
17c	Filter high-pass corner frequency (answer only if data was filtered)			Hz
18	What was the greatest challenge/switch you came across while modeling and analyzing the column?	Chosing the damping model and the damping ratios		



Concrete Column Blind Prediction Contest 2010



Questionnaire - Contestant/Team #10

1	Nonlinear Analysis Program used (select program from drop down menu in cell C9)	OpenSees	Other:	
2	Model Description - Column modeling (type of element)	Force based beam-column	Other:	
3	Model Description - Column cross section discretization	Force-based fibers		
4	Model Description - Column vertical discretization	3 nodes		
5	Model Description - Strain penetration i.e. longitudinal bar bond-slip in footing (explain if answer is yes)	No	Explanation:	
6	Model Description - Material strain rate effect (explain if answer is yes)	No	Explanation:	
7	Model Description - Additional Information (optional)	The concrete constitutive model is Concrete 02 of Opensees; the steel constitutive model is Steel 02 of Opensees. The number of Gauss integration points of the force-based beam column element are 4.		
8	Mass block formulation	Distributed	Other:	
9	Inertial block mass discretization (answer if masses were lumped)	Lumped on Hor DOF only	Other:	
10	Mass of inertial block (if mass was subdivided then show the sum of the masses)	233.35		kN-sec ² / m
11	Rotational mass (only if calculated and applied to the rotary degree of freedom)	0		kN-m-sec ²
12	Damping model	Rayleigh - mass & tangen stiffness	Other:	
12a	Damping ratio 1	0.3		(%)
12b	Corresponding frequency for damping ratio 1	1.76		Hz
12c	Damping ratio 2	1.2		(%)
12d	Corresponding frequency for damping ratio 2	2.16		Hz
13	Were damping forces included in the calculation of forces M, V and P?	No		
14	Integration scheme	Newmark Method	Other:	
15	Integration time-step	0.00389		sec
16	Type of analysis	Large-displacement theory		
17	Output acceleration data signal processing	None	Other:	
17a	Filter order (answer only if data was filtered)			
17b	Filter low-pass corner frequency (answer only if data was filtered)			Hz
17c	Filter high-pass corner frequency (answer only if data was filtered)			Hz
18	What was the greatest challenge/switch you came across while modeling and analyzing the column?	Chosing the damping model and the damping ratios		



Concrete Column Blind Prediction Contest 2010



Questionnaire - Contestant/Team #11

1	Nonlinear Analysis Program used (select program from drop down menu in cell C9)	OpenSees	Other:	
2	Model Description - Column modeling (type of element)	Force based beam-column	Other:	
3	Model Description - Column cross section discretization	Force-based fibers		
4	Model Description - Column vertical discretization	11+ nodes		
5	Model Description - Strain penetration i.e. longitudinal bar bond-slip in footing (explain if answer is yes)	No	Explanation:	
6	Model Description - Material strain rate effect (explain if answer is yes)	No	Explanation:	
7	Model Description - Additional Information (optional)	The section was discretize using Fiber Section. The core and cover concrete were modeled using concrete02 material. The steel was modeled using Steel02 material. The footing was not modeled as a reinforced concrete. Instead, assuming a linear behavior, it was modeled as a linear element with a flexural stiffness of a concrete box. This wasn't probably a good assumption.		
8	Mass block formulation	Lumped	Other:	
9	Inertial block mass discretization (answer if masses were lumped)	Lumped on Hor and Ver DOFs only	Other:	
10	Mass of inertial block (if mass was subdivided then show the sum of the masses)	231.9		kN-sec ² / m
11	Rotational mass (only if calculated and applied to the rotary degree of freedom)			kN-m-sec ²
12	Damping model	Rayleigh - mass & initial stiffness	Other:	
12a	Damping ratio 1	5		(%)
12b	Corresponding frequency for damping ratio 1	1		Hz
12c	Damping ratio 2	5		(%)
12d	Corresponding frequency for damping ratio 2	2		Hz
13	Were damping forces included in the calculation of forces M, V and P?	No		
14	Integration scheme	Newmark Method	Other:	
15	Integration time-step	0.00390625		sec
16	Type of analysis	Approximate P-Delta effects		
17	Output acceleration data signal processing	None	Other:	
17a	Filter order (answer only if data was filtered)			
17b	Filter low-pass corner frequency (answer only if data was filtered)			Hz
17c	Filter high-pass corner frequency (answer only if data was filtered)			Hz
18	What was the greatest challenge/switch you came across while modeling and analyzing the column?	Modeling the footing.		



Concrete Column Blind Prediction Contest 2010



Questionnaire - Contestant/Team #12

1	Nonlinear Analysis Program used (select program from drop down menu in cell C9)	OpenSees	Other:	
2	Model Description - Column modeling (type of element)	Force based beam-column	Other:	
3	Model Description - Column cross section discretization	Force-based fibers		
4	Model Description - Column vertical discretization	4 nodes		
5	Model Description - Strain penetration i.e. longitudinal bar bond-slip in footing (explain if answer is yes)	No	Explanation:	
6	Model Description - Material strain rate effect (explain if answer is yes)	No	Explanation:	
7	Model Description - Additional Information (optional)	The concrete constitutive model is Concrete 02 of opensees; the steel constitutive model is Steel 02 of Opensees. The number of Gauss integration points of the force-based beam column element are 4.		
8	Mass block formulation	Distributed	Other:	
9	Inertial block mass discretization (answer if masses were lumped)	Lumped on Hor DOF only	Other:	
10	Mass of inertial block (if mass was subdivided then show the sum of the masses)	249.7	kN-sec ² / m	
11	Rotational mass (only if calculated and applied to the rotary degree of freedom)	0	kN-m-sec ²	
12	Damping model	Rayleigh - mass & tangenl stiffness	Other:	
12a	Damping ratio 1	0.003	(%)	
12b	Corresponding frequency for damping ratio 1	1.608	Hz	
12c	Damping ratio 2	0.012	(%)	
12d	Corresponding frequency for damping ratio 2	2.008	Hz	
13	Were damping forces included in the calculation of forces M, V and P?	No		
14	Integration scheme	Newmark Method	Other:	
15	Integration time-step	0.00389	sec	
16	Type of analysis	Large-displacement theory		
17	Output acceleration data signal processing	None	Other:	
17a	Filter order (answer only if data was filtered)			
17b	Filter low-pass corner frequency (answer only if data was filtered)		Hz	
17c	Filter high-pass corner frequency (answer only if data was filtered)		Hz	
18	What was the greatest challenge/switch you came across while modeling and analyzing the column?	Chosing the damping model and the damping ratios		



Questionnaire - Contestant/Team #13

1	Nonlinear Analysis Program used (select program from drop down menu in cell C9)	OpenSees	Other:	
2	Model Description - Column modeling (type of element)	Force based beam-column	Other:	
3	Model Description - Column cross section discretization	Force-based fibers		
4	Model Description - Column vertical discretization	4 nodes		
5	Model Description - Strain penetration i.e. longitudinal bar bond-slip in footing (explain if answer is yes)	No	Explanation:	
6	Model Description - Material strain rate effect (explain if answer is yes)	No	Explanation:	
7	Model Description - Additional Information (optional)			
8	Mass block formulation	Lumped	Other:	
9	Inertial block mass discretization (answer if masses were lumped)	Lumped on Hor and Ver DOFs only	Other:	
10	Mass of inertial block (if mass was subdivided then show the sum of the masses)	228.85		kN-sec ² / m
11	Rotational mass (only if calculated and applied to the rotary degree of freedom)	0		kN-m-sec ²
12	Damping model	Rayleigh - mass & initial stiffness	Other:	
12a	Damping ratio 1	5		(%)
12b	Corresponding frequency for damping ratio 1	1.63		Hz
12c	Damping ratio 2	5		(%)
12d	Corresponding frequency for damping ratio 2	1.63		Hz
13	Were damping forces included in the calculation of forces M, V and P?	No		
14	Integration scheme	Newmark Method	Other:	
15	Integration time-step	0.00390625		sec
16	Type of analysis	Large-displacement theory		
17	Output acceleration data signal processing	None	Other:	
17a	Filter order (answer only if data was filtered)			
17b	Filter low-pass corner frequency (answer only if data was filtered)			Hz
17c	Filter high-pass corner frequency (answer only if data was filtered)			Hz
18	What was the greatest challenge/switch you came across while modeling and analyzing the column?			



Concrete Column Blind Prediction Contest 2010



Questionnaire - Contestant/Team #14

1	Nonlinear Analysis Program used (select program from drop down menu in cell C9)	Other (specify)	Other:	SeismoStruct
2	Model Description - Column modeling (type of element)	Displacement based beam-column	Other:	
3	Model Description - Column cross section discretization	Displacement-based fibers		
4	Model Description - Column vertical discretization	9 nodes		
5	Model Description - Strain penetration i.e. longitudinal bar bond-slip in footing (explain if answer is yes)	No	Explanation:	
6	Model Description - Material strain rate effect (explain if answer is yes)	No	Explanation:	
7	Model Description - Additional Information (optional)	Material constitutive relationships: The concrete was represented through a nonlinear constant confinement concrete model; it is a uniaxial nonlinear model following the constitutive relationship proposed by Mander et al. (1988), later modified by Martinez-Rueda and Elnashai (1997). The reinforcing steel was represented through the Menegotto-Pinto steel model (1973), as modified by Filippou et al. (1983) to include isotropic strain hardening. Buckling wasn't considered in the analysis.		
8	Mass block formulation	Lumped	Other:	
9	Inertial block mass discretization (answer if masses were lumped)	Lumped on 3DOFs	Other:	
10	Mass of inertial block (if mass was subdivided then show the sum of the masses)	228	kN-sec ² / m	
11	Rotational mass (only if calculated and applied to the rotary degree of freedom)	885	kN-m-sec ²	
12	Damping model	Other	Other:	None
12a	Damping ratio 1	-	(%)	
12b	Corresponding frequency for damping ratio 1	-	Hz	
12c	Damping ratio 2	-	(%)	
12d	Corresponding frequency for damping ratio 2	-	Hz	
13	Were damping forces included in the calculation of forces M, V and P?	No		
14	Integration scheme	Hilber-Hughes-Taylor Method	Other:	
15	Integration time-step	0.0039065	sec	
16	Type of analysis	Large-displacement theory		
17	Output acceleration data signal processing	None	Other:	
17a	Filter order (answer only if data was filtered)			
17b	Filter low-pass corner frequency (answer only if data was filtered)		Hz	
17c	Filter high-pass corner frequency (answer only if data was filtered)		Hz	
18	What was the greatest challenge/switch you came across while modeling and analyzing the column?			



Questionnaire - Contestant/Team #15

1	Nonlinear Analysis Program used (select program from drop down menu in cell C9)	Abaqus	Other:	
2	Model Description - Column modeling (type of element)	Displacement based beam-column	Other:	
3	Model Description - Column cross section discretization	Displacement-based fibers		
4	Model Description - Column vertical discretization	11+ nodes		
5	Model Description - Strain penetration i.e. longitudinal bar bond-slip in footing (explain if answer is	No	Explanation:	
6	Model Description - Material strain rate effect (explain if answer is yes)	No	Explanation:	
7	Model Description - Additional Information (optional)	Concrete fiber constitutive is similar to concrete02 in OpenSEES where stiffness deterioration is included. Steel fiber incorporated strength deterioration feature but seemed not an important issue in this analysis.		
8	Mass block formulation	Lumped	Other:	
9	Inertial block mass discretization (answer if masses were lumped)	Select	Other:	
10	Mass of inertial block (if mass was subdivided then show the sum of the masses)	249.9		kN-sec ² / m
11	Rotational mass (only if calculated and applied to the rotary degree of			kN-m-sec ²
12	Damping model	Other	Other:	Mass proportional
12a	Damping ratio 1	2		(%)
12b	Corresponding frequency for damping ratio 1	1.642		Hz
12c	Damping ratio 2			(%)
12d	Corresponding frequency for damping ratio 2			Hz
13	Were damping forces included in the calculation of forces M, V and P?	No		
14	Integration scheme	Hilber-Hughes-Taylor Method	Other:	
15	Integration time-step	0.04		sec
16	Type of analysis	Large-displacement theory		
17	Output acceleration data signal processing	None	Other:	
17a	Filter order (answer only if data was filtered)			
17b	Filter low-pass corner frequency (answer only if data was filtered)			Hz
17c	Filter high-pass corner frequency (answer only if data was filtered)			Hz
18	What was the greatest challenge/switch you came across while modeling and analyzing the column?	None		



Questionnaire - Contestant/Team #16

1	Nonlinear Analysis Program used (select program from drop down menu in cell C9)	Other (specify)	Other:	SAP Release 14
2	Model Description - Column modeling (type of element)	Displacement based beam-column	Other:	
3	Model Description - Column cross section discretization	Displacement-based fibers		
4	Model Description - Column vertical discretization	6 nodes		
5	Model Description - Strain penetration i.e. longitudinal bar bond-slip in footing (explain if answer is yes)	No	Explanation:	
6	Model Description - Material strain rate effect (explain if answer is yes)	No	Explanation:	
7	Model Description - Additional Information (optional)	Interaction with the column footing and response of the footing was not modeled (ie. fixed column base). We expect this contributed largely to our model reporting smaller displacements than the test specimen.		
8	Mass block formulation	Lumped	Other:	
9	Inertial block mass discretization (answer if masses were lumped)	Lumped on 3DOFs	Other:	
10	Mass of inertial block (if mass was subdivided then show the sum of the masses)	243.4	kN-sec ² / m	
11	Rotational mass (only if calculated and applied to the rotary degree of freedom)		kN-m-sec ²	
12	Damping model	Rayleigh - mass & initial stiffness	Other:	M & K directly specified in model
12a	Damping ratio 1	Mass coefficient = 1.81	(%)	
12b	Corresponding frequency for damping ratio 1	0.75	Hz	
12c	Damping ratio 2	Stiffness coefficient = 0.00053	(%)	
12d	Corresponding frequency for damping ratio 2	26.1	Hz	
13	Were damping forces included in the calculation of forces M, V and P?	No		
14	Integration scheme	Hilber-Hughes-Taylor Method	Other:	
15	Integration time-step	0.0039	sec	
16	Type of analysis	Approximate P-Delta effects		
17	Output acceleration data signal processing	None	Other:	
17a	Filter order (answer only if data was filtered)			
17b	Filter low-pass corner frequency (answer only if data was filtered)		Hz	
17c	Filter high-pass corner frequency (answer only if data was filtered)		Hz	
18	What was the greatest challenge/switch you came across while modeling and analyzing the column?	Initial elastic stiffness of concrete.		



Questionnaire - Contestant/Team #17

1	Nonlinear Analysis Program used (select program from drop down menu in cell C9)	OpenSees	Other:	SAP2000
2	Model Description - Column modeling (type of element)	Displacement based beam-column	Other:	
3	Model Description - Column cross section discretization	Displacement-based fibers		
4	Model Description - Column vertical discretization	2 nodes		
5	Model Description - Strain penetration i.e. longitudinal bar bond-slip in footing (explain if answer is yes)	No	Explanation:	
6	Model Description - Material strain rate effect (explain if answer is yes)	No	Explanation:	
7	Model Description - Additional Information (optional)			
8	Mass block formulation	Lumped	Other:	
9	Inertial block mass discretization (answer if masses were lumped)	Lumped on 3DOFs	Other:	
10	Mass of inertial block (if mass was subdivided then show the sum of the masses)	244.9		kN-sec ² / m
11	Rotational mass (only if calculated and applied to the rotary degree of freedom)	0		kN-m-sec ²
12	Damping model	Rayleigh - tangenl stiffness	Other:	
12a	Damping ratio 1	5		(%)
12b	Corresponding frequency for damping ratio 1	1.13		Hz
12c	Damping ratio 2	5		(%)
12d	Corresponding frequency for damping ratio 2	N/A		Hz
13	Were damping forces included in the calculation of forces M, V and P?	No		
14	Integration scheme	Newmark Method	Other:	
15	Integration time-step	0.0039		sec
16	Type of analysis	Approximate P-Delta effects		
17	Output acceleration data signal processing	None	Other:	
17a	Filter order (answer only if data was filtered)			
17b	Filter low-pass corner frequency (answer only if data was filtered)			Hz
17c	Filter high-pass corner frequency (answer only if data was filtered)			Hz
18	What was the greatest challenge/switch you came across while modeling and analyzing the column?			



Questionnaire - Contestant/Team #18

- 1 Nonlinear Analysis Program used
(select program from drop down menu in cell C9)
- 2 Model Description - Column modeling (type of element)
- 3 Model Description - Column cross section discretization
- 4 Model Description - Column vertical discretization
- 5 Model Description - Strain penetration
i.e. longitudinal bar bond-slip in footing (explain if answer is yes)
- 6 Model Description - Material strain rate effect (explain if answer is yes)
- 7 Model Description - Additional Information (optional)

ANSR II		
Beam with distributed plastic hinges		
Lumped Plasticity		
10 nodes		
No		
No		
Bi-linear backbone curve, with 2.5% strain hardening (post-yield stiffness). Cracked section properties were assumed by applying stiffness reduction factors based on the recommendations of NZS 3101:2006 for columns subjected to high ductility demands and low levels of axial load. Strength degradation was based on ASCE 41-06 Supplement 1 provisions. Unloading stiffness was degrading using $\alpha=0.3$ per Prestley, Seible & Calvi ("Seismic Design & Retrofit of Bridges"), which is probably reasonable for a well confined reinforced concrete section. Parameters such as strain hardening and verification that failure mechanisms such as bar rupture would not occur at the maximum expected curvature demand were obtained from a preliminary moment-curvature analysis of the section. The moment-curvature analysis used the Mander Model and incorporated a pseudo-cyclic (simplified) moment-curvature analysis to account for Bauschinger Effects in the longitudinal		
Lumped		
Multiple Lumped Masses in Hor and Ver DOFs		
228	kN-sec ² / m	
		kN-m-sec ²
Rayleigh - mass & initial stiffness		
2.5	(%)	
0.77	Hz	
2.5	(%)	
4.35	Hz	
Yes		
Newmark Method		
0.00005	sec	
Large-displacement theory		
None		

- 8 Mass block formulation
- 9 Inertial block mass discretization (answer if masses were lumped)
- 10 Mass of inertial block
(if mass was subdivided then show the sum of the masses)
- 11 Rotational mass
(only if calculated and applied to the rotary degree of freedom)
- 12 Damping model
- 12a Damping ratio 1
- 12b Corresponding frequency for damping ratio 1
- 12c Damping ratio 2
- 12d Corresponding frequency for damping ratio 2
- 13 Were damping forces included in the calculation of forces M, V and P?
- 14 Integration scheme
- 15 Integration time-step
- 16 Type of analysis
- 17 Output acceleration data signal processing

18 What was the greatest challenge/switch you came across while modeling and analyzing the column?

1. Selection of an appropriate time step provided to be an iterative process. Initial time step estimates (of similar duration to supplied record time step) resulted in convergence issues with the analysis, likely due to the highly non-linear and degrading response. Thus, the time step was established by progressively reducing the duration until the analysis was stable and peak response results "converged" with the preceding larger time step. 2. Establishing initial model parameters that would be suitable for use throughout all of the 6 sequentially applied earthquakes proved to be an iterative and somewhat judgement based process. This applied to the following parameters in particular: stiffness degradation, cracked section modifiers (eg assume fully cracked section properties from the outset, as this could only be defined at the start?) & damping. As an aside, in a "design office" environment we would typically attempt to capture the response sensitivity by bounding these parameters, running multiple earthquake records (non-sequentially) and perhaps enveloping or averaging the response; but the sequential and highly non-linear nature of the experimental test sequence made this approach overly conservative and thus inappropriate. For example, using our in-house default modeling parameters for the initial analyses, it was interesting to note that the model suggested collapse under the intermediate levels of shaking (excessive displacement due to P-delta effects).



Concrete Column Blind Prediction Contest 2010



Questionnaire - Contestant/Team #19

1	Nonlinear Analysis Program used (select program from drop down menu in cell C9)	OpenSees	Other:	CUMBIA
2	Model Description - Column modeling (type of element)	Beam with distributed plastic hinges	Other:	
3	Model Description - Column cross section discretization	Force-based fibers		
4	Model Description - Column vertical discretization	2 nodes		
5	Model Description - Strain penetration i.e. longitudinal bar bond-slip in footing (explain if answer is yes)	Yes	Explanation:	Accounted for in the plastic hinge length
6	Model Description - Material strain rate effect (explain if answer is yes)	No	Explanation:	
7	Model Description - Additional Information (optional)	ReinforcedSteelMaterial was used to model cyclic degradation. Concrete01 with parameters estimated using Mander (98) model was used to model confined and unconfined concrete		
8	Mass block formulation	Lumped	Other:	
9	Inertial block mass discretization (answer if masses were lumped)	Lumped on Hor and Ver DOFs only	Other:	
10	Mass of inertial block (if mass was subdivided then show the sum of the masses)	236.2		kN-sec ² / m
11	Rotational mass (only if calculated and applied to the rotary degree of freedom)	no		kN-m-sec ²
12	Damping model	Rayleigh - tangent stiffness	Other:	
12a	Damping ratio 1	0.50%		(%)
12b	Corresponding frequency for damping ratio 1			Hz
12c	Damping ratio 2	no		(%)
12d	Corresponding frequency for damping ratio 2	no		Hz
13	Were damping forces included in the calculation of forces M, V and P?	No		
14	Integration scheme	Newmark Method	Other:	
15	Integration time-step	0.005		sec
16	Type of analysis	Approximate P-Delta effects		
17	Output acceleration data signal processing	None	Other:	
17a	Filter order (answer only if data was filtered)			
17b	Filter low-pass corner frequency (answer only if data was filtered)			Hz
17c	Filter high-pass corner frequency (answer only if data was filtered)			Hz
18	What was the greatest challenge/switch you came across while modeling and analyzing the column?	modelind of rebar buckling		



Questionnaire - Contestant/Team #20

1	Nonlinear Analysis Program used (select program from drop down menu in cell C9)	Other (specify)	Other:	MSC.Marc
2	Model Description - Column modeling (type of element)	Beam with distributed plastic hinges	Other:	
3	Model Description - Column cross section discretization	Displacement-based fibers		
4	Model Description - Column vertical discretization	11+ nodes		
5	Model Description - Strain penetration i.e. longitudinal bar bond-slip in footing (explain if answer is yes)	Yes	Explanation:	Extend the column and fix the horizontal displacement of extended
6	Model Description - Material strain rate effect (explain if answer is yes)	No	Explanation:	
7	Model Description - Additional Information (optional)	Shear deformation is roughly taken into account with one elastic nonlinear spring in the middle of column, which is modeled by fiber element.		
8	Mass block formulation	Distributed	Other:	
9	Inertial block mass discretization (answer if masses were lumped)	Select	Other:	
10	Mass of inertial block (if mass was subdivided then show the sum of the masses)	250.3		kN-sec ² / m
11	Rotational mass (only if calculated and applied to the rotary degree of freedom)			kN-m-sec ²
12	Damping model	Rayleigh - mass & initial stiffness	Other:	
12a	Damping ratio 1	2		(%)
12b	Corresponding frequency for damping ratio 1			Hz
12c	Damping ratio 2			(%)
12d	Corresponding frequency for damping ratio 2			Hz
13	Were damping forces included in the calculation of forces M, V and P?	Yes		
14	Integration scheme	Newmark Method	Other:	
15	Integration time-step	1/256		sec
16	Type of analysis	Large-displacement theory		
17	Output acceleration data signal processing	None	Other:	
17a	Filter order (answer only if data was filtered)			
17b	Filter low-pass corner frequency (answer only if data was filtered)			Hz
17c	Filter high-pass corner frequency (answer only if data was filtered)			Hz
18	What was the greatest challenge/switch you came across while modeling and analyzing the column?	the possible shear failure in the column		



Questionnaire - Contestant/Team #21

1	Nonlinear Analysis Program used (select program from drop down menu in cell C9)	PC-ANSR	Other:	
2	Model Description - Column modeling (type of element)	Other	Other:	Fiber hinge elements connected to linear-elastic beam elements
3	Model Description - Column cross section discretization	Multi-spring		
4	Model Description - Column vertical discretization	11+ nodes		
5	Model Description - Strain penetration i.e. longitudinal bar bond-slip in footing (explain if answer is yes)	Yes	Explanation:	Fiber hinge element at base had extended fiber lengths to account for
6	Model Description - Material strain rate effect (explain if answer is yes)	No	Explanation:	
7	Model Description - Additional Information (optional)	Fiber hinge model: Concrete fibers (bi-linear with slip effect (pinching upon reloading), stiffness softening with cycling), Steel fibers (bi-linear with strength deterioration in compression, hardening strength increase with cycling))		
8	Mass block formulation	Lumped	Other:	
9	Inertial block mass discretization (answer if masses were lumped)	Lumped on Hor and Ver DOFs only	Other:	
10	Mass of inertial block (if mass was subdivided then show the sum of the masses)	234		kN-sec ² / m
11	Rotational mass (only if calculated and applied to the rotary degree of freedom)			kN-m-sec ²
12	Damping model	Rayleigh - mass & initial stiffness	Other:	
12a	Damping ratio 1	0.01		(%)
12b	Corresponding frequency for damping ratio 1	2		Hz
12c	Damping ratio 2	0.01		(%)
12d	Corresponding frequency for damping ratio 2	0.67		Hz
13	Were damping forces included in the calculation of forces M, V and P?	No		
14	Integration scheme	Newmark Method	Other:	
15	Integration time-step	0.002		sec
16	Type of analysis	Small-displacement theory		
17	Output acceleration data signal processing	None	Other:	
17a	Filter order (answer only if data was filtered)			
17b	Filter low-pass corner frequency (answer only if data was filtered)			Hz
17c	Filter high-pass corner frequency (answer only if data was filtered)			Hz
18	What was the greatest challenge/switch you came across while modeling and analyzing the column?	The multiple earthquakes meant that how the cyclic material behavior was modeled was key (upon cycling: strength increase in steel and strength decrease in concrete)		



Questionnaire - Contestant/Team #22

1	Nonlinear Analysis Program used (select program from drop down menu in cell C9)	Canny	Other:	
2	Model Description - Column modeling (type of element)	Select	Other:	
3	Model Description - Column cross section discretization	Multi-spring		
4	Model Description - Column vertical discretization	11+ nodes		
5	Model Description - Strain penetration i.e. longitudinal bar bond-slip in footing (explain if answer is yes)	No	Explanation:	
6	Model Description - Material strain rate effect (explain if answer is yes)	No	Explanation:	
7	Model Description - Additional Information (optional)	2688 Concrete Spring / 18 Steel Spring / No bar buckling / Concrete Material has compression ascending curve in exponential function + Step Down Technique in descending branch / Steel Material Model from Dr. Tanaka at Technological Research Institute in Fujita Corporation type Ramberg-Osgood.		
8	Mass block formulation	Lumped	Other:	
9	Inertial block mass discretization (answer if masses were lumped)	Lumped on 3DOFs	Other:	
10	Mass of inertial block (if mass was subdivided then show the sum of the masses)	229.9	kN-sec ² / m	
11	Rotational mass (only if calculated and applied to the rotary degree of freedom)		kN-m-sec ²	
12	Damping model	Other	Other:	Proportional Damping
12a	Damping ratio 1	2.50%	(%)	
12b	Corresponding frequency for damping ratio 1		Hz	
12c	Damping ratio 2		(%)	
12d	Corresponding frequency for damping ratio 2		Hz	
13	Were damping forces included in the calculation of forces M, V and P?	Yes		
14	Integration scheme	Newmark Method	Other:	
15	Integration time-step	0.000975	sec	
16	Type of analysis	Large-displacement theory		
17	Output acceleration data signal processing	None	Other:	
17a	Filter order (answer only if data was filtered)			
17b	Filter low-pass corner frequency (answer only if data was filtered)		Hz	
17c	Filter high-pass corner frequency (answer only if data was filtered)		Hz	
18	What was the greatest challenge/switch you came across while modeling and analyzing the column?	Curvature and Strain determination at intermediate locations. Also residual displacements if one chooses to not use the White Noise record for easing time computing.		



Concrete Column Blind Prediction Contest 2010



Questionnaire - Contestant/Team #23

1	Nonlinear Analysis Program used (select program from drop down menu in cell C9)	ANSR II	Other:	
2	Model Description - Column modeling (type of element)	Beam with springs	Other:	
3	Model Description - Column cross section discretization	Multi-spring		
4	Model Description - Column vertical discretization	8 nodes		
5	Model Description - Strain penetration i.e. longitudinal bar bond-slip in footing (explain if answer is yes)	No	Explanation:	
6	Model Description - Material strain rate effect (explain if answer is yes)	No	Explanation:	
7	Model Description - Additional Information (optional)	At each bar location, a pair of gap-truss elements in parallel was used to model the base hinging. The bars used a bi-linear yield function in both tension and compression and the gaps were bilinear in compression. Above this hinge, the column was linear elastic.		
8	Mass block formulation	Lumped	Other:	
9	Inertial block mass discretization (answer if masses were lumped)	Multiple Lumped Masses in Hor and Ver DOFs	Other:	
10	Mass of inertial block (if mass was subdivided then show the sum of the masses)	240	kN-sec ² / m	
11	Rotational mass (only if calculated and applied to the rotary degree of freedom)	0	kN-m-sec ²	
12	Damping model	Rayleigh - mass & initial stiffness	Other:	
12a	Damping ratio 1	0.03	(%)	
12b	Corresponding frequency for damping ratio 1	1.25	Hz	
12c	Damping ratio 2	0.03	(%)	
12d	Corresponding frequency for damping ratio 2	2	Hz	
13	Were damping forces included in the calculation of forces M, V and P?	Yes		
14	Integration scheme	Newmark Method	Other:	
15	Integration time-step	0.003906	sec	
16	Type of analysis	Approximate P-Delta effects		
17	Output acceleration data signal processing	None	Other:	
17a	Filter order (answer only if data was filtered)			
17b	Filter low-pass corner frequency (answer only if data was filtered)		Hz	
17c	Filter high-pass corner frequency (answer only if data was filtered)		Hz	
18	What was the greatest challenge/switch you came across while modeling and analyzing the column?	The model used was based on design office use and so was developed for ultimate level loads. It did not well represent the serviceability level earthquake response. It might have been better to have used different model properties for different earthquakes. Damping is also difficult to estimate for a bare structure with no cladding, contents etc.		



Questionnaire - Contestant/Team #24

1	Nonlinear Analysis Program used (select program from drop down menu in cell C9)	Other (specify)	Other:	SAP2000
2	Model Description - Column modeling (type of element)	Other	Other:	Beam with concentrated plastic hinges
3	Model Description - Column cross section discretization	Lumped Plasticity		
4	Model Description - Column vertical discretization	2 nodes		
5	Model Description - Strain penetration i.e. longitudinal bar bond-slip in footing (explain if answer is yes)	Yes	Explanation:	Included estimated strain penetration length in assumed plastic hinge length for calculating stiffness of lumped
6	Model Description - Material strain rate effect (explain if answer is yes)	No	Explanation:	
7	Model Description - Additional Information (optional)			
8	Mass block formulation	Lumped	Other:	
9	Inertial block mass discretization (answer if masses were lumped)	Lumped on 3DOFs	Other:	
10	Mass of inertial block (if mass was subdivided then show the sum of the masses)	234		kN-sec ² / m
11	Rotational mass (only if calculated and applied to the rotary degree of freedom)	1056		kN-m-sec ²
12	Damping model	Rayleigh - mass & initial stiffness	Other:	
12a	Damping ratio 1	1.5		(%)
12b	Corresponding frequency for damping ratio 1	0.727		Hz
12c	Damping ratio 2	1.5		(%)
12d	Corresponding frequency for damping ratio 2	3.18		Hz
13	Were damping forces included in the calculation of forces M, V and P?	No		
14	Integration scheme	Hilber-Hughes-Taylor Method	Other:	
15	Integration time-step	0.00391		sec
16	Type of analysis	Approximate P-Delta effects		
17	Output acceleration data signal processing	Butterworth	Other:	
17a	Filter order (answer only if data was filtered)			
17b	Filter low-pass corner frequency (answer only if data was filtered)			Hz
17c	Filter high-pass corner frequency (answer only if data was filtered)			Hz
18	What was the greatest challenge/switch you came across while modeling and analyzing the column?	Accurately capturing hysteretic behavior.		



Concrete Column Blind Prediction Contest 2010



Questionnaire - Contestant/Team #25

1	Nonlinear Analysis Program used (select program from drop down menu in cell C9)	Canny	Other:	
2	Model Description - Column modeling (type of element)	Select	Other:	
3	Model Description - Column cross section discretization	Multi-spring		
4	Model Description - Column vertical discretization	2 nodes		
5	Model Description - Strain penetration i.e. longitudinal bar bond-slip in footing (explain if answer is yes)	No	Explanation:	
6	Model Description - Material strain rate effect (explain if answer is yes)	No	Explanation:	
7	Model Description - Additional Information (optional)	2688 Concrete Spring / 18 Steel Spring / No bar buckling / Concrete Material has compression ascending curve in exponential function + Step Down Technique in descending branch / Steel Material Model from Dr. Tanaka at Technological Research Institute in Fujita Corporation type Ramberg-Osgood.		
8	Mass block formulation	Lumped	Other:	
9	Inertial block mass discretization (answer if masses were lumped)	Lumped on 3DOFs	Other:	
10	Mass of inertial block (if mass was subdivided then show the sum of the masses)	228.9		kN-sec ² / m
11	Rotational mass (only if calculated and applied to the rotary degree of freedom)			kN-m-sec ²
12	Damping model	Other	Other:	Proportional Damping in damping factor affecting [K]
12a	Damping ratio 1	5.00%		(%)
12b	Corresponding frequency for damping ratio 1			Hz
12c	Damping ratio 2			(%)
12d	Corresponding frequency for damping ratio 2			Hz
13	Were damping forces included in the calculation of forces M, V and P?	Yes		
14	Integration scheme	Newmark Method	Other:	
15	Integration time-step	0.000975		sec
16	Type of analysis	Large-displacement theory		
17	Output acceleration data signal processing	None	Other:	
17a	Filter order (answer only if data was filtered)			
17b	Filter low-pass corner frequency (answer only if data was filtered)			Hz
17c	Filter high-pass corner frequency (answer only if data was filtered)			Hz
18	What was the greatest challenge/switch you came across while modeling and analyzing the column?			

PEER REPORTS

PEER reports are available as a free PDF download from http://peer.berkeley.edu/publications/peer_reports_complete.html. Printed hard copies of PEER reports can be ordered directly from our printer by following the instructions at http://peer.berkeley.edu/publications/peer_reports.html. For other related questions about the PEER Report Series, contact the Pacific Earthquake Engineering Research Center, 325 Davis Hall mail code 1792, Berkeley, CA 94720. Tel.: (510) 642-3437; Fax: (510) 665-1655; Email: peer_editor@berkeley.edu

- PEER 2015/01** *Concrete Column Blind Prediction Contest 2010: Outcomes and Observations.* Vesna Terzic, Matthew J. Schoettler, José I. Restrepo, and Stephen A Mahin. March 2015.
- PEER 2014/20** *Stochastic Modeling and Simulation of Near-Fault Ground Motions for Performance-Based Earthquake Engineering.* Mayssa Dabaghi and Armen Der Kiureghian. December 2014.
- PEER 2014/19** *Seismic Response of a Hybrid Fiber-Reinforced Concrete Bridge Column Detailed for Accelerated Bridge Construction.* Wilson Nguyen, William Trono, Marios Panagiotou, and Claudia P. Ostertag. December 2014.
- PEER 2014/18** *Three-Dimensional Beam-Truss Model for Reinforced Concrete Walls and Slabs Subjected to Cyclic Static or Dynamic Loading.* Yuan Lu, Marios Panagiotou, and Ioannis Koutromanos. December 2014.
- PEER 2014/17** *PEER NGA-East Database.* Christine A. Goulet, Tadahiro Kishida, Timothy D. Ancheta, Chris H. Cramer, Robert B. Darragh, Walter J. Silva, Youssef M.A. Hashash, Joseph Harmon, Jonathan P. Stewart, Katie E. Wooddell, and Robert R. Youngs. October 2014.
- PEER 2014/16** *Guidelines for Performing Hazard-Consistent One-Dimensional Ground Response Analysis for Ground Motion Prediction.* Jonathan P. Stewart, Kioumars Afshari, and Youssef M.A. Hashash. October 2014.
- PEER 2014/15** *NGA-East Regionalization Report: Comparison of Four Crustal Regions within Central and Eastern North America using Waveform Modeling and 5%-Damped Pseudo-Spectral Acceleration Response.* Jennifer Dreiling, Marius P. Isken, Walter D. Mooney, Martin C. Chapman, and Richard W. Godbee. October 2014.
- PEER 2014/14** *Scaling Relations between Seismic Moment and Rupture Area of Earthquakes in Stable Continental Regions.* Paul Somerville. August 2014.
- PEER 2014/13** *PEER Preliminary Notes and Observations on the August 24, 2014, South Napa Earthquake.* Grace S. Kang (Editor), Stephen A. Mahin (Editors). September 2014.
- PEER 2014/12** *Reference-Rock Site Conditions for Central and Eastern North America: Part II – Attenuation (Kappa) Definition.* Kenneth W. Campbell, Youssef M.A. Hashash, Byungmin Kim, Albert R. Kottke, Ellen M. Rathje, Walter J. Silva, and Jonathan P. Stewart. August 2014.
- PEER 2014/11** *Reference-Rock Site Conditions for Central and Eastern North America: Part I - Velocity Definition.* Youssef M.A. Hashash, Albert R. Kottke, Jonathan P. Stewart, Kenneth W. Campbell, Byungmin Kim, Ellen M. Rathje, Walter J. Silva, Sissy Nikolaou, and Cheryl Moss. August 2014.
- PEER 2014/10** *Evaluation of Collapse and Non-Collapse of Parallel Bridges Affected by Liquefaction and Lateral Spreading.* Benjamin Turner, Scott J. Brandenberg, and Jonathan P. Stewart. August 2014.
- PEER 2014/09** *PEER Arizona Strong-Motion Database and GMPEs Evaluation.* Tadahiro Kishida, Robert E. Kayen, Olga-Joan Ktenidou, Walter J. Silva, Robert B. Darragh, and Jennie Watson-Lamprey. June 2014.
- PEER 2014/08** *Unbonded Pretensioned Bridge Columns with Rocking Detail.* Jeffrey A. Schaefer, Bryan Kennedy, Marc O. Eberhard, John F. Stanton. June 2014.
- PEER 2014/07** *Northridge 20 Symposium Summary Report: Impacts, Outcomes, and Next Steps.* May 2014.
- PEER 2014/06** *Report of the Tenth Planning Meeting of NEES/E-Defense Collaborative Research on Earthquake Engineering.* December 2013.
- PEER 2014/05** *Seismic Velocity Site Characterization of Thirty-One Chilean Seismometer Stations by Spectral Analysis of Surface Wave Dispersion.* Robert Kayen, Brad D. Carkin, Skye Corbet, Camilo Pinilla, Allan Ng, Edward Gorbis, and Christine Truong. April 2014.
- PEER 2014/04** *Effect of Vertical Acceleration on Shear Strength of Reinforced Concrete Columns.* Hyerin Lee and Khalid M. Mosalam. April 2014.
- PEER 2014/03** *Retest of Thirty-Year-Old Neoprene Isolation Bearings.* James M. Kelly and Niel C. Van Engelen. March 2014.
- PEER 2014/02** *Theoretical Development of Hybrid Simulation Applied to Plate Structures.* Ahmed A. Bakhaty, Khalid M. Mosalam, and Sanjay Govindjee. January 2014.

- PEER 2014/01** *Performance-Based Seismic Assessment of Skewed Bridges*. Peyman Kaviani, Farzin Zareian, and Ertugrul Taciroglu. January 2014.
- PEER 2013/26** *Urban Earthquake Engineering. Proceedings of the U.S.-Iran Seismic Workshop*. December 2013.
- PEER 2013/25** *Earthquake Engineering for Resilient Communities: 2013 PEER Internship Program Research Report Collection*. Heidi Tremayne (Editor), Stephen A. Mahin (Editor), Jorge Archbold Monterossa, Matt Brosman, Shelly Dean, Katherine deLaveaga, Curtis Fong, Donovan Holder, Rakeeb Khan, Elizabeth Jachens, David Lam, Daniela Martinez Lopez, Mara Minner, Geffen Oren, Julia Pavicic, Melissa Quinonez, Lorena Rodriguez, Sean Salazar, Kelli Slaven, Vivian Steyert, Jenny Taing, and Salvador Tena. December 2013.
- PEER 2013/24** *NGA-West2 Ground Motion Prediction Equations for Vertical Ground Motions*. September 2013.
- PEER 2013/23** *Coordinated Planning and Preparedness for Fire Following Major Earthquakes*. Charles Scawthorn. November 2013.
- PEER 2013/22** *GEM-PEER Task 3 Project: Selection of a Global Set of Ground Motion Prediction Equations*. Jonathan P. Stewart, John Douglas, Mohammad B. Javanbarg, Carola Di Alessandro, Yousef Bozorgnia, Norman A. Abrahamson, David M. Boore, Kenneth W. Campbell, Elise Delavaud, Mustafa Erdik and Peter J. Stafford. December 2013.
- PEER 2013/21** *Seismic Design and Performance of Bridges with Columns on Rocking Foundations*. Grigorios Antonellis and Marios Panagiotou. September 2013.
- PEER 2013/20** *Experimental and Analytical Studies on the Seismic Behavior of Conventional and Hybrid Braced Frames*. Jiun-Wei Lai and Stephen A. Mahin. September 2013.
- PEER 2013/19** *Toward Resilient Communities: A Performance-Based Engineering Framework for Design and Evaluation of the Built Environment*. Michael William Mieler, Bozidar Stojadinovic, Robert J. Budnitz, Stephen A. Mahin and Mary C. Comerio. September 2013.
- PEER 2013/18** *Identification of Site Parameters that Improve Predictions of Site Amplification*. Ellen M. Rathje and Sara Navidi. July 2013.
- PEER 2013/17** *Response Spectrum Analysis of Concrete Gravity Dams Including Dam-Water-Foundation Interaction*. Arnkjell Løkke and Anil K. Chopra. July 2013.
- PEER 2013/16** *Effect of hoop reinforcement spacing on the cyclic response of large reinforced concrete special moment frame beams*. Marios Panagiotou, Tea Visnjic, Grigorios Antonellis, Panagiotis Galanis, and Jack P. Moehle. June 2013.
- PEER 2013/15** *A Probabilistic Framework to Include the Effects of Near-Fault Directivity in Seismic Hazard Assessment*. Shrey Kumar Shahi, Jack W. Baker. October 2013.
- PEER 2013/14** *Hanging-Wall Scaling using Finite-Fault Simulations*. Jennifer L. Donahue and Norman A. Abrahamson. September 2013.
- PEER 2013/13** *Semi-Empirical Nonlinear Site Amplification and its Application in NEHRP Site Factors*. Jonathan P. Stewart and Emel Seyhan. November 2013.
- PEER 2013/12** *Nonlinear Horizontal Site Response for the NGA-West2 Project*. Ronnie Kamai, Norman A. Abramson, Walter J. Silva. May 2013.
- PEER 2013/11** *Epistemic Uncertainty for NGA-West2 Models*. Linda Al Atik and Robert R. Youngs. May 2013.
- PEER 2013/10** *NGA-West 2 Models for Ground-Motion Directionality*. Shrey K. Shahi and Jack W. Baker. May 2013.
- PEER 2013/09** *Final Report of the NGA-West2 Directivity Working Group*. Paul Spudich, Jeffrey R. Bayless, Jack W. Baker, Brian S.J. Chiou, Badie Rowshandel, Shrey Shahi, and Paul Somerville. May 2013.
- PEER 2013/08** *NGA-West2 Model for Estimating Average Horizontal Values of Pseudo-Absolute Spectral Accelerations Generated by Crustal Earthquakes*. I. M. Idriss. May 2013.
- PEER 2013/07** *Update of the Chiou and Youngs NGA Ground Motion Model for Average Horizontal Component of Peak Ground Motion and Response Spectra*. Brian Chiou and Robert Youngs. May 2013.
- PEER 2013/06** *NGA-West2 Campbell-Bozorgnia Ground Motion Model for the Horizontal Components of PGA, PGV, and 5%-Damped Elastic Pseudo-Acceleration Response Spectra for Periods Ranging from 0.01 to 10 sec*. Kenneth W. Campbell and Yousef Bozorgnia. May 2013.
- PEER 2013/05** *NGA-West 2 Equations for Predicting Response Spectral Accelerations for Shallow Crustal Earthquakes*. David M. Boore, Jonathan P. Stewart, Emel Seyhan, Gail M. Atkinson. May 2013.
- PEER 2013/04** *Update of the AS08 Ground-Motion Prediction Equations Based on the NGA-West2 Data Set*. Norman Abrahamson, Walter Silva, and Ronnie Kamai. May 2013.

- PEER 2013/03** *PEER NGA-West2 Database*. Timothy D. Ancheta, Robert B. Darragh, Jonathan P. Stewart, Emel Seyhan, Walter J. Silva, Brian S.J. Chiou, Katie E. Wooddell, Robert W. Graves, Albert R. Kottke, David M. Boore, Tadahiro Kishida, and Jennifer L. Donahue. May 2013.
- PEER 2013/02** *Hybrid Simulation of the Seismic Response of Squat Reinforced Concrete Shear Walls*. Catherine A. Whyte and Bozidar Stojadinovic. May 2013.
- PEER 2013/01** *Housing Recovery in Chile: A Qualitative Mid-program Review*. Mary C. Comerio. February 2013.
- PEER 2012/08** *Guidelines for Estimation of Shear Wave Velocity*. Bernard R. Wair, Jason T. DeJong, and Thomas Shantz. December 2012.
- PEER 2012/07** *Earthquake Engineering for Resilient Communities: 2012 PEER Internship Program Research Report Collection*. Heidi Tremayne (Editor), Stephen A. Mahin (Editor), Collin Anderson, Dustin Cook, Michael Erceg, Carlos Esparza, Jose Jimenez, Dorian Krausz, Andrew Lo, Stephanie Lopez, Nicole McCurdy, Paul Shipman, Alexander Strum, Eduardo Vega. December 2012.
- PEER 2012/06** *Fragilities for Precarious Rocks at Yucca Mountain*. Matthew D. Purvance, Rasool Anooshehpour, and James N. Brune. December 2012.
- PEER 2012/05** *Development of Simplified Analysis Procedure for Piles in Laterally Spreading Layered Soils*. Christopher R. McGann, Pedro Arduino, and Peter Mackenzie-Helnwein. December 2012.
- PEER 2012/04** *Unbonded Pre-Tensioned Columns for Bridges in Seismic Regions*. Phillip M. Davis, Todd M. Janes, Marc O. Eberhard, and John F. Stanton. December 2012.
- PEER 2012/03** *Experimental and Analytical Studies on Reinforced Concrete Buildings with Seismically Vulnerable Beam-Column Joints*. Sangjoon Park and Khalid M. Mosalam. October 2012.
- PEER 2012/02** *Seismic Performance of Reinforced Concrete Bridges Allowed to Uplift during Multi-Directional Excitation*. Andres Oscar Espinoza and Stephen A. Mahin. July 2012.
- PEER 2012/01** *Spectral Damping Scaling Factors for Shallow Crustal Earthquakes in Active Tectonic Regions*. Sanaz Rezaeian, Yousef Bozorgnia, I. M. Idriss, Kenneth Campbell, Norman Abrahamson, and Walter Silva. July 2012.
- PEER 2011/10** *Earthquake Engineering for Resilient Communities: 2011 PEER Internship Program Research Report Collection*. Eds. Heidi Faison and Stephen A. Mahin. December 2011.
- PEER 2011/09** *Calibration of Semi-Stochastic Procedure for Simulating High-Frequency Ground Motions*. Jonathan P. Stewart, Emel Seyhan, and Robert W. Graves. December 2011.
- PEER 2011/08** *Water Supply in regard to Fire Following Earthquake*. Charles Scawthorn. November 2011.
- PEER 2011/07** *Seismic Risk Management in Urban Areas. Proceedings of a U.S.-Iran-Turkey Seismic Workshop*. September 2011.
- PEER 2011/06** *The Use of Base Isolation Systems to Achieve Complex Seismic Performance Objectives*. Troy A. Morgan and Stephen A. Mahin. July 2011.
- PEER 2011/05** *Case Studies of the Seismic Performance of Tall Buildings Designed by Alternative Means*. Task 12 Report for the Tall Buildings Initiative. Jack Moehle, Yousef Bozorgnia, Nirmal Jayaram, Pierson Jones, Mohsen Rahnama, Nilesh Shome, Zeynep Tuna, John Wallace, Tony Yang, and Farzin Zareian. July 2011.
- PEER 2011/04** *Recommended Design Practice for Pile Foundations in Laterally Spreading Ground*. Scott A. Ashford, Ross W. Boulanger, and Scott J. Brandenburg. June 2011.
- PEER 2011/03** *New Ground Motion Selection Procedures and Selected Motions for the PEER Transportation Research Program*. Jack W. Baker, Ting Lin, Shrey K. Shahi, and Nirmal Jayaram. March 2011.
- PEER 2011/02** *A Bayesian Network Methodology for Infrastructure Seismic Risk Assessment and Decision Support*. Michelle T. Bensi, Armen Der Kiureghian, and Daniel Straub. March 2011.
- PEER 2011/01** *Demand Fragility Surfaces for Bridges in Liquefied and Laterally Spreading Ground*. Scott J. Brandenburg, Jian Zhang, Pirooz Kashighandi, Yili Huo, and Minxing Zhao. March 2011.
- PEER 2010/05** *Guidelines for Performance-Based Seismic Design of Tall Buildings*. Developed by the Tall Buildings Initiative. November 2010.
- PEER 2010/04** *Application Guide for the Design of Flexible and Rigid Bus Connections between Substation Equipment Subjected to Earthquakes*. Jean-Bernard Dastous and Armen Der Kiureghian. September 2010.
- PEER 2010/03** *Shear Wave Velocity as a Statistical Function of Standard Penetration Test Resistance and Vertical Effective Stress at Caltrans Bridge Sites*. Scott J. Brandenburg, Naresh Bellana, and Thomas Shantz. June 2010.
- PEER 2010/02** *Stochastic Modeling and Simulation of Ground Motions for Performance-Based Earthquake Engineering*. Sanaz Rezaeian and Armen Der Kiureghian. June 2010.

- PEER 2010/01** *Structural Response and Cost Characterization of Bridge Construction Using Seismic Performance Enhancement Strategies.* Ady Aviram, Božidar Stojadinović, Gustavo J. Parra-Montesinos, and Kevin R. Mackie. March 2010.
- PEER 2009/03** *The Integration of Experimental and Simulation Data in the Study of Reinforced Concrete Bridge Systems Including Soil-Foundation-Structure Interaction.* Matthew Dryden and Gregory L. Fenves. November 2009.
- PEER 2009/02** *Improving Earthquake Mitigation through Innovations and Applications in Seismic Science, Engineering, Communication, and Response. Proceedings of a U.S.-Iran Seismic Workshop.* October 2009.
- PEER 2009/01** *Evaluation of Ground Motion Selection and Modification Methods: Predicting Median Interstory Drift Response of Buildings.* Curt B. Haselton, Ed. June 2009.
- PEER 2008/10** *Technical Manual for Strata.* Albert R. Kottke and Ellen M. Rathje. February 2009.
- PEER 2008/09** *NGA Model for Average Horizontal Component of Peak Ground Motion and Response Spectra.* Brian S.-J. Chiou and Robert R. Youngs. November 2008.
- PEER 2008/08** *Toward Earthquake-Resistant Design of Concentrically Braced Steel Structures.* Patxi Uriz and Stephen A. Mahin. November 2008.
- PEER 2008/07** *Using OpenSees for Performance-Based Evaluation of Bridges on Liquefiable Soils.* Stephen L. Kramer, Pedro Arduino, and HyungSuk Shin. November 2008.
- PEER 2008/06** *Shaking Table Tests and Numerical Investigation of Self-Centering Reinforced Concrete Bridge Columns.* Hyung IL Jeong, Junichi Sakai, and Stephen A. Mahin. September 2008.
- PEER 2008/05** *Performance-Based Earthquake Engineering Design Evaluation Procedure for Bridge Foundations Undergoing Liquefaction-Induced Lateral Ground Displacement.* Christian A. Ledezma and Jonathan D. Bray. August 2008.
- PEER 2008/04** *Benchmarking of Nonlinear Geotechnical Ground Response Analysis Procedures.* Jonathan P. Stewart, Annie On-Lei Kwok, Youssef M. A. Hashash, Neven Matasovic, Robert Pyke, Zhiliang Wang, and Zhaohui Yang. August 2008.
- PEER 2008/03** *Guidelines for Nonlinear Analysis of Bridge Structures in California.* Ady Aviram, Kevin R. Mackie, and Božidar Stojadinović. August 2008.
- PEER 2008/02** *Treatment of Uncertainties in Seismic-Risk Analysis of Transportation Systems.* Evangelos Stergiou and Anne S. Kiremidjian. July 2008.
- PEER 2008/01** *Seismic Performance Objectives for Tall Buildings.* William T. Holmes, Charles Kircher, William Petak, and Nabih Youssef. August 2008.
- PEER 2007/12** *An Assessment to Benchmark the Seismic Performance of a Code-Conforming Reinforced Concrete Moment-Frame Building.* Curt Haselton, Christine A. Goulet, Judith Mitrani-Reiser, James L. Beck, Gregory G. Deierlein, Keith A. Porter, Jonathan P. Stewart, and Ertugrul Taciroglu. August 2008.
- PEER 2007/11** *Bar Buckling in Reinforced Concrete Bridge Columns.* Wayne A. Brown, Dawn E. Lehman, and John F. Stanton. February 2008.
- PEER 2007/10** *Computational Modeling of Progressive Collapse in Reinforced Concrete Frame Structures.* Mohamed M. Talaat and Khalid M. Mosalam. May 2008.
- PEER 2007/09** *Integrated Probabilistic Performance-Based Evaluation of Benchmark Reinforced Concrete Bridges.* Kevin R. Mackie, John-Michael Wong, and Božidar Stojadinović. January 2008.
- PEER 2007/08** *Assessing Seismic Collapse Safety of Modern Reinforced Concrete Moment-Frame Buildings.* Curt B. Haselton and Gregory G. Deierlein. February 2008.
- PEER 2007/07** *Performance Modeling Strategies for Modern Reinforced Concrete Bridge Columns.* Michael P. Berry and Marc O. Eberhard. April 2008.
- PEER 2007/06** *Development of Improved Procedures for Seismic Design of Buried and Partially Buried Structures.* Linda Al Atik and Nicholas Sitar. June 2007.
- PEER 2007/05** *Uncertainty and Correlation in Seismic Risk Assessment of Transportation Systems.* Renee G. Lee and Anne S. Kiremidjian. July 2007.
- PEER 2007/04** *Numerical Models for Analysis and Performance-Based Design of Shallow Foundations Subjected to Seismic Loading.* Sivapalan Gajan, Tara C. Hutchinson, Bruce L. Kutter, Prishati Raychowdhury, José A. Ugalde, and Jonathan P. Stewart. May 2008.
- PEER 2007/03** *Beam-Column Element Model Calibrated for Predicting Flexural Response Leading to Global Collapse of RC Frame Buildings.* Curt B. Haselton, Abbie B. Liel, Sarah Taylor Lange, and Gregory G. Deierlein. May 2008.
- PEER 2007/02** *Campbell-Bozorgnia NGA Ground Motion Relations for the Geometric Mean Horizontal Component of Peak and Spectral Ground Motion Parameters.* Kenneth W. Campbell and Yousef Bozorgnia. May 2007.

- PEER 2007/01** *Boore-Atkinson NGA Ground Motion Relations for the Geometric Mean Horizontal Component of Peak and Spectral Ground Motion Parameters.* David M. Boore and Gail M. Atkinson. May. May 2007.
- PEER 2006/12** *Societal Implications of Performance-Based Earthquake Engineering.* Peter J. May. May 2007.
- PEER 2006/11** *Probabilistic Seismic Demand Analysis Using Advanced Ground Motion Intensity Measures, Attenuation Relationships, and Near-Fault Effects.* Polsak Tothong and C. Allin Cornell. March 2007.
- PEER 2006/10** *Application of the PEER PBEE Methodology to the I-880 Viaduct.* Sashi Kunnath. February 2007.
- PEER 2006/09** *Quantifying Economic Losses from Travel Forgone Following a Large Metropolitan Earthquake.* James Moore, Sungbin Cho, Yue Yue Fan, and Stuart Werner. November 2006.
- PEER 2006/08** *Vector-Valued Ground Motion Intensity Measures for Probabilistic Seismic Demand Analysis.* Jack W. Baker and C. Allin Cornell. October 2006.
- PEER 2006/07** *Analytical Modeling of Reinforced Concrete Walls for Predicting Flexural and Coupled-Shear-Flexural Responses.* Kutay Orakcal, Leonardo M. Massone, and John W. Wallace. October 2006.
- PEER 2006/06** *Nonlinear Analysis of a Soil-Drilled Pier System under Static and Dynamic Axial Loading.* Gang Wang and Nicholas Sitar. November 2006.
- PEER 2006/05** *Advanced Seismic Assessment Guidelines.* Paolo Bazzurro, C. Allin Cornell, Charles Menun, Maziar Motahari, and Nicolas Luco. September 2006.
- PEER 2006/04** *Probabilistic Seismic Evaluation of Reinforced Concrete Structural Components and Systems.* Tae Hyung Lee and Khalid M. Mosalam. August 2006.
- PEER 2006/03** *Performance of Lifelines Subjected to Lateral Spreading.* Scott A. Ashford and Teerawut Juinarongrit. July 2006.
- PEER 2006/02** *Pacific Earthquake Engineering Research Center Highway Demonstration Project.* Anne Kiremidjian, James Moore, Yue Yue Fan, Nesrin Basoz, Ozgur Yazali, and Meredith Williams. April 2006.
- PEER 2006/01** *Bracing Berkeley. A Guide to Seismic Safety on the UC Berkeley Campus.* Mary C. Comerio, Stephen Tobriner, and Ariane Fehrenkamp. January 2006.
- PEER 2005/16** *Seismic Response and Reliability of Electrical Substation Equipment and Systems.* Junho Song, Armen Der Kiureghian, and Jerome L. Sackman. April 2006.
- PEER 2005/15** *CPT-Based Probabilistic Assessment of Seismic Soil Liquefaction Initiation.* R. E. S. Moss, R. B. Seed, R. E. Kayen, J. P. Stewart, and A. Der Kiureghian. April 2006.
- PEER 2005/14** *Workshop on Modeling of Nonlinear Cyclic Load-Deformation Behavior of Shallow Foundations.* Bruce L. Kutter, Geoffrey Martin, Tara Hutchinson, Chad Harden, Sivapalan Gajan, and Justin Phalen. March 2006.
- PEER 2005/13** *Stochastic Characterization and Decision Bases under Time-Dependent Aftershock Risk in Performance-Based Earthquake Engineering.* Gee Liek Yeo and C. Allin Cornell. July 2005.
- PEER 2005/12** *PEER Testbed Study on a Laboratory Building: Exercising Seismic Performance Assessment.* Mary C. Comerio, editor. November 2005.
- PEER 2005/11** *Van Nuys Hotel Building Testbed Report: Exercising Seismic Performance Assessment.* Helmut Krawinkler, editor. October 2005.
- PEER 2005/10** *First NEES/E-Defense Workshop on Collapse Simulation of Reinforced Concrete Building Structures.* September 2005.
- PEER 2005/09** *Test Applications of Advanced Seismic Assessment Guidelines.* Joe Maffei, Karl Telleen, Danya Mohr, William Holmes, and Yuki Nakayama. August 2006.
- PEER 2005/08** *Damage Accumulation in Lightly Confined Reinforced Concrete Bridge Columns.* R. Tyler Ranf, Jared M. Nelson, Zach Price, Marc O. Eberhard, and John F. Stanton. April 2006.
- PEER 2005/07** *Experimental and Analytical Studies on the Seismic Response of Freestanding and Anchored Laboratory Equipment.* Dimitrios Konstantinidis and Nicos Makris. January 2005.
- PEER 2005/06** *Global Collapse of Frame Structures under Seismic Excitations.* Luis F. Ibarra and Helmut Krawinkler. September 2005.
- PEER 2005/05** *Performance Characterization of Bench- and Shelf-Mounted Equipment.* Samit Ray Chaudhuri and Tara C. Hutchinson. May 2006.
- PEER 2005/04** *Numerical Modeling of the Nonlinear Cyclic Response of Shallow Foundations.* Chad Harden, Tara Hutchinson, Geoffrey R. Martin, and Bruce L. Kutter. August 2005.

- PEER 2005/03** *A Taxonomy of Building Components for Performance-Based Earthquake Engineering.* Keith A. Porter. September 2005.
- PEER 2005/02** *Fragility Basis for California Highway Overpass Bridge Seismic Decision Making.* Kevin R. Mackie and Božidar Stojadinović. June 2005.
- PEER 2005/01** *Empirical Characterization of Site Conditions on Strong Ground Motion.* Jonathan P. Stewart, Yoojoong Choi, and Robert W. Graves. June 2005.
- PEER 2004/09** *Electrical Substation Equipment Interaction: Experimental Rigid Conductor Studies.* Christopher Stearns and André Filiatrault. February 2005.
- PEER 2004/08** *Seismic Qualification and Fragility Testing of Line Break 550-kV Disconnect Switches.* Shakhzod M. Takhirov, Gregory L. Fenves, and Eric Fujisaki. January 2005.
- PEER 2004/07** *Ground Motions for Earthquake Simulator Qualification of Electrical Substation Equipment.* Shakhzod M. Takhirov, Gregory L. Fenves, Eric Fujisaki, and Don Clyde. January 2005.
- PEER 2004/06** *Performance-Based Regulation and Regulatory Regimes.* Peter J. May and Chris Koski. September 2004.
- PEER 2004/05** *Performance-Based Seismic Design Concepts and Implementation: Proceedings of an International Workshop.* Peter Fajfar and Helmut Krawinkler, editors. September 2004.
- PEER 2004/04** *Seismic Performance of an Instrumented Tilt-up Wall Building.* James C. Anderson and Vitelmo V. Bertero. July 2004.
- PEER 2004/03** *Evaluation and Application of Concrete Tilt-up Assessment Methodologies.* Timothy Graf and James O. Malley. October 2004.
- PEER 2004/02** *Analytical Investigations of New Methods for Reducing Residual Displacements of Reinforced Concrete Bridge Columns.* Junichi Sakai and Stephen A. Mahin. August 2004.
- PEER 2004/01** *Seismic Performance of Masonry Buildings and Design Implications.* Kerri Anne Taeko Tokoro, James C. Anderson, and Vitelmo V. Bertero. February 2004.
- PEER 2003/18** *Performance Models for Flexural Damage in Reinforced Concrete Columns.* Michael Berry and Marc Eberhard. August 2003.
- PEER 2003/17** *Predicting Earthquake Damage in Older Reinforced Concrete Beam-Column Joints.* Catherine Pagni and Laura Lowes. October 2004.
- PEER 2003/16** *Seismic Demands for Performance-Based Design of Bridges.* Kevin Mackie and Božidar Stojadinović. August 2003.
- PEER 2003/15** *Seismic Demands for Nondeteriorating Frame Structures and Their Dependence on Ground Motions.* Ricardo Antonio Medina and Helmut Krawinkler. May 2004.
- PEER 2003/14** *Finite Element Reliability and Sensitivity Methods for Performance-Based Earthquake Engineering.* Terje Haukaas and Armen Der Kiureghian. April 2004.
- PEER 2003/13** *Effects of Connection Hysteretic Degradation on the Seismic Behavior of Steel Moment-Resisting Frames.* Janise E. Rodgers and Stephen A. Mahin. March 2004.
- PEER 2003/12** *Implementation Manual for the Seismic Protection of Laboratory Contents: Format and Case Studies.* William T. Holmes and Mary C. Comerio. October 2003.
- PEER 2003/11** *Fifth U.S.-Japan Workshop on Performance-Based Earthquake Engineering Methodology for Reinforced Concrete Building Structures.* February 2004.
- PEER 2003/10** *A Beam-Column Joint Model for Simulating the Earthquake Response of Reinforced Concrete Frames.* Laura N. Lowes, Nilanjan Mitra, and Arash Altoontash. February 2004.
- PEER 2003/09** *Sequencing Repairs after an Earthquake: An Economic Approach.* Marco Casari and Simon J. Wilkie. April 2004.
- PEER 2003/08** *A Technical Framework for Probability-Based Demand and Capacity Factor Design (DCFD) Seismic Formats.* Fatemeh Jalayer and C. Allin Cornell. November 2003.
- PEER 2003/07** *Uncertainty Specification and Propagation for Loss Estimation Using FOSM Methods.* Jack W. Baker and C. Allin Cornell. September 2003.
- PEER 2003/06** *Performance of Circular Reinforced Concrete Bridge Columns under Bidirectional Earthquake Loading.* Mahmoud M. Hachem, Stephen A. Mahin, and Jack P. Moehle. February 2003.
- PEER 2003/05** *Response Assessment for Building-Specific Loss Estimation.* Eduardo Miranda and Shahram Taghavi. September 2003.

- PEER 2003/04** *Experimental Assessment of Columns with Short Lap Splices Subjected to Cyclic Loads.* Murat Melek, John W. Wallace, and Joel Conte. April 2003.
- PEER 2003/03** *Probabilistic Response Assessment for Building-Specific Loss Estimation.* Eduardo Miranda and Hesameddin Aslani. September 2003.
- PEER 2003/02** *Software Framework for Collaborative Development of Nonlinear Dynamic Analysis Program.* Jun Peng and Kincho H. Law. September 2003.
- PEER 2003/01** *Shake Table Tests and Analytical Studies on the Gravity Load Collapse of Reinforced Concrete Frames.* Kenneth John Elwood and Jack P. Moehle. November 2003.
- PEER 2002/24** *Performance of Beam to Column Bridge Joints Subjected to a Large Velocity Pulse.* Natalie Gibson, André Filiatrault, and Scott A. Ashford. April 2002.
- PEER 2002/23** *Effects of Large Velocity Pulses on Reinforced Concrete Bridge Columns.* Greg L. Orozco and Scott A. Ashford. April 2002.
- PEER 2002/22** *Characterization of Large Velocity Pulses for Laboratory Testing.* Kenneth E. Cox and Scott A. Ashford. April 2002.
- PEER 2002/21** *Fourth U.S.-Japan Workshop on Performance-Based Earthquake Engineering Methodology for Reinforced Concrete Building Structures.* December 2002.
- PEER 2002/20** *Barriers to Adoption and Implementation of PBEE Innovations.* Peter J. May. August 2002.
- PEER 2002/19** *Economic-Engineered Integrated Models for Earthquakes: Socioeconomic Impacts.* Peter Gordon, James E. Moore II, and Harry W. Richardson. July 2002.
- PEER 2002/18** *Assessment of Reinforced Concrete Building Exterior Joints with Substandard Details.* Chris P. Pantelides, Jon Hansen, Justin Nadauld, and Lawrence D. Reaveley. May 2002.
- PEER 2002/17** *Structural Characterization and Seismic Response Analysis of a Highway Overcrossing Equipped with Elastomeric Bearings and Fluid Dampers: A Case Study.* Nicos Makris and Jian Zhang. November 2002.
- PEER 2002/16** *Estimation of Uncertainty in Geotechnical Properties for Performance-Based Earthquake Engineering.* Allen L. Jones, Steven L. Kramer, and Pedro Arduino. December 2002.
- PEER 2002/15** *Seismic Behavior of Bridge Columns Subjected to Various Loading Patterns.* Asadollah Esmaeily-Gh. and Yan Xiao. December 2002.
- PEER 2002/14** *Inelastic Seismic Response of Extended Pile Shaft Supported Bridge Structures.* T.C. Hutchinson, R.W. Boulanger, Y.H. Chai, and I.M. Idriss. December 2002.
- PEER 2002/13** *Probabilistic Models and Fragility Estimates for Bridge Components and Systems.* Paolo Gardoni, Armen Der Kiureghian, and Khalid M. Mosalam. June 2002.
- PEER 2002/12** *Effects of Fault Dip and Slip Rake on Near-Source Ground Motions: Why Chi-Chi Was a Relatively Mild M7.6 Earthquake.* Brad T. Aagaard, John F. Hall, and Thomas H. Heaton. December 2002.
- PEER 2002/11** *Analytical and Experimental Study of Fiber-Reinforced Strip Isolators.* James M. Kelly and Shakhzod M. Takhirov. September 2002.
- PEER 2002/10** *Centrifuge Modeling of Settlement and Lateral Spreading with Comparisons to Numerical Analyses.* Sivapalan Gajan and Bruce L. Kutter. January 2003.
- PEER 2002/09** *Documentation and Analysis of Field Case Histories of Seismic Compression during the 1994 Northridge, California, Earthquake.* Jonathan P. Stewart, Patrick M. Smith, Daniel H. Whang, and Jonathan D. Bray. October 2002.
- PEER 2002/08** *Component Testing, Stability Analysis and Characterization of Buckling-Restrained Unbonded Braces™.* Cameron Black, Nicos Makris, and Ian Aiken. September 2002.
- PEER 2002/07** *Seismic Performance of Pile-Wharf Connections.* Charles W. Roeder, Robert Graff, Jennifer Soderstrom, and Jun Han Yoo. December 2001.
- PEER 2002/06** *The Use of Benefit-Cost Analysis for Evaluation of Performance-Based Earthquake Engineering Decisions.* Richard O. Zerbe and Anthony Falit-Baiamonte. September 2001.
- PEER 2002/05** *Guidelines, Specifications, and Seismic Performance Characterization of Nonstructural Building Components and Equipment.* André Filiatrault, Constantin Christopoulos, and Christopher Stearns. September 2001.
- PEER 2002/04** *Consortium of Organizations for Strong-Motion Observation Systems and the Pacific Earthquake Engineering Research Center Lifelines Program: Invited Workshop on Archiving and Web Dissemination of Geotechnical Data, 4–5 October 2001.* September 2002.

- PEER 2002/03** *Investigation of Sensitivity of Building Loss Estimates to Major Uncertain Variables for the Van Nuys Testbed.* Keith A. Porter, James L. Beck, and Rustem V. Shaikhutdinov. August 2002.
- PEER 2002/02** *The Third U.S.-Japan Workshop on Performance-Based Earthquake Engineering Methodology for Reinforced Concrete Building Structures.* July 2002.
- PEER 2002/01** *Nonstructural Loss Estimation: The UC Berkeley Case Study.* Mary C. Comerio and John C. Stallmeyer. December 2001.
- PEER 2001/16** *Statistics of SDF-System Estimate of Roof Displacement for Pushover Analysis of Buildings.* Anil K. Chopra, Rakesh K. Goel, and Chatpan Chintanapakdee. December 2001.
- PEER 2001/15** *Damage to Bridges during the 2001 Nisqually Earthquake.* R. Tyler Ranf, Marc O. Eberhard, and Michael P. Berry. November 2001.
- PEER 2001/14** *Rocking Response of Equipment Anchored to a Base Foundation.* Nicos Makris and Cameron J. Black. September 2001.
- PEER 2001/13** *Modeling Soil Liquefaction Hazards for Performance-Based Earthquake Engineering.* Steven L. Kramer and Ahmed-W. Elgamal. February 2001.
- PEER 2001/12** *Development of Geotechnical Capabilities in OpenSees.* Boris Jeremić. September 2001.
- PEER 2001/11** *Analytical and Experimental Study of Fiber-Reinforced Elastomeric Isolators.* James M. Kelly and Shakhzod M. Takhirov. September 2001.
- PEER 2001/10** *Amplification Factors for Spectral Acceleration in Active Regions.* Jonathan P. Stewart, Andrew H. Liu, Yoojoong Choi, and Mehmet B. Baturay. December 2001.
- PEER 2001/09** *Ground Motion Evaluation Procedures for Performance-Based Design.* Jonathan P. Stewart, Shyh-Jeng Chiou, Jonathan D. Bray, Robert W. Graves, Paul G. Somerville, and Norman A. Abrahamson. September 2001.
- PEER 2001/08** *Experimental and Computational Evaluation of Reinforced Concrete Bridge Beam-Column Connections for Seismic Performance.* Clay J. Naito, Jack P. Moehle, and Khalid M. Mosalam. November 2001.
- PEER 2001/07** *The Rocking Spectrum and the Shortcomings of Design Guidelines.* Nicos Makris and Dimitrios Konstantinidis. August 2001.
- PEER 2001/06** *Development of an Electrical Substation Equipment Performance Database for Evaluation of Equipment Fragilities.* Thalia Agnanos. April 1999.
- PEER 2001/05** *Stiffness Analysis of Fiber-Reinforced Elastomeric Isolators.* Hsiang-Chuan Tsai and James M. Kelly. May 2001.
- PEER 2001/04** *Organizational and Societal Considerations for Performance-Based Earthquake Engineering.* Peter J. May. April 2001.
- PEER 2001/03** *A Modal Pushover Analysis Procedure to Estimate Seismic Demands for Buildings: Theory and Preliminary Evaluation.* Anil K. Chopra and Rakesh K. Goel. January 2001.
- PEER 2001/02** *Seismic Response Analysis of Highway Overcrossings Including Soil-Structure Interaction.* Jian Zhang and Nicos Makris. March 2001.
- PEER 2001/01** *Experimental Study of Large Seismic Steel Beam-to-Column Connections.* Egor P. Popov and Shakhzod M. Takhirov. November 2000.
- PEER 2000/10** *The Second U.S.-Japan Workshop on Performance-Based Earthquake Engineering Methodology for Reinforced Concrete Building Structures.* March 2000.
- PEER 2000/09** *Structural Engineering Reconnaissance of the August 17, 1999 Earthquake: Kocaeli (Izmit), Turkey.* Halil Sezen, Kenneth J. Elwood, Andrew S. Whittaker, Khalid Mosalam, John J. Wallace, and John F. Stanton. December 2000.
- PEER 2000/08** *Behavior of Reinforced Concrete Bridge Columns Having Varying Aspect Ratios and Varying Lengths of Confinement.* Anthony J. Calderone, Dawn E. Lehman, and Jack P. Moehle. January 2001.
- PEER 2000/07** *Cover-Plate and Flange-Plate Reinforced Steel Moment-Resisting Connections.* Taejin Kim, Andrew S. Whittaker, Amir S. Gilani, Vitelmo V. Bertero, and Shakhzod M. Takhirov. September 2000.
- PEER 2000/06** *Seismic Evaluation and Analysis of 230-kV Disconnect Switches.* Amir S. J. Gilani, Andrew S. Whittaker, Gregory L. Fenves, Chun-Hao Chen, Henry Ho, and Eric Fujisaki. July 2000.
- PEER 2000/05** *Performance-Based Evaluation of Exterior Reinforced Concrete Building Joints for Seismic Excitation.* Chandra Clyde, Chris P. Pantelides, and Lawrence D. Reaveley. July 2000.
- PEER 2000/04** *An Evaluation of Seismic Energy Demand: An Attenuation Approach.* Chung-Che Chou and Chia-Ming Uang. July 1999.

- PEER 2000/03** *Framing Earthquake Retrofitting Decisions: The Case of Hillside Homes in Los Angeles.* Detlof von Winterfeldt, Nels Roselund, and Alicia Kitsuse. March 2000.
- PEER 2000/02** *U.S.-Japan Workshop on the Effects of Near-Field Earthquake Shaking.* Andrew Whittaker, ed. July 2000.
- PEER 2000/01** *Further Studies on Seismic Interaction in Interconnected Electrical Substation Equipment.* Armen Der Kiureghian, Kee-Jeung Hong, and Jerome L. Sackman. November 1999.
- PEER 1999/14** *Seismic Evaluation and Retrofit of 230-kV Porcelain Transformer Bushings.* Amir S. Gilani, Andrew S. Whittaker, Gregory L. Fenves, and Eric Fujisaki. December 1999.
- PEER 1999/13** *Building Vulnerability Studies: Modeling and Evaluation of Tilt-up and Steel Reinforced Concrete Buildings.* John W. Wallace, Jonathan P. Stewart, and Andrew S. Whittaker, editors. December 1999.
- PEER 1999/12** *Rehabilitation of Nonductile RC Frame Building Using Encasement Plates and Energy-Dissipating Devices.* Mehrdad Sasani, Vitelmo V. Bertero, James C. Anderson. December 1999.
- PEER 1999/11** *Performance Evaluation Database for Concrete Bridge Components and Systems under Simulated Seismic Loads.* Yael D. Hose and Frieder Seible. November 1999.
- PEER 1999/10** *U.S.-Japan Workshop on Performance-Based Earthquake Engineering Methodology for Reinforced Concrete Building Structures.* December 1999.
- PEER 1999/09** *Performance Improvement of Long Period Building Structures Subjected to Severe Pulse-Type Ground Motions.* James C. Anderson, Vitelmo V. Bertero, and Raul Bertero. October 1999.
- PEER 1999/08** *Envelopes for Seismic Response Vectors.* Charles Menun and Armen Der Kiureghian. July 1999.
- PEER 1999/07** *Documentation of Strengths and Weaknesses of Current Computer Analysis Methods for Seismic Performance of Reinforced Concrete Members.* William F. Cofer. November 1999.
- PEER 1999/06** *Rocking Response and Overturning of Anchored Equipment under Seismic Excitations.* Nicos Makris and Jian Zhang. November 1999.
- PEER 1999/05** *Seismic Evaluation of 550 kV Porcelain Transformer Bushings.* Amir S. Gilani, Andrew S. Whittaker, Gregory L. Fenves, and Eric Fujisaki. October 1999.
- PEER 1999/04** *Adoption and Enforcement of Earthquake Risk-Reduction Measures.* Peter J. May, Raymond J. Burby, T. Jens Feeley, and Robert Wood.
- PEER 1999/03** *Task 3 Characterization of Site Response General Site Categories.* Adrian Rodriguez-Marek, Jonathan D. Bray, and Norman Abrahamson. February 1999.
- PEER 1999/02** *Capacity-Demand-Diagram Methods for Estimating Seismic Deformation of Inelastic Structures: SDF Systems.* Anil K. Chopra and Rakesh Goel. April 1999.
- PEER 1999/01** *Interaction in Interconnected Electrical Substation Equipment Subjected to Earthquake Ground Motions.* Armen Der Kiureghian, Jerome L. Sackman, and Kee-Jeung Hong. February 1999.
- PEER 1998/08** *Behavior and Failure Analysis of a Multiple-Frame Highway Bridge in the 1994 Northridge Earthquake.* Gregory L. Fenves and Michael Ellery. December 1998.
- PEER 1998/07** *Empirical Evaluation of Inertial Soil-Structure Interaction Effects.* Jonathan P. Stewart, Raymond B. Seed, and Gregory L. Fenves. November 1998.
- PEER 1998/06** *Effect of Damping Mechanisms on the Response of Seismic Isolated Structures.* Nicos Makris and Shih-Po Chang. November 1998.
- PEER 1998/05** *Rocking Response and Overturning of Equipment under Horizontal Pulse-Type Motions.* Nicos Makris and Yiannis Roussos. October 1998.
- PEER 1998/04** *Pacific Earthquake Engineering Research Invitational Workshop Proceedings, May 14–15, 1998: Defining the Links between Planning, Policy Analysis, Economics and Earthquake Engineering.* Mary Comerio and Peter Gordon. September 1998.
- PEER 1998/03** *Repair/Upgrade Procedures for Welded Beam to Column Connections.* James C. Anderson and Xiaojing Duan. May 1998.
- PEER 1998/02** *Seismic Evaluation of 196 kV Porcelain Transformer Bushings.* Amir S. Gilani, Juan W. Chavez, Gregory L. Fenves, and Andrew S. Whittaker. May 1998.
- PEER 1998/01** *Seismic Performance of Well-Confined Concrete Bridge Columns.* Dawn E. Lehman and Jack P. Moehle. December 2000.

ONLINE PEER REPORTS

The following PEER reports are available by Internet only at http://peer.berkeley.edu/publications/peer_reports_complete.html.

- PEER 2012/103** *Performance-Based Seismic Demand Assessment of Concentrically Braced Steel Frame Buildings*. Chui-Hsin Chen and Stephen A. Mahin. December 2012.
- PEER 2012/102** *Procedure to Restart an Interrupted Hybrid Simulation: Addendum to PEER Report 2010/103*. Vesna Terzic and Božidar Stojadinovic. October 2012.
- PEER 2012/101** *Mechanics of Fiber Reinforced Bearings*. James M. Kelly and Andrea Calabrese. February 2012.
- PEER 2011/107** *Nonlinear Site Response and Seismic Compression at Vertical Array Strongly Shaken by 2007 Niigata-ken Chuetsu-oki Earthquake*. Eric Yee, Jonathan P. Stewart, and Kohji Tokimatsu. December 2011.
- PEER 2011/106** *Self Compacting Hybrid Fiber Reinforced Concrete Composites for Bridge Columns*. Pardeep Kumar, Gabriel Jen, William Trono, Marios Panagiotou, and Claudia Ostertag. September 2011.
- PEER 2011/105** *Stochastic Dynamic Analysis of Bridges Subjected to Spatially Varying Ground Motions*. Katerina Konakli and Armen Der Kiureghian. August 2011.
- PEER 2011/104** *Design and Instrumentation of the 2010 E-Defense Four-Story Reinforced Concrete and Post-Tensioned Concrete Buildings*. Takuya Nagae, Kenichi Tahara, Taizo Matsumori, Hitoshi Shiohara, Toshimi Kabeyasawa, Susumu Kono, Minehiro Nishiyama (Japanese Research Team) and John Wallace, Wassim Ghannoum, Jack Moehle, Richard Sause, Wesley Keller, Zeynep Tuna (U.S. Research Team). June 2011.
- PEER 2011/103** *In-Situ Monitoring of the Force Output of Fluid Dampers: Experimental Investigation*. Dimitrios Konstantinidis, James M. Kelly, and Nicos Makris. April 2011.
- PEER 2011/102** *Ground-motion prediction equations 1964 - 2010*. John Douglas. April 2011.
- PEER 2011/101** *Report of the Eighth Planning Meeting of NEES/E-Defense Collaborative Research on Earthquake Engineering*. Convened by the Hyogo Earthquake Engineering Research Center (NIED), NEES Consortium, Inc. February 2011.
- PEER 2010/111** *Modeling and Acceptance Criteria for Seismic Design and Analysis of Tall Buildings*. Task 7 Report for the Tall Buildings Initiative - Published jointly by the Applied Technology Council. October 2010.
- PEER 2010/110** *Seismic Performance Assessment and Probabilistic Repair Cost Analysis of Precast Concrete Cladding Systems for Multistory Buildings*. Jeffrey P. Hunt and Božidar Stojadinovic. November 2010.
- PEER 2010/109** *Report of the Seventh Joint Planning Meeting of NEES/E-Defense Collaboration on Earthquake Engineering. Held at the E-Defense, Miki, and Shin-Kobe, Japan, September 18–19, 2009*. August 2010.
- PEER 2010/108** *Probabilistic Tsunami Hazard in California*. Hong Kie Thio, Paul Somerville, and Jascha Polet, preparers. October 2010.
- PEER 2010/107** *Performance and Reliability of Exposed Column Base Plate Connections for Steel Moment-Resisting Frames*. Ady Aviram, Božidar Stojadinovic, and Armen Der Kiureghian. August 2010.
- PEER 2010/106** *Verification of Probabilistic Seismic Hazard Analysis Computer Programs*. Patricia Thomas, Ivan Wong, and Norman Abrahamson. May 2010.
- PEER 2010/105** *Structural Engineering Reconnaissance of the April 6, 2009, Abruzzo, Italy, Earthquake, and Lessons Learned*. M. Selim Günay and Khalid M. Mosalam. April 2010.
- PEER 2010/104** *Simulating the Inelastic Seismic Behavior of Steel Braced Frames, Including the Effects of Low-Cycle Fatigue*. Yuli Huang and Stephen A. Mahin. April 2010.
- PEER 2010/103** *Post-Earthquake Traffic Capacity of Modern Bridges in California*. Vesna Terzic and Božidar Stojadinović. March 2010.
- PEER 2010/102** *Analysis of Cumulative Absolute Velocity (CAV) and JMA Instrumental Seismic Intensity (I_{JMA}) Using the PEER–NGA Strong Motion Database*. Kenneth W. Campbell and Yousef Bozorgnia. February 2010.
- PEER 2010/101** *Rocking Response of Bridges on Shallow Foundations*. Jose A. Ugalde, Bruce L. Kutter, and Boris Jeremic. April 2010.
- PEER 2009/109** *Simulation and Performance-Based Earthquake Engineering Assessment of Self-Centering Post-Tensioned Concrete Bridge Systems*. Won K. Lee and Sarah L. Billington. December 2009.

- PEER 2009/108** *PEER Lifelines Geotechnical Virtual Data Center.* J. Carl Stepp, Daniel J. Ponti, Loren L. Turner, Jennifer N. Swift, Sean Devlin, Yang Zhu, Jean Benoit, and John Bobbitt. September 2009.
- PEER 2009/107** *Experimental and Computational Evaluation of Current and Innovative In-Span Hinge Details in Reinforced Concrete Box-Girder Bridges: Part 2: Post-Test Analysis and Design Recommendations.* Matias A. Hube and Khalid M. Mosalam. December 2009.
- PEER 2009/106** *Shear Strength Models of Exterior Beam-Column Joints without Transverse Reinforcement.* Sangjoon Park and Khalid M. Mosalam. November 2009.
- PEER 2009/105** *Reduced Uncertainty of Ground Motion Prediction Equations through Bayesian Variance Analysis.* Robb Eric S. Moss. November 2009.
- PEER 2009/104** *Advanced Implementation of Hybrid Simulation.* Andreas H. Schellenberg, Stephen A. Mahin, Gregory L. Fenves. November 2009.
- PEER 2009/103** *Performance Evaluation of Innovative Steel Braced Frames.* T. Y. Yang, Jack P. Moehle, and Božidar Stojadinovic. August 2009.
- PEER 2009/102** *Reinvestigation of Liquefaction and Nonliquefaction Case Histories from the 1976 Tangshan Earthquake.* Robb Eric Moss, Robert E. Kayen, Liyuan Tong, Songyu Liu, Guojun Cai, and Jiaer Wu. August 2009.
- PEER 2009/101** *Report of the First Joint Planning Meeting for the Second Phase of NEES/E-Defense Collaborative Research on Earthquake Engineering.* Stephen A. Mahin et al. July 2009.
- PEER 2008/104** *Experimental and Analytical Study of the Seismic Performance of Retaining Structures.* Linda Al Atik and Nicholas Sitar. January 2009.
- PEER 2008/103** *Experimental and Computational Evaluation of Current and Innovative In-Span Hinge Details in Reinforced Concrete Box-Girder Bridges. Part 1: Experimental Findings and Pre-Test Analysis.* Matias A. Hube and Khalid M. Mosalam. January 2009.
- PEER 2008/102** *Modeling of Unreinforced Masonry Infill Walls Considering In-Plane and Out-of-Plane Interaction.* Stephen Kadsiewicz and Khalid M. Mosalam. January 2009.
- PEER 2008/101** *Seismic Performance Objectives for Tall Buildings.* William T. Holmes, Charles Kircher, William Petak, and Nabih Youssef. August 2008.
- PEER 2007/101** *Generalized Hybrid Simulation Framework for Structural Systems Subjected to Seismic Loading.* Tarek Elkhoraibi and Khalid M. Mosalam. July 2007.
- PEER 2007/100** *Seismic Evaluation of Reinforced Concrete Buildings Including Effects of Masonry Infill Walls.* Alidad Hashemi and Khalid M. Mosalam. July 2007.

The Pacific Earthquake Engineering Research Center (PEER) is a multi-institutional research and education center with headquarters at the University of California, Berkeley. Investigators from over 20 universities, several consulting companies, and researchers at various state and federal government agencies contribute to research programs focused on performance-based earthquake engineering.

These research programs aim to identify and reduce the risks from major earthquakes to life safety and to the economy by including research in a wide variety of disciplines including structural and geotechnical engineering, geology/seismology, lifelines, transportation, architecture, economics, risk management, and public policy.

PEER is supported by federal, state, local, and regional agencies, together with industry partners.



PEER Core Institutions:
University of California, Berkeley (Lead Institution)
California Institute of Technology
Oregon State University
Stanford University
University of California, Davis
University of California, Irvine
University of California, Los Angeles
University of California, San Diego
University of Southern California
University of Washington

PEER reports can be ordered at http://peer.berkeley.edu/publications/peer_reports.html or by contacting

Pacific Earthquake Engineering Research Center
University of California, Berkeley
325 Davis Hall, mail code 1792
Berkeley, CA 94720-1792
Tel: 510-642-3437
Fax: 510-642-1655
Email: peer_editor@berkeley.edu

ISSN 1547-0587X